Summer 5-26-2022

Microbial Sociality in Biofilms

Swetha Kasetty
Dartmouth College, swetha.kasetty.gr@dartmouth.edu

Microbial Sociality in Biofilms

A Thesis
Submitted to the Faculty
in partial fulfillment of the requirements for the
degree of

Doctor of Philosophy

in

Ecology, Evolution, Environment and Society

by Swetha Kasetty

Guarini School of Graduate and Advanced Studies
Dartmouth College
Hanover, New Hampshire
May 2022

Examining Committee

_____

(chair) Carey D. Nadell, PhD

_____

Deborah A. Hogan, PhD

_____

Mark A. McPeek, PhD

_____

David R. Andes, MD

_____

F. Jon Kull, Ph.D.
Dean of the Guarini School of Graduate and Advanced Studies

Abstract

Biofilms are communities of microorganisms attached to surfaces through various self-secreted matrix materials. Biofilms are dynamic communities with extensive interactions between their residents. Microorganisms compete, cooperate, and communicate with each other in biofilms. These ecological interactions determine the emergence or loss of strains/species and are critical in the formation and proliferation of biofilms. Furthermore, most natural biofilms are formed by multiple microbial species and strains and these interactions within the biofilm dramatically influence community composition and structure over time. Microbial interactions also influence clinically relevant outcomes such as antibiotic resistance and host virulence. In this thesis we explore the potential interactions of microbial populations with their environment, different strains and species using a combination of molecular techniques, microfluidics, and confocal microscopy. In the first study we explored surface competition and biofilm invasion strategies of two strains of *Pseudomonas aeruginosa*. We found that different extracellular matrix composition and biofilm production strategies effect their direct competition. One strain was able to outcompete the later during early colonization and growth. In contrast the later strain was able to better invade existing biofilms and more inclined to stay during starvation conditions. This sheds light on the advantages of different colonization strategies and their advantages in diverse environmental settings. In the second project, we explored the effect of nutrition on *Candida albicans* biofilms by growing them in different media. We studied *C. albicans* biofilm characteristics in three distinct nutritional niches and found that biofilm architecture and properties were distinct in each nutritional niche. This study highlights the importance of nutrient media, and the effects metabolism has on biofilm formation. Finally, in the last project we studied the interaction of *Pseudomonas aeruginosa* and *Candida albicans* in a Cystic Fibrosis (CF) lung environment. We found an increase in biovolume for both species and this result was specific to the biofilm environment. Although we could not identify the mechanism of action, we saw this robust result of increase of biovolume in dual species biofilms across multiple mutants and CF isolates. These studies showcase the importance of microbial ecology in understanding biofilm properties and characteristics.

Acknowledgements

To my guide and mentor Carey, thank you! I am so grateful to have been able to work with you and be a part of your lab or your extended family as you once called the lab. Your excitement for science is unparalleled and inspiring. Your unwavering support and confidence in me over the years has kept me going. Thank you for giving me the opportunity and space for exploring all the ideas I have had. I have learnt so much about science from you, I also learnt to be understanding, approachable and generally kind and helpful to the community. It's been an amazing journey being the first person in the lab and watching it grow to be such a wonderful and supportive place to work at. I have enjoyed the work I have done in the lab so much. Thank you, Carey!

To our first collaborators Deb and Dallas. Thank you, Deb, for sharing all your knowledge and expertise with us. I am so grateful you were so welcoming and opened your lab for us. Thank you, Dallas, for teaching me the ropes of cloning and helping me get a foothold on all the protocols. I very much enjoyed all our conversations. You were always happy to answer my questions and talk through ideas, I very much appreciate it.

To my committee members, Mark and David, Thank you for your time and thoughts. I appreciate all your insights and advice on my projects. To the collaborators on the Pseudomonas project George and Stefan, I have very much enjoyed working together. I have learnt what a good collaboration should be like and how to proceed when conflict arises, thank you! A shout out to my advisors at Rutgers Dr. Both and Dr. Barkey who were instrumental in helping me get to Dartmouth, thank you for all the guidance and support as I was transitioning into a new country and culture.

To my lab mates, Matt, Ben, Emilia, Alice, Lia, Jay and Jake, thank you for making the lab such a fun, interactive and supportive place to work in. I am so grateful for having met all of you. I have learnt so much from everyone from fixing things to plants to cows to knives to movies to unwavering love of phages. A special mention to Matt who I've spent the

longest time in the lab with. Thank you for always listening and always being so positive and most importantly disliking the cold weather as much as I do.

To the EEES community and my cohort, thank you for being so inclusive. To my friends in the upper valley, thank you for being supportive and understanding throughout my graduate school life. All the social activities kept me sane and refreshed through the years. The home cooked food has been amazing. To my friends across the continents, thank you for all the phone calls, love, and support. It has been so wonderful relishing all the memories we have had and looking forward to all the new memories we will make.

To my family, thank you for being so supportive. For encouraging me to follow my interests even though it meant being so far away. To my sister Sneha, thank you for being so full of excitement and intrigue and listening to all my science. To my mother Anitha, who has pushed me to pursue excellence and instilled in me the importance of hard work and persistence. Finally, to my partner Ajay who has constantly supported me through the years and has been ever so patient and kind to me. You have been my rock, Thank you! And of course, thank you to my kitties, Adi and Soma my stress busters. Could not have done any of this without you all. I am very grateful and feel so humbled to have this amazing support system.

Table of Contents

List of Tables

List of Figures

Chapter 1

Introduction

Biofilms as a System to Study Sociality in Microorganisms

Swetha Kasetty[1] and Carey D. Nadell[1]

[1]Department of Biological Sciences, Dartmouth College, Hanover, NH

Author contributions

S.K. wrote the original draft of the chapter. C.D.N. provided critical input and assisted in writing, organizing, and editing the chapter.

1.1 Abstract

Microorganisms commonly exist as communities and constantly interact with each other and their environment. They can interact positively, negatively, or neutrally and these interactions have a big impact on shaping the community as well as their environment. Microorganisms can exist as spatially structured communities called biofilms, the spatial structure enables swifter interactions because of spatial proximity to their neighboring cells. Studying the spatial structure of microbial biofilms can enable us to understand their underlying interactions, for example if species or strains are competing, they are likely to spatially separate from each other. The sessile nature of biofilms allows us to track microbial interactions changes temporally. The spatial structure and non-motile lifestyle make microbial biofilms a good system to study microbial interactions.

1.2 Introduction

Microorganisms or microbes include bacteria, archaea, fungi, protists, and viruses and are a highly diverse group of organisms. They are distributed globally ranging from the human guts [1] to deep-sea hydrothermal vents [2] to aerosolized droplets [3]. Rather than existing as single free-living or planktonic cells, microbes are known to form complex interactive groups within their ecosystem. Microbes interact with other microbes of the same species, of different species or with vastly different families and phyla[4], [5]. Microbial interactions can span a multitude of mechanisms such as genetic or metabolic exchange,

and chemical signaling. Microbe-microbe interactions are critical for the survival and replication of microbial populations in various environments [6].

The basic unit of microbial interaction is gene expression in response to chemical or physical stimuli. Differential expression of multiple genes leads production of chemical molecules or microbial appendages that microbes use to interact with their environment [7]. The nature and significance of these interactions depends on both abundance and type of interacting organisms present as well as the physical environment and available nutritional source. Microbes are not limited to a single kind of interaction, the transient nature of their physical, chemical, and biological environment results in highly complex and dynamic interactions[5], [8], [9].

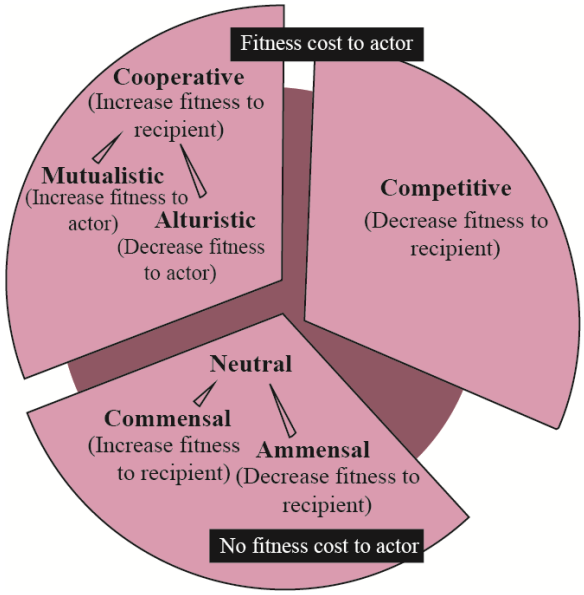

FIG. 1: Classification of microbial interactions based on fitness cost to actor and recipient. Cooperative and competition interactions cause a fitness decrease in the actors whereas there is no fitness cost to the actor in neutral interaction.

Microbial interactions can be broadly classified based on fitness consequence for the microbial actor and the microbial recipient (Figure 1). When there is an increase in fitness for the recipient, the behavior is termed cooperative. These interactions can manifest as

mutualistic interactions, for example *Vibrio cholerae* produces chitinase, a secreted enzyme to degrade its nutrient source, within the environment. When multiple *V. cholerae* cells produce and secrete this enzyme into the environment, the increased concentration of the enzyme can be beneficial for all producing members by increasing access to nutrients [10]. Cooperative interactions can alternately be altruistic, where there is a fitness cost incurred by the actor. For example, when E*scherichia coli* cells are faced with antibiotic stress, a portion of cells produce a signaling molecule, at a cost to themselves, that helps non-producing cells cope with the stress [11]. Interactions leading to fitness decrease for the recipients is referred to as competitive interaction. Scarce nutrients and limited space have led to several competitive behaviors in microbes using which they can outcompete and displace their competitors. For example, *Burkholderia thailandensis* inhibits growth of *Bacillus subtilis* by the production of antibiotics [12]. Finally, neutral interactions exist when the actor does not incur an energy cost, but the recipient is positively or negatively affected. For example, *Bacillus cereus* produces peptidoglycans as a product of its own metabolism, and the presence of this peptidoglycan has shown to stimulate growth of Rhizosphere bacteria [13].

Disentangling of microbial interactions and their underlying mechanisms can unravel strategies that microbes use to establish and survive in different environments and ecosystems. Understanding the effects of these interactions is essential to improving the performance of many ecological systems that are important in diverse processes like biological waste treatment, industrial fermentations, human or animal health, and disease and in soil systems[6]–[8], [14], [15]. Microbial interactions research is still in its nascency. Little is understood about the multidimensional nature of communication channels microbe's use. Exhaustive descriptions and detailed characterization of microbial interactions will enable us to manipulate microbial communities and utilize them for clinical, industrial, and biotechnological applications.

1.3 Microbial interactions: Cooperation and Competition

(i) Competition

Microbial populations need space and nutrients to grow and multiply. Most microbes live in environments that have finite space and nutrients. The need to access these common resources, gives rise to microbial competition [12]. Microbes usually overlap in resource use and invest energy to cause a fitness decrease in their competitor. Antagonistic or competitive behaviors can occur between unrelated species of different kingdoms or even between the same strains of a species differing by a single mutation [16].

Microbes can compete two distinct ways (Figure 2) depending on whether they are actively or passively engaging with their competitors.

1. **Exploitative Competition**

   This kind of competition occurs passively through the consumption of a limiting resource thereby denying access to the competitor. The indirect competition to nutrients can occur through the increased uptake of nutrients and through release of extracellular molecules that can harvest nutrients from their surroundings. Additionally, competition can occur for space; microbes can rapidly colonize a space and prevent the entry of others. Alternatively, microbes can push out or move existing competitors as a consequence of faster growth or extracellular molecule production to make space for themselves [17]. The fast growth or extracellular molecule provides an advantage to the species producing it, however it is still passive in the sense that it is also produced in the absence of the competitor.

2. **Interference Competition**

   This in an active form of competition where the microbes directly interact and physically impair their competitors. Secretion of toxic chemicals like antibiotics can kill or damage competitors. Secretion of certain molecules can manipulate competitor's metabolism and prove advantageous to the secretor. Cells can also starve their competitors and cut off access to nutrients through physical barriers. Furthermore, direct competition can occur through physical contact, for example

type VI secretion systems, where cells inject syringe-like protrusions containing toxins and other molecules into neighboring cells [17].

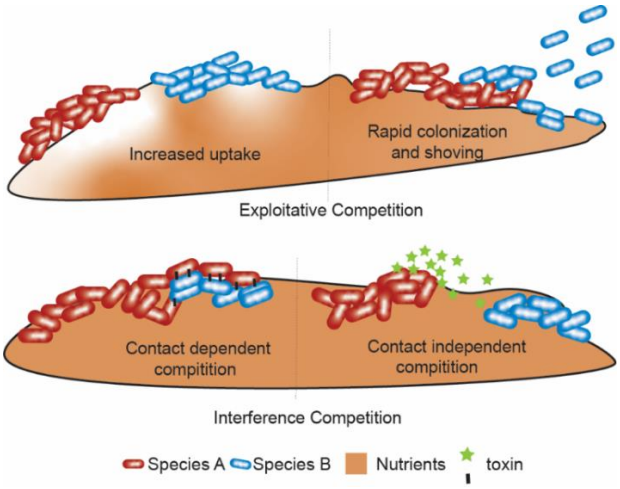

FIG. 2: Diagrammatic representative of types of competitive behaviors. Exploitative competition occurs passively through increase uptake of nutrients or rapid colonization / shoving behavior. Interference competition on the other hand occurs through direct interaction.

A landmark study by Foster and Bell [18] compared pairwise interactions of 72 strains of bacteria and found that the net benefits to the species involved remain relatively modest. Based on these results they predicted that there are larger numbers of competitive interactions between many species and fewer cooperative interactions. We know that microbes have evolved a wide range of mechanisms to harm and kill their competitors that include a multitude of chemical weapons and mechanical techniques. Microbial competition is very diverse and complex shaped by many factors, including cell density, nutrient abundance and spatial arranged of cells[12], [19]. The existence of all these multiple competitive strategies reflects the principal role of microbial competition in microbial ecology.

(ii) Cooperation

As referenced earlier, the key determinants of social behavior are fitness costs for the actor and the recipient. An increase in fitness for the recipient, is termed cooperative. Cooperative behavior could be mutually beneficial for the actor or altruistic (negative) for the actor (Figure 3). In contrast, antagonistic behaviors result in a fitness decrease for the recipients and could provide an advantage for the actor. This makes antagonistic and mutually beneficial behaviors easier to explain in an ecological sense in relation to altruistic behaviors.

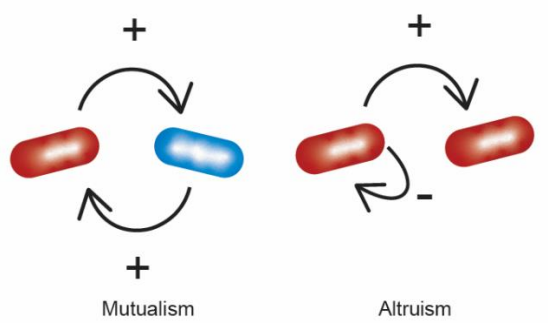

FIG. 3: Diagrammatic representation of fitness cost to microbial actor on the left and recipient on the right. Mutualistic interactions are positive to both actor and recipient. Altruistic interactions are beneficial to the recipient and harmful to actor.

Cooperation presents two major theoretical challenges that must be understood in order to determine how cooperation can arise:

1. The first challenge is to understand why an individual would carry out a costly behavior for the benefit of other individuals.

   Cooperative behaviors can be divided into two broad groups. The first is a direct fitness advantage to the actor, the fitness advantage outweighs the cost of performing the behavior. In this situation the cooperation is beneficial to both the actor and receiver and there is usually a mechanism in place to enforce the cooperating behavior and remove non-cooperators. A second kind of cooperative behaviors decrease the direct fitness of the actor, however, there is an overall increase in the fitness of that genotype. Altruistic behaviors are usually targeted towards close relatives or clonemates and is termed as indirect fitness or inclusive fitness.

To dive a little deeper, altruistic behavior can be explained by kin selection theory. Helping a close relative to reproduce benefits the actor by passing on its own genes to the next generation. This provides an indirect fitness advantage for the actor and a direct fitness benefit for the receiver. The theory is encapsulated mathematically in the form of Hamilton's rule [20], which states that altruistic cooperation is favored when $rb-c > 0$; r is genetic relatedness, b is the benefit to the recipient and c is the cost of behavior to the actor. Altruistic cooperation can be expected when relatedness or benefit are high, and cost of cooperation is low. For predominantly asexual organisms like microorganisms, the concept of relatedness can be reduced to genotypic view of the behavior. Genotypic identity could be a result of recent clonal growth or horizontal gene transfer. If the genotypes that drive the interaction are identical, altruistic cooperation is favored [16] .

2. In mutualistic cooperation, there is the problem of non-cooperative individuals or cheaters, who could benefit by not cooperating and obtain a competitive advantage. This concept can be illustrated by Hardin's theory of the tragedy of the commons. Consider a shared pastureland that many shepherds can use. Cooperation can exist between the shepherds if they have fixed small number of sheep. This ensures the pasture is not overgrazed, providing a net benefit for all the shepherds. But it is in each individual shepherd's benefit to add sheep to his flock, even though it may cause exhaustion of the shared resource (grazing pasture) and reduce the benefit for all shepherds. This leads to the collapse of cooperation.

   Studies, however, have shown the existence of cooperative behaviors in microorganisms. Take for example the production of public goods. Public goods are products that are costly for an individual to produce but provide a benefit to the population [21]. Iron scavenging molecules called siderophores are an example of public goods produced by many bacteria in iron limiting conditions. Experiments with *P. aeruginosa* [22] have demonstrated that wild type strains that produce the siderophore and can grow faster in iron limiting conditions than do siderophore non-producing mutant strains. However, in iron rich conditions, the siderophore

mutants grew faster demonstrating that there is cost to siderophore production. However, it is possible in mixed populations the mutants can gain benefit of siderophore production without paying the cost and able to out compete the wild type of strain. In natural systems, this kind of invasion by non-cooperators or cheaters can be minimized by a multiple stabilization mechanism like density dependence, spatial structure, pleiotropy, metabolic prudence, and policing behaviors [23]. These different techniques help keep cheaters out and ensure cooperators are not outcompeted.

1.4 System to study microbial interactions: Biofilms

An ideal system to study microbial interactions given the size of the organisms, is one which not only has a large enough population but also is non motile enabling tracking changes spatially and temporally. Biofilms are such a system; we know that 40-80% of microbial life exist as biofilms making them a very relevant system to study [24].

Biofilms are communities of microbes attached to surfaces through various self-secreted matrix materials. The matrix, a canonical feature of biofilms, can be made of polysaccharides, proteins, lipids, and extracellular DNA [25]. Biofilms are extremely widespread in nature, they can colonize a variety of substrata like minerals, metals, plant and animal cells and implanted medical devices like catheters and metal implants [8], [26]–[29]. Fossil records have shown that biofilm formation is ancient process indicating that it is a fundamental process in the microbial life cycle. A diverse spectrum of microorganisms, including bacteria, fungi, and protists, have displayed biofilm formation likely indicating that it is beneficial for survival.

Biofilms interact with their environment in ways that contrast with their planktonic counter parts. For example, antimicrobial resistance of biofilm dwelling microbes is considerably higher than their planktonic counter parts. Anti-microbial protection can be achieved by reduction in metabolic and growth rates, protection by extracellular matrix and resistance mechanisms conferred by the altered physiology of biofilm microbes [24]. Biofilm mode of life confers other advantages to its members, such as adhesion/cohesion capabilities,

mechanical properties, nutritional sources, metabolite exchange platform, cellular communication, protection from environmental stresses and host immune, and shear forces [29].

Further, biofilms are a critical area of study because they are the most widely distributed and successful modes of life on Earth. They drive biogeochemical cycling processes of many elements in water, soil, sediment, and subsurface environments [30]. Biotechnological applications of biofilms include the filtration of drinking water, the degradation of wastewater and solid waste, and biocatalysts in biotechnological processes, such as the production of bulk and fine chemicals, as well as biofuels[31]. All higher organisms, including humans, are colonized by microorganisms that form biofilms, which can be associated with persistent infections in plants and animals, and with the contamination of medical devices and implants[32], [33]. Biofilms also present technical challenges and are responsible for biofouling and contamination of process water, deterioration of the hygienic quality of drinking water and microbially influenced corrosion [34], [35]. Understanding how biofilms form and function will allow use not only to mitigate their negative effects but also maximize utilities they provide.

The exact molecular mechanisms of biofilm formation vary substantially among microorganisms. However, the broad stages of biofilm development (Figure 4) are conserved among them: (i) Initial attachment (ii) Microcolony formation (iii) Mature biofilm (iv) Dispersal. It is important to note that different environmental stimuli can trigger different biofilm developmental pathways, indicating that the process of biofilm formation is very dynamic. Once attached, they start secreting a glue like material called matrix and multiplying to give rise to small microcolony which eventually mature into larger three-dimensional biofilms. Eventually the cells from the biofilm disperse into the environment to find a new region to colonize [25], [29].

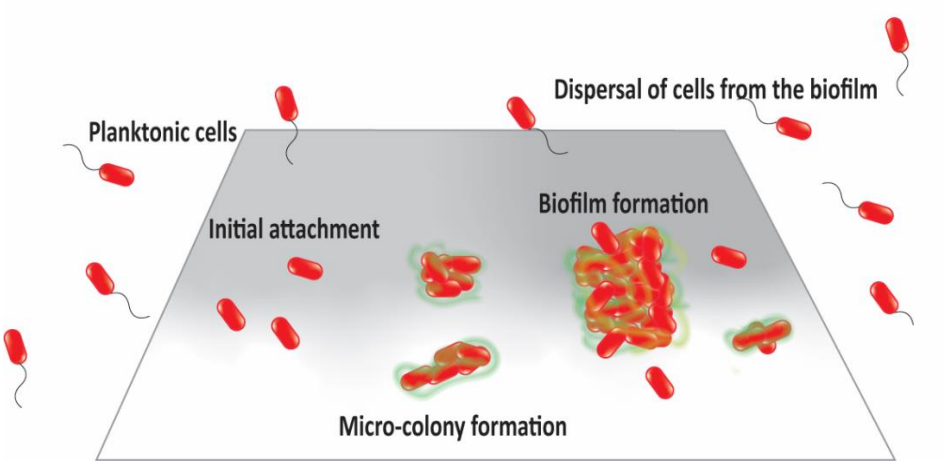

FIG. 4: Representation of stages of biofilm formation for bacteria *Pseudomonas aeruginosa*. Planktonic or free-floating cells attach to a surface after which they start to multiply and produce matrix. The cells then expand vertically to form a three-dimensional amature biofilm. Finally, planktonic cells are released from the biofilm back into the environment to find a new niche to colonize.

1.5 Effect of internal factors on spatial structure

(i) Interactions

We know microbial biofilms can contain a diversity of strains (subtype of a species) and species. As surface attached cells start to grow, they interact with other cells around them and their environment causing the structure of their community to change. Because biofilms are stationary, microbial social behaviors are limited to neighbors making spatial structure crucial. Cells immigrating and emigrating from the biofilm, environmental stress, predation, nutrient availability can all affect the structure and composition of biofilms [36].

Social interactions have been increasingly recognized as one of the major influencers that contribute to microbial biofilms including their spatial structure [37]. To briefly consider how interactions can shape biofilm dynamics and their spatial structure, consider an initial population of three distinct cell lineages A, B and C (example from [37]). In the first scenario, A is antagonistic and kills B and C, leading to a biofilm that contains only A. Alternatively, in a scenario where B and C are mutualistic, they may tend to cluster towards each other to maximize their shared benefit. In a third scenario, where B produces public

goods, B is likely to spatially localize with themselves away from A and C to prevent cheating behavior. Therefore, studying the spatial structure of the biofilm could help us understand underlying interaction and how these interactions in turn shape biofilm characteristics and emergent properties.

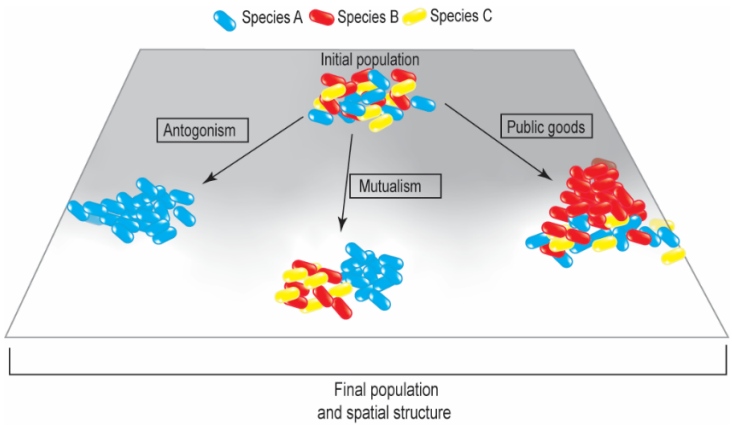

FIG. 5: Representation of the effect of interactions on spatial structure of biofilms. If an initial population starts with equal number of cells from three species (i) Species A is antagonistic and kills all other cells, to a final population with only species A (ii) If species B and C are mutualistic, leads to a final population where B and C might spatial collocate (iii) if species B produces public goods, it may spatially isolate itself from other species to maximize its own benefits and prevent cheating behavior.

1.6 Effect of external factors on spatial structure

(i) Fluid flow

Flow around a biofilm influences transport of solutes in and out of the biofilm and applies forces to the biofilm that can affect its ability to attach and detach [38]. Flow primarily exerts shear force onto the biofilm usually in the main direction of fluid flow, but complex fluid mechanics like eddies and turbulent bursts can also result in additional force components[39]. The movement of liquids and consequently the stress they introduce have been shown to have physical effects on biofilms rolling, development of streamers, oscillatory movement, and detachment [38]–[43]. Fluid flow around biofilms can also affect mass transfer, they can act for example as an insulator for diffusive exchange. This

in turn can exacerbate oxygen or nutrient limitation, affect quorum sensing, and contribute to changes in spatial structure of the biofilm [44].

The flow regime can also affect the morphology and biofilm characteristic at their microscale architectural space. For example, adaptation shear stress at cellular scale has influenced the evolution of bacterial surface motility, surface colonization mechanisms, extracellular matrix secretion, bacterial cell shape, planktonic aggregate formation, and biofilm community assembly and function[39], [41], [42], [45]. However, flow mediated changes in solute environment are another important fluid flow function that not explored as well (Figure 6). Additionally, if and how shear stress initiates or represses the production of certain secreted molecules used for microbial communication in unknown.

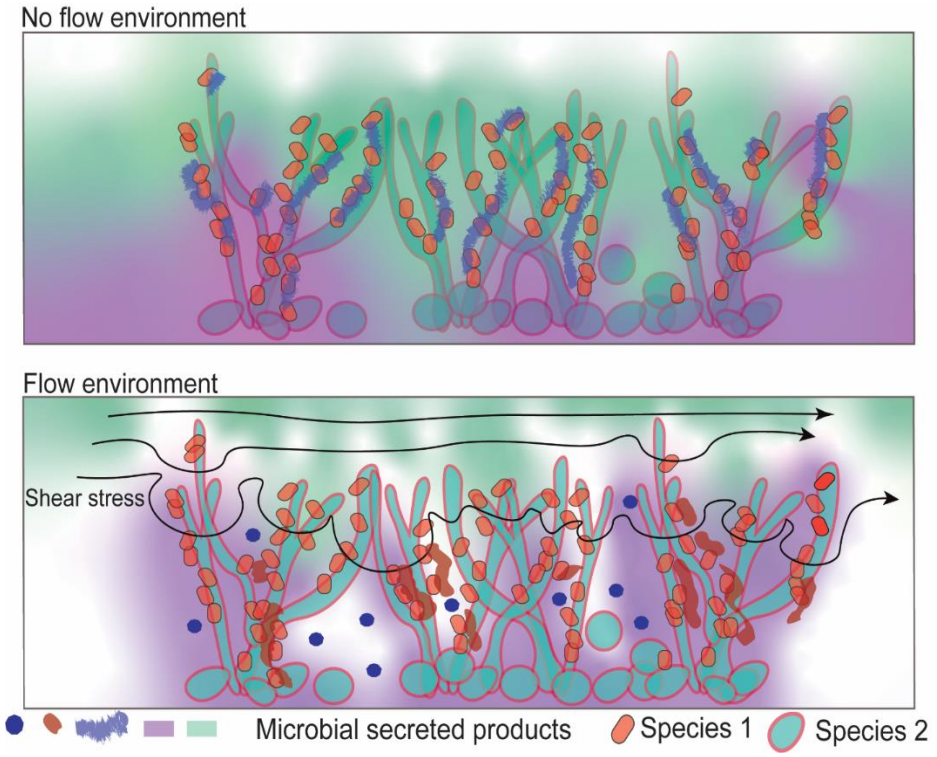

FIG. 6: Representation of potential effects of flow on secreted microbial products. The presence of fluid flow may change concentration gradients and spatial location of microbially secreted products. Flow may also induce production of novel products and inhibition of those produced under conditions without flow.

(ii) Nutrient environment

Biofilm formation is a multistep process, involving multiple physiological changes that takes place in response to environmental and biochemical factors. The amounts and types of nutrients in the environment influence the development and composition of biofilms [46]. In oligotrophic environments, for example, organisms respond to nutrient stress by alterations in their cell morphology and cell surfaces, changing their adherence properties [47].

Microbes can initiate, accelerate, facilitate, and block certain behaviours depending on the amount and type of nutrients available. Although there have been studies of the effects of nutrient concentrations on biofilm growth there have been fewer studies exploring the how different kinds of nutrients effect biofilms [48], [49]. Biofilms are known to grow in a multitude of habitats, these habitats are very nutritionally diverse and complex. In addition, the metabolic flexibility of different microbes has been explored and documented. However, the combination of these two areas is still under studied. An interesting area in microbial biofilm research is to explore biofilm ecology in diverse nutritional environments and to study the effect of nutrient type on biofilm form and function.

1.7 Microbial model system

(i) *Pseudomonas aeruginosa* biofilms

P. aeruginosa is a gram-negative soil bacterium that is the focus of intense research because of its role in disease because of long-term colonization and persistence. Metabolic flexibility allows it to exploit several niches. Being an opportunistic pathogen, *P. aeruginosa* is frequently isolates from human hosts with compromised immune systems. Treatment of *P. aeruginosa* infections are hindered by its ability to form biofilms. Biofilms not only protect the microbe from anti-microbial treatments but also provide protection from environmental stress, and host defenses [50].

Biofilm formation in *P. aeruginosa* starts with surface attachment (Figure 7). Planktonic cells first contact a surface through reversible attachment [51]. Once this contact is made the cells can move using twitching motility using type IV pilli or flagella and surfactants to move across the surface[51]. Finally, cells can also commit to irreversible attachment through the long axis of the cell. Following which surface proteins such as SadB or LapA and secreted matrix components assist in adhesion between the cell and the surface [52], [53]. c-di-GMP is a signaling molecule and secondary messenger molecule that regulates transition from motile to sessile mode of growth. c-di-GMP is thought to act as a checkpoint through the different stages of biofilm formation, increase in c-di-GMP can modulate matrix production, stress responses, and inhibit motility [54]. cAMP is another secondary molecule that has been shown to promote attachment and stimulate microcolony formation [55]. Changes in cAMP concentrations by cells that have encountered a surface have also been shown to be passed down temporally through clonemates. This temporal passage of information can help in faster attachment to a surface [56].

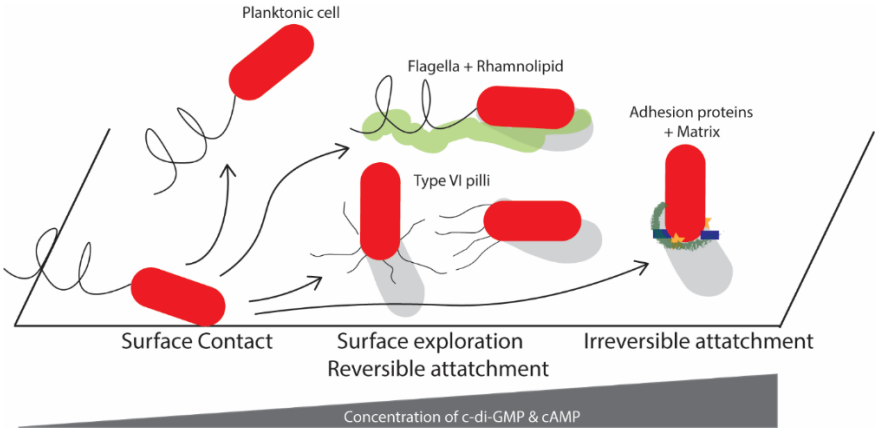

FIG. 7: Surface attachment by *P. aeruginosa*. Once the cell contacts a surface it can leave, explore the surface using type IV pilli or flagella and rhamnolipids. The cells can alternately, commit to irreversible attachment by the production of adhesion proteins and secretion of matrix.

.

Following attachment, cells start to multiply and produce extracellular matrix. A canonical feature of biofilms is their production of an extracellular matrix. The matrix provides a protective environment and three-dimensional structure to the cells present in the biofilm [57], [58]. Biofilm matrix composition varies depending on *P. aeruginosa* strain, although

the different components of matrix are documented (Figure 8A), the trade-offs, preferences, and advantages of different combinations of matrix composition are still under investigation. The matrix of *P. aeruginosa* is largely made of exopolysaccharides – Psl and Pel. Psl and Pel have been proposed to be involved in cell-cell and cell-surface adhesion. They are also important in binding other matrix components like extracellular DNA and host polymers like hyaluronan and mucin. Psl and Pel seem to be redundant in function, some strains of *P. aeruginosa* only have Pel [57], [59], [60]. Another polysaccharide, alginate was initially thought to be an important component of biofilm formation; however, it is now accepted that alginate is not a significant component of the matrix. While *P. aeruginosa* biofilms can be formed without alginate, alginate seems to be an important component of defense mechanisms against host immune systems [61].

In addition to polysaccharides, the *P. aeruginosa* biofilm matrix also contains proteins and extracellular DNA (eDNA). The protein CdrA has been shown to be important in biofilm formation by anchoring Psl to the bacteria or by crosslinking of CdrA and Psl in addition to retaining Psl in the biofilm matrix. CdrA-CdrA interactions have been shown to be important in cell-cell packing in an aggregate that is resistant to physical shear [62]. LecA and LecB are proteins also thought to be involved biofilm formation. LecA is believed to be involved in cell-to-cell interactions within the biofilm thereby connecting the bacterial cells together in biofilms [63]. LecB on the other hand is thought to be involved in cell-matrix EPS interactions [64]. eDNA in the *P. aeruginosa* matrix has been shown to provide structural support. eDNA isolated from *in vitro* biofilms was identified to be derived from *P. aeruginosa* genomic DNA in biofilms suggesting that eDNA was actively produced for biofilm matrix [65], [66].

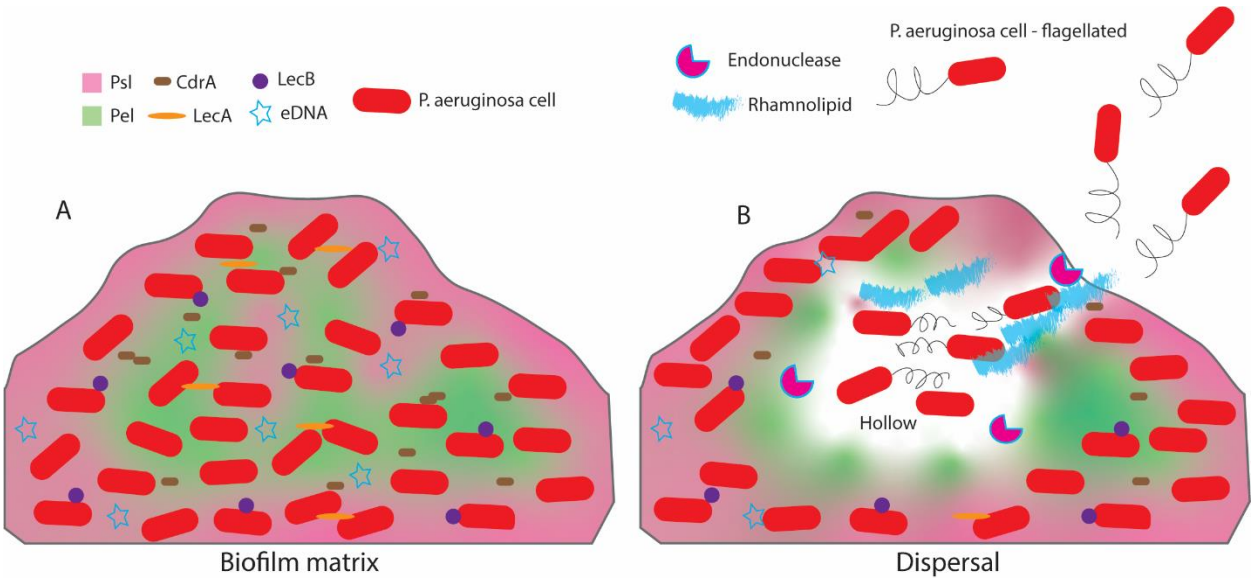

FIG. 8: *P. aeruginosa* biofilm matrix composition and mechanism of dispersal. (A) Diagrammatic representation of matrix components (B) representation of mechanisms involved in dispersal from a *P. aeruginosa* biofilm.

Dispersal, a mode of biofilm detachment, indicates active mechanisms that cause individual cells to separate from the biofilm and return to planktonic life. Since biofilm cells are cemented and surrounded by EPSs, dispersal is not simple to do, and many researchers are now paying more attention to this active detachment process. c-di-GMP as mentioned earlier is an intracellular signal that regulates the transition from sessile to planktonic growth in a variety of bacteria. Increased levels of c-di-GMP generally result in an increase in exopolysaccharide and fimbriae production, and a decrease in motility, whereas decreased levels of c-di-GMP exert the opposite effects and induce biofilm dispersal [54]. *P. aeruginosa* dispersal from biofilms can occur through one or combination of mechanisms. Cells can detach from the biofilm through the degradation of biofilm matrix using an endonuclease EndA, they can also return to motile lifestyle by investing in flagella [67], [68]. Alternately, they have been also shown to produce surfactants called rhamnolipids which have shown to be important in motility [69]. *P. aeruginosa* can also differentiate spatially ahead of dispersal to form hollows inside biofilms form which planktonic cells reenter the environment [70] (Figure 8B).

(ii) *Candida albicans* biofilms

C. albicans is a prevalent polymorphic fungal commensal and colonizes many areas of the body in healthy individuals. However, any alterations in host immunity can lead to *C. albicans* infection. They are known to notoriously colonize implanted medical devices like catheters, pacemakers, dentures and prosthetic joints. *C. albicans*, like *P. aeruginosa*, depends on its ability to thrive as a biofilm [71].

C. albicans biofilm formation is represented in Figure 9 and begins with yeast cells contacting a surface, these early interactions are thought to comprise non-specific factors like attractive forces and electrostatic interactions facilitate initial surface contact[72]. Following surface contact, cell-wall associated molecules are expressed to attach. Agglutinin-like sequence (Als) family of proteins have been shown to facilitate yeast cell-cell and cell-substrate adhesion [73]. Once the yeast cell is attached to a surface, it starts to germinate to form hyphae and psuedohyphae [71]. In addition to Als family of adhesion proteins hyphal wall proteins and Iff/Hyr family of adhesion proteins have been shown to be important in cell-cell and cell-surface adhesion maintenance [74].

Adhesion is followed by biofilm development, which includes changes in morphology, increase in biomass and secretion of extracellular matrix. Filamentous morphology provides support and structural integrity to the biofilm in addition to providing a scaffold for yeast cell attachment [75]. Mutants defective in hyphae production for example were shown to be defective in biofilm formation [76]. The extracellular matrix is essential for biofilm development and maturation. *C. albicans* matrix contains 55% exopolysaccharides, most common of which are β-1,6 glucan and α-mannan, which interact to form a mannose glucose complex. A total of 565 different proteins have been identified in the *C. albicans* matrix that constitute 25% of the biofilm matrix. This suggests a non-canonical secretion pathway or the accumulation of proteins after cell death. *C. albicans* biofilms also contain eDNA (5%) in their matrix, it was demonstrated that *C. albicans* eDNA is largely composed of random non-coding sequences. Finally, the matrix has about 15% lipids that are yet to be characterised and studied [77], [78].

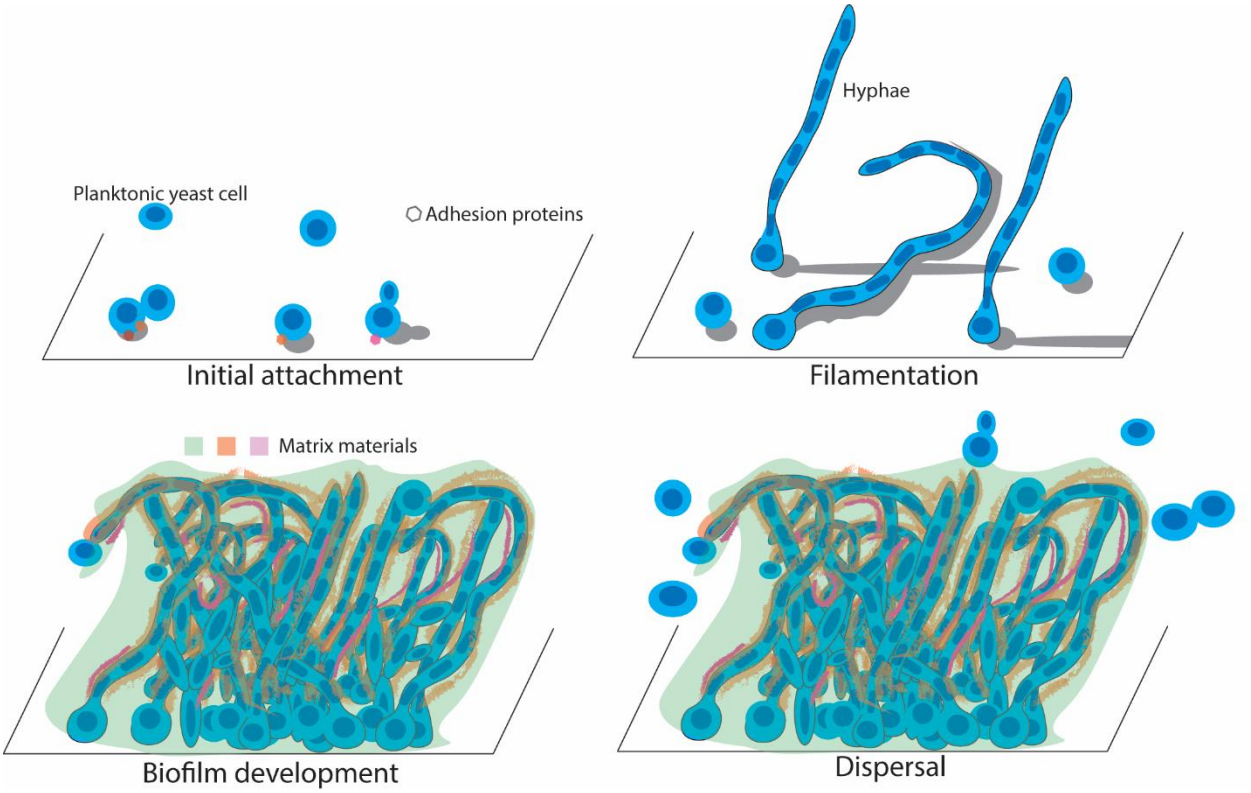

FIG. 9: Diagrammatic representation of biofilm formation by C. albicans. Yeast cells attach to a surface through adhesion proteins followed by filamentation. This is followed by matrix production and cell multiplication. Final step in biofilm formation is dispersal, yeast cells are released from the top layers of the biofilm.

The final piece of biofilm lifestyle is dispersal, where cells are released from mature biofilms into the environment to find a new niche to colonize. The majority of dispersal in *C. albicans* biofilms occurs from the top layers of the biofilm and associated with yeast cells [79]. Additionally, studies of *in vitro* biofilm development indicate that cells are probably dispersed continuously throughout biofilm formation [80]. Although these dispersed cells morphologically resemble the round yeast cells seen in the planktonic mode of growth, they have distinct characteristics. For example, the dispersed cells have increased adherence properties, and have a higher capacity to form biofilms, relative to planktonic cells. Although these dispersed cells morphologically resemble the round yeast cells seen in the planktonic mode of growth, they have distinct characteristics. For example,

the dispersed cells have increased adherence properties, and have a higher capacity to form biofilms, relative to planktonic cells [81].

Transcriptional regulators are DNA binding proteins that regulate transcription; they play pivotal roles in co-regulating target genes that function together to achieve a specific function. A primary study of transcriptional regulators by Nobile et al led to the identification of six master regulators responsible for biofilm formation. The regulators form an elaborate interconnected network, each regulator controlling the other and each target controlled by more than one regulator. The authors present the explanation for the complexity of the circuit as a response to a wide range of environmental cues. Consistent with this idea they provide the example of the regulator Bcr1 that plays an important role in biofilm formation in the catheter model but has less pronounced role in the denture model [82]. Currently it is approximated that there are about 58 transcriptional factors collectively influencing close to 1000 genes involved in different stages of biofilm formation that include filamentation, adhesion, metabolism, and production of matrix [83].

(iii) *Pseudomonas aeruginosa – Candida albicans* interactions and dual species biofilms

In the context of disease microbes usually grow as biofilm communities, these communities are often polymicrobial in nature. Although most natural biofilms are polymicrobial, most of our current knowledge about biofilms comes from study of single species [14], [84]. Interactions between members of different species can alter host responses, virulence and pathogenesis and usually increase the severity of the infection [14]. Examples of human polymicrobial infections include cystic fibrosis lung infections, biomaterials and implants related infections, urinary tract infections and diabetic ulcers. *P. aeruginosa* and *C. albicans* are two opportunistic pathogens often co-isolated from a variety of these human polymicrobial infections[8], [83]–[88].

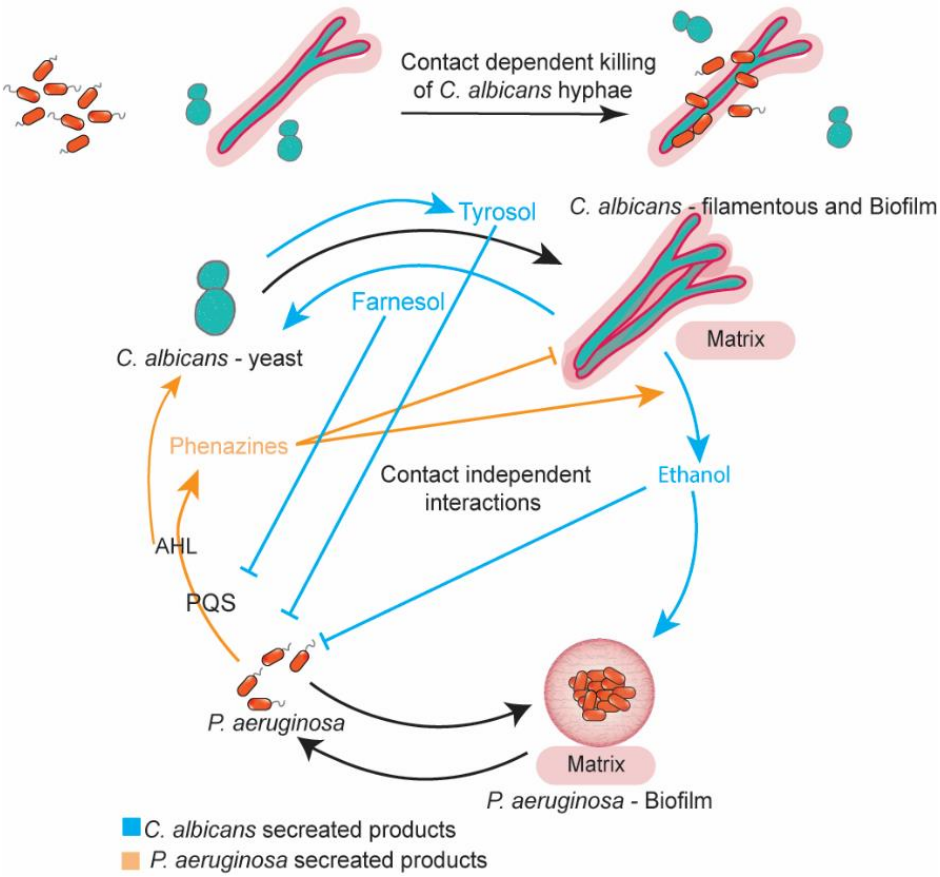

FIG. 10: Diagrammatic representation of microbial interactions between *P. aeruginosa* and *C. albicans*. These interactions include both contact dependent and independent mechanisms.

P. aeruginosa and *C. albicans* have been known to form recalcitrant polymicrobial biofilms that place considerable burden in infections they are involved in, explaining the bulk of research on their interactions (Figure 10). The primary findings reported *P. aeruginosa* killing the *C. albicans* hyphal cells however this did not extend to yeast cells [89]. This effect was further confirmed to be morphology specific, with the bacteria showing extensive attachment to the fungal hyphae. This colocalization and killing has been implicated in nutrient competition, with *P. aeruginosa* using type IV pilli and lectin binding carbohydrates to make the physical association [90]. *P. aeruginosa* has known to secrete acyl-homoserine lactone (AHL) molecule called 3-oxo-C12-HSL a quorum sensing molecule controlled by the *Pseudomonas* quinolone signal (PQS) sensing circuit which can inhibit yeast to hyphal switch [91]. This inhibition compromises *C. albicans* ability to form biofilms. The bacterium also produces a suit of toxins called phenazines, one of which is

pyocyanin. Pyocyanin has been shown to reduce cAM required of biofilm formation and generates ROS both negatively affect the biofilm formation of the fungus [88]. On the contrary, *P. aeruginosa* proteolytic enzymes have been shown to increase *C. albicans* virulence and *in vivo* experiments using a zebrafish model have indicated mutually enhanced virulence of the two species, suggesting that environmental shifts may have strong impacts on the properties of cocultures of these microbes [92].

C. albicans also secretes several factors that have been shown to effect *P. aeruginosa* metabolism and biofilm formation. One such secreted molecule is Farnesol, it can inhibit pyocyanin production and rhamnolipid mediated swarming motility. Farnesol has traditionally been associated with hyphal to yeast transition [93]. Another secreted molecule called Tyrosol which is involved in yeast to hyphal switch has been shown to decrease *P. aeruginosa* virulence [94]. Ethanol is a common fermentation product produced by many bacteria and fungi; it has been shown to influence *P. aeruginosa* in diverse polymicrobial settings. In polymicrobial infections where *P. aeruginosa* coexists with *C. albicans*, exogenous fungal-produced ethanol has been shown to inhibit phenazine production and promote biofilm formation. In addition, ethanol enhances bacterial Pel matrix production and represses surface motility. This is believed to be a feedback loop whereby *C. albicans* produces ethanol, which increases biofilm formation, inhibits swarming motility, and enhances the production of antifungal phenazines on the part of *P. aeruginosa* [95], [96]. Competition for iron is also one of the main antagonistic interactions occurring in *P. aeruginosa*-*C. albicans* infections. Enhanced secretion of *P. aeruginosa* siderophore pyoverdine in mixed species biofilms leads to a decrease in iron availability on *C. albicans* and inhibits yeast growth [97].

1.8 Conclusions and Outlook

Biofilms are surfaced attached groups of microbial cells; they are believed to be the dominant mode of growth for microbial cells. Biofilms have distinct properties in relation to their planktonic counter parts, spatial location of cells especially plays an important role [24]. The spatial proximity of cells in biofilms not only creates a conducive environment for contact dependent interactions but also for contact independent interactions. Most secreted molecules move as a consequence of diffusion and bulk transport, the spatial structure of the population will determine the extent to which these molecules will be consumed by or effect neighbouring cells [43]. Microbial cells are also influenced by the availability of nutrients and environmental factors like shear stress from flow. These factors funnel into changes in metabolism which in turn effect microbial interactions and secreted molecules which ultimately influence biofilm characteristics [38], [39].

In recent years, the number of studies examining microbial interactions in biofilms has increased however, we have only begun to scratch the surface of a very important topic in microbiology. These studies are relevant to multiple microbial environments that include medicine, industry, and biogeocycling, highlighting importance of microbial interactions and their influence on biofilm form and function. One of the challenges of establishing model systems for studying microbial biofilms under controlled, laboratory conditions is to preserve or recreate the relevant microenvironment. Microbial interactions are important at the microscale in biofilms, however most studies on biofilms often lack the microhabitat and spatial information.

Advances in new technologies like microfluidics coupled with microscopy have improved our ability to study a variety of microbial habitats along with providing spatial information at single cell resolution. Nonetheless, there is much to understand about the details of microbial interactions in ecologically relevant niches. Several important questions are yet to be explored. How do microbial interactions shaped by spatial structure, nutrient availability, and other environmental factors and in turn effect their environment? How do specific environments shape microbial spatial structure? What effect does microbial metabolism have on spatial structure? What typical effects do spatial structure have on biofilm function? Using established biofilm models like those of *P. aeruginosa* and *C.*

albicans we can start to answer these questions that will ultimately help us understand the ecological dynamics that occur within biofilms that relate to the compositional changes in community structure and biofilm function.

1.9 References

[1] E. Thursby and N. Juge, "Introduction to the human gut microbiota," *Biochemical Journal*, vol. 474, no. 11, pp. 1823–1836, Jun. 2017, doi: 10.1042/BCJ20160510.

[2] G. J. Dick, K. Anantharaman, B. J. Baker, M. Li, D. C. Reed, and C. S. Sheik, "The microbiology of deep-sea hydrothermal vent plumes: ecological and biogeographic linkages to seafloor and water column habitats," *Front. Microbiol.*, vol. 4, 2013, doi: 10.3389/fmicb.2013.00124.

[3] Y. S. Joung, Z. Ge, and C. R. Buie, "Bioaerosol generation by raindrops on soil," *Nat Commun*, vol. 8, no. 1, p. 14668, Apr. 2017, doi: 10.1038/ncomms14668.

[4] M. J. Wargo and D. A. Hogan, "Fungal—bacterial interactions: a mixed bag of mingling microbes," *Current Opinion in Microbiology*, vol. 9, no. 4, pp. 359–364, Aug. 2006, doi: 10.1016/j.mib.2006.06.001.

[5] R. M. Braga, M. N. Dourado, and W. L. Araújo, "Microbial interactions: ecology in a molecular perspective," *Brazilian Journal of Microbiology*, vol. 47, pp. 86–98, Dec. 2016, doi: 10.1016/j.bjm.2016.10.005.

[6] M. Burmølle, “Interspecific Bacterial Interactions Are Reflected in Multispecies Biofilm Spatial Organization,” *Frontiers in Microbiology*, vol. 7, p. 8, 2016.

[7] N. Weiland-Bräuer, “Friends or Foes—Microbial Interactions in Nature,” *Biology*, vol. 10, no. 6, p. 496, Jun. 2021, doi: 10.3390/biology10060496.

[8] W. H. Bowen, R. A. Burne, H. Wu, and H. Koo, “Oral Biofilms: Pathogens, Matrix, and Polymicrobial Interactions in Microenvironments,” *Trends in Microbiology*, vol. 26, no. 3, pp. 229–242, Mar. 2018, doi: 10.1016/j.tim.2017.09.008.

[9] A. Deveau *et al.*, “Bacterial–fungal interactions: ecology, mechanisms and challenges,” *FEMS Microbiology Reviews*, vol. 42, no. 3, pp. 335–352, May 2018, doi: 10.1093/femsre/fuy008.

[10] K. Drescher, C. D. Nadell, H. A. Stone, N. S. Wingreen, and B. L. Bassler, “Solutions to the Public Goods Dilemma in Bacterial Biofilms,” *Current Biology*, vol. 24, no. 1, pp. 50–55, Jan. 2014, doi: 10.1016/j.cub.2013.10.030.

[11] H. H. Lee, M. N. Molla, C. R. Cantor, and J. J. Collins, “Bacterial charity work leads to population-wide resistance,” *Nature*, vol. 467, no. 7311, pp. 82–85, Sep. 2010, doi: 10.1038/nature09354.

[12] M. E. Hibbing, C. Fuqua, M. R. Parsek, and S. B. Peterson, “Bacterial competition: surviving and thriving in the microbial jungle,” *Nat Rev Microbiol*, vol. 8, no. 1, pp. 15–25, Jan. 2010, doi: 10.1038/nrmicro2259.

[13] “Peptidoglycan from Bacillus cereus Mediates Commensalism with Rhizosphere Bacteria from the Cytophaga-Flavobacterium Group.” https://journals.asm.org/doi/epub/10.1128/AEM.02928-05 (accessed Feb. 27, 2022).

[14] B. M. Peters, M. A. Jabra-Rizk, G. A. O’May, J. W. Costerton, and M. E. Shirtliff, “Polymicrobial Interactions: Impact on Pathogenesis and Human Disease,” *Clinical Microbiology Reviews*, vol. 25, no. 1, pp. 193–213, Jan. 2012, doi: 10.1128/CMR.00013-11.

[15] O. X. Cordero and M. S. Datta, “Microbial interactions and community assembly at microscales,” *Current Opinion in Microbiology*, vol. 31, pp. 227–234, Jun. 2016, doi: 10.1016/j.mib.2016.03.015.

[16] S. Mitri and K. Richard Foster, “The Genotypic View of Social Interactions in Microbial Communities,” *Annu. Rev. Genet.*, vol. 47, no. 1, pp. 247–273, Nov. 2013, doi: 10.1146/annurev-genet-111212-133307.

[17] “Multifaceted Interfaces of Bacterial Competition.” https://journals.asm.org/doi/epub/10.1128/JB.00275-16 (accessed Apr. 02, 2022).

[18] K. R. Foster and T. Bell, “Competition, Not Cooperation, Dominates Interactions among Culturable Microbial Species,” *Current Biology*, vol. 22, no. 19, pp. 1845–1850, Oct. 2012, doi: 10.1016/j.cub.2012.08.005.

[19] “Microbial Competition.” https://www.science.org/doi/10.1126/science.7268409 (accessed Jan. 28, 2022).

[20] R. Axelrod and W. D. Hamilton, “The Evolution of Cooperation,” vol. 211, p. 8, 1981.

[21] S. A. FRANK, “A general model of the public goods dilemma,” *Journal of Evolutionary Biology*, vol. 23, pp. 1245–1250, 2010, doi: 10.1111/j.1420-9101.2010.01986.x.

[22] A. Griffin, S. A. West, and A. Buckling, “Cooperation and competition in pathogenic bacteria,” *Nature*, vol. 430, Aug. 2004.

[23] C. N. Wilder, S. P. Diggle, and M. Schuster, “Cooperation and cheating in Pseudomonas aeruginosa: the roles of the las, rhl and pqs quorum-sensing systems,” *ISME J*, vol. 5, no. 8, pp. 1332–1343, Aug. 2011, doi: 10.1038/ismej.2011.13.

[24] M. E. Davey and G. A. O’toole, “Microbial Biofilms: from Ecology to Molecular Genetics,” *Microbiol. Mol. Biol. Rev.*, vol. 64, no. 4, pp. 847–867, Dec. 2000, doi: 10.1128/MMBR.64.4.847-867.2000.

[25] S. S. Branda, Å. Vik, L. Friedman, and R. Kolter, “Biofilms: the matrix revisited,” *Trends in Microbiology*, vol. 13, no. 1, pp. 20–26, Jan. 2005, doi: 10.1016/j.tim.2004.11.006.

[26] K. Besemer *et al.*, “Biophysical Controls on Community Succession in Stream Biofilms,” *AEM*, vol. 73, no. 15, pp. 4966–4974, Aug. 2007, doi: 10.1128/AEM.00588-07.

[27] O. Ciofu, T. Tolker-Nielsen, P. Ø. Jensen, H. Wang, and N. Høiby, “Antimicrobial resistance, respiratory tract infections and role of biofilms in lung infections in cystic fibrosis patients,” *Advanced Drug Delivery Reviews*, vol. 85, pp. 7–23, May 2015, doi: 10.1016/j.addr.2014.11.017.

[28] C. Delcaru *et al.*, “Microbial Biofilms in Urinary Tract Infections and Prostatitis: Etiology, Pathogenicity, and Combating strategies,” *Pathogens*, vol. 5, no. 4, p. 65, Nov. 2016, doi: 10.3390/pathogens5040065.

[29] H.-C. Flemming, J. Wingender, U. Szewzyk, P. Steinberg, S. A. Rice, and S. Kjelleberg, “Biofilms: an emergent form of bacterial life,” *Nat Rev Microbiol*, vol. 14, no. 9, pp. 563–575, Sep. 2016, doi: 10.1038/nrmicro.2016.94.

[30] H.-C. Flemming and S. Wuertz, “Bacteria and archaea on Earth and their abundance in biofilms,” vol. 17, 2019.

[31] J. T. Boock *et al.*, “Engineered microbial biofuel production and recovery under supercritical carbon dioxide,” *Nat Commun*, vol. 10, no. 1, p. 587, Dec. 2019, doi: 10.1038/s41467-019-08486-6.

[32] A. Silverstein and C. F. Donatucci, “Bacterial Biofilms and implantable prosthetic devices,” *Int J Impot Res*, vol. 15, no. S5, pp. S150–S154, Oct. 2003, doi: 10.1038/sj.ijir.3901093.

[33] L. Hall-Stoodley, J. W. Costerton, and P. Stoodley, “Bacterial biofilms: from the Natural environment to infectious diseases,” *Nat Rev Microbiol*, vol. 2, no. 2, pp. 95–108, Feb. 2004, doi: 10.1038/nrmicro821.

[34] N. Kip and J. A. van Veen, “The dual role of microbes in corrosion,” *ISME J*, vol. 9, no. 3, pp. 542–551, Mar. 2015, doi: 10.1038/ismej.2014.169.

[35] J. Wingender and H.-C. Flemming, “Biofilms in drinking water and their role as reservoir for pathogens,” *International Journal of Hygiene and Environmental Health*, vol. 214, no. 6, pp. 417–423, Nov. 2011, doi: 10.1016/j.ijheh.2011.05.009.

[36] L. Yang, Y. Liu, H. Wu, N. Høiby, S. Molin, and Z. Song, “Current understanding of multi-species biofilms,” *Int J Oral Sci*, vol. 3, no. 2, pp. 74–81, Apr. 2011, doi: 10.4248/IJOS11027.

[37] C. D. Nadell, K. Drescher, and K. R. Foster, “Spatial structure, cooperation and competition in biofilms,” *Nat Rev Microbiol*, vol. 14, no. 9, pp. 589–600, Sep. 2016, doi: 10.1038/nrmicro.2016.84.

[38] J. D. Wheeler, E. Secchi, R. Rusconi, and R. Stocker, “Not Just Going with the Flow: The Effects of Fluid Flow on Bacteria and Plankton,” *Annu. Rev. Cell Dev. Biol.*, vol. 35, no. 1, pp. 213–237, Oct. 2019, doi: 10.1146/annurev-cellbio-100818-125119.

[39] C. D. Nadell, D. Ricaurte, J. Yan, K. Drescher, and B. L. Bassler, “Flow environment and matrix structure interact to determine spatial competition in Pseudomonas aeruginosa biofilms,” *eLife*, vol. 6, p. e21855, Jan. 2017, doi: 10.7554/eLife.21855.

[40] A. Kannan, Z. Yang, M. K. Kim, H. A. Stone, and A. Siryaporn, “Dynamic switching enables efficient bacterial colonization in flow,” *Proc Natl Acad Sci USA*, vol. 115, no. 21, pp. 5438–5443, May 2018, doi: 10.1073/pnas.1718813115.

[41] O. Kroukamp, R. G. Dumitrache, and G. M. Wolfaardt, “Pronounced Effect of the Nature of the Inoculum on Biofilm Development in Flow Systems,” *Appl Environ Microbiol*, vol. 76, no. 18, pp. 6025–6031, Sep. 2010, doi: 10.1128/AEM.00070-10.

[42] R. Martínez-García, C. D. Nadell, R. Hartmann, K. Drescher, and J. A. Bonachela, “Cell adhesion and fluid flow jointly initiate genotype spatial distribution in biofilms,” *PLoS Comput Biol*, vol. 14, no. 4, p. e1006094, Apr. 2018, doi: 10.1371/journal.pcbi.1006094.

[43] “Microbes in flow | Elsevier Enhanced Reader.” https://reader.elsevier.com/reader/sd/pii/S1369527415000387?token=6DEB71EA2AF28

849DE8658D1DDF00D9BDDB2CECD642223973A2ADFBDBDFE9D500044043BC88
96ED251CB9E5334382E07 (accessed Aug. 27, 2020).

[44] P. S. Stewart, “Mini-review: Convection around biofilms,” *Biofouling*, vol. 28, no. 2, pp. 187–198, Feb. 2012, doi: 10.1080/08927014.2012.662641.

[45] B. R. Wucher, T. M. Bartlett, M. Hoyos, K. Papenfort, A. Persat, and C. D. Nadell, “Vibrio cholerae filamentation promotes chitin surface attachment at the expense of competition in biofilms,” *PNAS*, vol. 116, no. 28, pp. 14216–14221, Jul. 2019, doi: 10.1073/pnas.1819016116.

[46] G. H. W. Bowden and Y. H. Li, “Nutritional Influences on Biofilm Development,” *Advances in Dental Research*, 1997, doi: https://doi.org/10.1177/08959374970110012101.

[47] D. C. Yang, K. M. Blair, and N. R. Salama, “Staying in Shape: the Impact of Cell Shape on Bacterial Survival in Diverse Environments,” *Microbiol. Mol. Biol. Rev.*, vol. 80, no. 1, pp. 187–203, Mar. 2016, doi: 10.1128/MMBR.00031-15.

[48] S. J. Salgar-Chaparro, K. Lepkova, T. Pojtanabuntoeng, A. Darwin, and L. L. Machuca, “Nutrient Level Determines Biofilm Characteristics and Subsequent Impact on Microbial Corrosion and Biocide Effectiveness,” *Appl Environ Microbiol*, vol. 86, no. 7, pp. e02885-19, /aem/86/7/AEM.02885-19.atom, Jan. 2020, doi: 10.1128/AEM.02885-19.

[49] P. Stoodley, I. Dodds, J. D. Boyle, and H. M. Lappin-Scott, “Influence of hydrodynamics and nutrients on biofilm structure,” *Journal of Applied Microbiology*, vol. 85, no. S1, pp. 19S-28S, Dec. 1998, doi: 10.1111/j.1365-2672.1998.tb05279.x.

[50] L. R. Mulcahy, V. M. Isabella, and K. Lewis, “Pseudomonas aeruginosa Biofilms in Disease,” *Microb Ecol*, vol. 68, no. 1, pp. 1–12, Jul. 2014, doi: 10.1007/s00248-013-0297-x.

[51] C. K. Lee *et al.*, “Social Cooperativity of Bacteria during Reversible Surface Attachment in Young Biofilms: a Quantitative Comparison of *Pseudomonas aeruginosa* PA14 and PAO1,” *mBio*, vol. 11, no. 1, pp. e02644-19, /mbio/11/1/mBio.02644-19.atom, Feb. 2020, doi: 10.1128/mBio.02644-19.

[52] N. C. Caiazza and G. A. O'Toole, "SadB Is Required for the Transition from Reversible to Irreversible Attachment during Biofilm Formation by *Pseudomonas aeruginosa* PA14," *J Bacteriol*, vol. 186, no. 14, pp. 4476–4485, Jul. 2004, doi: 10.1128/JB.186.14.4476-4485.2004.

[53] R. D. Monds, P. D. Newell, R. H. Gross, and G. A. O'Toole, "Phosphate-dependent modulation of c-di-GMP levels regulates Pseudomonas fluorescens Pf0-1 biofilm formation by controlling secretion of the adhesin LapA," *Mol Microbiol*, vol. 63, no. 3, Feb. 2007, doi: 10.1111/j.1365-2958.2006.05539.x.

[54] D.-G. Ha and G. A. O'Toole, "c-di-GMP and its Effects on Biofilm Formation and Dispersion: a Pseudomonas Aeruginosa Review," p. 12.

[55] K. Ono *et al.*, "cAMP Signaling Affects Irreversible Attachment During Biofilm Formation by *Pseudomonas aeruginosa* PAO1," *Microb. Environ.*, vol. 29, no. 1, pp. 104–106, 2014, doi: 10.1264/jsme2.ME13151.

[56] C. K. Lee *et al.*, "Multigenerational memory and adaptive adhesion in early bacterial biofilm communities," *Proc. Natl. Acad. Sci. U.S.A.*, vol. 115, no. 17, pp. 4471–4476, Apr. 2018, doi: 10.1073/pnas.1720071115.

[57] L. Ma, M. Conover, H. Lu, M. R. Parsek, K. Bayles, and D. J. Wozniak, "Assembly and Development of the Pseudomonas aeruginosa Biofilm Matrix," *PLoS Pathog*, vol. 5, no. 3, p. e1000354, Mar. 2009, doi: 10.1371/journal.ppat.1000354.

[58] L. Friedman and R. Kolter, "Genes involved in matrix formation in Pseudomonas aeruginosa PA14 biofilms," *Molecular Microbiology*, vol. 51, no. 3, pp. 675–690, 2004, doi: 10.1046/j.1365-2958.2003.03877.x.

[59] L. K. Jennings *et al.*, "Pel is a cationic exopolysaccharide that cross-links extracellular DNA in the *Pseudomonas aeruginosa* biofilm matrix," *Proc Natl Acad Sci USA*, vol. 112, no. 36, pp. 11353–11358, Sep. 2015, doi: 10.1073/pnas.1503058112.

[60] C. Reichhardt and M. R. Parsek, "Confocal Laser Scanning Microscopy for Analysis of Pseudomonas aeruginosa Biofilm Architecture and Matrix Localization," *Front. Microbiol.*, vol. 10, p. 677, Apr. 2019, doi: 10.3389/fmicb.2019.00677.

[61] D. J. Wozniak *et al.*, “Alginate is not a significant component of the extracellular polysaccharide matrix of PA14 and PAO1 *Pseudomonas aeruginosa* biofilms,” *Proc. Natl. Acad. Sci. U.S.A.*, vol. 100, no. 13, pp. 7907–7912, Jun. 2003, doi: 10.1073/pnas.1231792100.

[62] C. Reichhardt, C. Wong, D. Passos da Silva, D. J. Wozniak, and M. R. Parsek, “CdrA Interactions within the *Pseudomonas aeruginosa* Biofilm Matrix Safeguard It from Proteolysis and Promote Cellular Packing,” *mBio*, vol. 9, no. 5, pp. e01376-18, /mbio/9/5/mBio.01376-18.atom, Sep. 2018, doi: 10.1128/mBio.01376-18.

[63] S. P. Diggle, R. E. Stacey, C. Dodd, M. Camara, P. Williams, and K. Winzer, “The galactophilic lectin, LecA, contributes to biofilm development in Pseudomonas aeruginosa,” *Environ Microbiol*, vol. 8, no. 6, pp. 1095–1104, Jun. 2006, doi: 10.1111/j.1462-2920.2006.001001.x.

[64] D. Passos da Silva *et al.*, “The Pseudomonas aeruginosa lectin LecB binds to the exopolysaccharide Psl and stabilizes the biofilm matrix,” *Nat Commun*, vol. 10, no. 1, p. 2183, Dec. 2019, doi: 10.1038/s41467-019-10201-4.

[65] J. R. Buzzo *et al.*, “Z-form extracellular DNA is a structural component of the bacterial biofilm matrix,” *Cell*, vol. 184, no. 23, pp. 5740-5758.e17, Nov. 2021, doi: 10.1016/j.cell.2021.10.010.

[66] V. Svarcova, K. Zdenkova, M. Sulakova, K. Demnerova, and J. Pazlarova, “Contribution to determination of extracellular DNA origin in the biofilm matrix,” *J Basic Microbiol*, p. jobm.202100090, May 2021, doi: 10.1002/jobm.202100090.

[67] S. B. Guttenplan and D. B. Kearns, “Regulation of flagellar motility during biofilm formation,” *FEMS Microbiol Rev*, vol. 37, no. 6, pp. 849–871, Nov. 2013, doi: 10.1111/1574-6976.12018.

[68] K. E. Cherny and K. Sauer, “Pseudomonas aeruginosa Requires the DNA-Specific Endonuclease EndA To Degrade Extracellular Genomic DNA To Disperse from the Biofilm,” *J Bacteriol*, vol. 201, no. 18, Sep. 2019, doi: 10.1128/JB.00059-19.

[69] S. R. Schooling, U. K. Charaf, D. G. Allison, and P. Gilbert, “A role for rhamnolipid in biofilm dispersion,” *Biofilms*, vol. 1, no. 2, pp. 91–99, Apr. 2004, doi: 10.1017/S147905050400119X.

[70] B. R. Boles, M. Thoendel, and P. K. Singh, “Rhamnolipids mediate detachment of *Pseudomonas aeruginosa* from biofilms: Rhamnolipid-mediated biofilm detachment,” *Molecular Microbiology*, vol. 57, no. 5, pp. 1210–1223, Sep. 2005, doi: 10.1111/j.1365-2958.2005.04743.x.

[71] J. V. Desai and A. P. Mitchell, “Candida albicans Biofilm Development and Its Genetic Control,” *Microbiology Spectrum*, vol. 3, no. 3, Jun. 2015, doi: 10.1128/microbiolspec.MB-0005-2014.

[72] T. Atriwal *et al.*, “Mechanistic Understanding of Candida albicans Biofilm Formation and Approaches for Its Inhibition,” *Front. Microbiol.*, vol. 12, p. 638609, Apr. 2021, doi: 10.3389/fmicb.2021.638609.

[73] L. L. Hoyer and E. Cota, “Candida albicans Agglutinin-Like Sequence (Als) Family Vignettes: A Review of Als Protein Structure and Function,” *Front. Microbiol.*, vol. 7, Mar. 2016, doi: 10.3389/fmicb.2016.00280.

[74] P. W. J. de Groot, O. Bader, A. D. de Boer, M. Weig, and N. Chauhan, “Adhesins in Human Fungal Pathogens: Glue with Plenty of Stick,” *Eukaryot Cell*, vol. 12, no. 4, pp. 470–481, Apr. 2013, doi: 10.1128/EC.00364-12.

[75] P. J. Cullen and G. F. Sprague, “The Regulation of Filamentous Growth in Yeast,” *Genetics*, vol. 190, no. 1, pp. 23–49, Jan. 2012, doi: 10.1534/genetics.111.127456.

[76] M. L. Richard, C. J. Nobile, V. M. Bruno, and A. P. Mitchell, “Candida albicans Biofilm-Defective Mutants,” *Eukaryotic Cell*, vol. 4, no. 8, pp. 1493–1502, Aug. 2005, doi: 10.1128/EC.4.8.1493-1502.2005.

[77] M. A. Al-Fattani, “Biofilm matrix of Candida albicans and Candida tropicalis: chemical composition and role in drug resistance,” *Journal of Medical Microbiology*, vol. 55, no. 8, pp. 999–1008, Aug. 2006, doi: 10.1099/jmm.0.46569-0.

[78] C. Pierce *et al.*, "The Candida albicans Biofilm Matrix: Composition, Structure and Function," *JoF*, vol. 3, no. 1, p. 14, Mar. 2017, doi: 10.3390/jof3010014.

[79] P. Uppuluri *et al.*, "Dispersion as an Important Step in the Candida albicans Biofilm Developmental Cycle," *PLoS Pathog*, vol. 6, no. 3, p. e1000828, Mar. 2010, doi: 10.1371/journal.ppat.1000828.

[80] G. Wall, D. Montelongo-Jauregui, B. Vidal Bonifacio, J. L. Lopez-Ribot, and P. Uppuluri, "Candida albicans biofilm growth and dispersal: contributions to pathogenesis," *Current Opinion in Microbiology*, vol. 52, pp. 1–6, Dec. 2019, doi: 10.1016/j.mib.2019.04.001.

[81] P. Uppuluri *et al.*, "*Candida albicans* Dispersed Cells Are Developmentally Distinct from Biofilm and Planktonic Cells," *mBio*, vol. 9, no. 4, pp. e01338-18, Sep. 2018, doi: 10.1128/mBio.01338-18.

[82] C. J. Nobile *et al.*, "A Recently Evolved Transcriptional Network Controls Biofilm Development in Candida albicans," *Cell*, vol. 148, no. 1–2, pp. 126–138, Jan. 2012, doi: 10.1016/j.cell.2011.10.048.

[83] N. O. Ponde, L. Lortal, G. Ramage, J. R. Naglik, and J. P. Richardson, "*Candida albicans* biofilms and polymicrobial interactions," *Critical Reviews in Microbiology*, vol. 47, no. 1, pp. 91–111, Jan. 2021, doi: 10.1080/1040841X.2020.1843400.

[84] A. Stacy, L. McNally, S. E. Darch, S. P. Brown, and M. Whiteley, "The biogeography of polymicrobial infection," *Nat Rev Microbiol*, vol. 14, no. 2, pp. 93–105, Feb. 2016, doi: 10.1038/nrmicro.2015.8.

[85] R. C. Costa *et al.*, "Fitting pieces into the puzzle: The impact of titanium-based dental implant surface modifications on bacterial accumulation and polymicrobial infections," *Advances in Colloid and Interface Science*, vol. 298, p. 102551, Dec. 2021, doi: 10.1016/j.cis.2021.102551.

[86] L. M. Filkins and G. A. O'Toole, "Cystic Fibrosis Lung Infections: Polymicrobial, Complex, and Hard to Treat," *PLoS Pathog*, vol. 11, no. 12, p. e1005258, Dec. 2015, doi: 10.1371/journal.ppat.1005258.

[87] J. R. Gaston, A. O. Johnson, K. L. Bair, A. N. White, and C. E. Armbruster, "Polymicrobial Interactions in the Urinary Tract: Is the Enemy of My Enemy My Friend?," *Infect Immun*, vol. 89, no. 4, Mar. 2021, doi: 10.1128/IAI.00652-20.

[88] J. Gibson, A. Sood, and D. A. Hogan, "Pseudomonas aeruginosa-Candida albicans Interactions: Localization and Fungal Toxicity of a Phenazine Derivative," *Applied and Environmental Microbiology*, vol. 75, no. 2, pp. 504–513, Jan. 2009, doi: 10.1128/AEM.01037-08.

[89] D. A. Hogan and R. Kolter, "Interactions: An Ecological Role for Virulence Factors," vol. 296, p. 5, 2002.

[90] A. Brand, J. D. Barnes, K. S. Mackenzie, F. C. Odds, and N. A. R. Gow, "Cell wall glycans and soluble factors determine the interactions between the hyphae of *Candida albicans* and *Pseudomonas aeruginosa*," *FEMS Microbiology Letters*, vol. 287, no. 1, pp. 48–55, Oct. 2008, doi: 10.1111/j.1574-6968.2008.01301.x.

[91] F. J. Reen *et al.*, "The Pseudomonas quinolone signal (PQS), and its precursor HHQ, modulate interspecies and interkingdom behaviour: Quinolone signal molecules modulate interkingdom behaviour," *FEMS Microbiology Ecology*, vol. 77, no. 2, pp. 413–428, Aug. 2011, doi: 10.1111/j.1574-6941.2011.01121.x.

[92] A. C. Bergeron, B. G. Seman, J. H. Hammond, L. S. Archambault, D. A. Hogan, and R. T. Wheeler, "Candida albicans and Pseudomonas aeruginosa Interact To Enhance Virulence of Mucosal Infection in Transparent Zebrafish," *Infect. Immun.*, vol. 85, no. 11, pp. e00475-17, /iai/85/11/e00475-17.atom, Nov. 2017, doi: 10.1128/IAI.00475-17.

[93] G. McAlester, F. O'Gara, and J. P. Morrissey, "Signal-mediated interactions between Pseudomonas aeruginosa and Candida albicans," *Journal of Medical Microbiology*, vol. 57, no. 5, pp. 563–569, May 2008, doi: 10.1099/jmm.0.47705-0.

[94] E. F. Dixon and R. A. Hall, "Noisy neighbourhoods: quorum sensing in fungal-polymicrobial infections: Quorum sensing in fungal infections," *Cellular Microbiology*, vol. 17, no. 10, pp. 1431–1441, Oct. 2015, doi: 10.1111/cmi.12490.

[95] A. I. Chen *et al.*, “Candida albicans Ethanol Stimulates Pseudomonas aeruginosa WspR-Controlled Biofilm Formation as Part of a Cyclic Relationship Involving Phenazines,” *PLoS Pathog*, vol. 10, no. 10, p. e1004480, Oct. 2014, doi: 10.1371/journal.ppat.1004480.

[96] K. A. Lewis *et al.*, “Ethanol Decreases *Pseudomonas aeruginosa* Flagellar Motility through the Regulation of Flagellar Stators,” *J Bacteriol*, vol. 201, no. 18, pp. e00285-19, /jb/201/18/JB.00285-19.atom, May 2019, doi: 10.1128/JB.00285-19.

[97] A. Trejo-Hernández, A. Andrade-Domínguez, M. Hernández, and S. Encarnación, “Interspecies competition triggers virulence and mutability in Candida albicans–Pseudomonas aeruginosa mixed biofilms,” *ISME J*, vol. 8, no. 10, pp. 1974–1988, Oct. 2014, doi: 10.1038/ismej.2014.53.

Chapter 2

Differential Surface Competition and Biofilm Invasion Strategies of *Pseudomonas aeruginosa* PA14 and PAO1

Swetha Kasetty [a], Stefan Katharios-Lanwermeyer [b], George A. O'Toole [b] and Carey D. Nadell [a]

Swetha Kasetty and Stefan Katharios-Lanwermeyer contributed equally to this work.

a Department of Biological Sciences, Dartmouth, Hanover, New Hampshire, USA
b Department of Microbiology and Immunology, Geisel School of Medicine at Dartmouth, Hanover, New Hampshire, USA

Published in Journal of bacteriology 2021; https://doi.org/10.1128/JB.00265-21

Author contributions

S.K-L. and G.A.O. conceived the project. C.D.N. and G.A.O. supervised the project. S.K., S.K-L., G.A.O. and C.D.N. designed experiments. S.K. and S.K-L. performed experiments and image analysis. S.K. S.K-L., G.A.O. and C.D.N. finalized figures. S.K., D.K-L., G.A.O., and C.D.N. wrote the paper.

2.1 Abstract

Pseudomonas aeruginosa strains PA14 and PAO1 are among the two best-characterized model organisms used to study the mechanisms of biofilm formation while also representing two distinct lineages of *P. aeruginosa*. Previous work has shown that PA14 and PAO1 use different strategies for surface colonization; they also have different extracellular matrix composition and different propensities to disperse from biofilms back into the planktonic phase surrounding them. We expand on this work here by exploring the consequences of these different biofilm production strategies during direct competition. Using differentially labeled strains and microfluidic culture methods, we show that PAO1 can outcompete PA14 in direct competition during early colonization and subsequent biofilm growth, that they can do so in constant and perturbed environments, and that this advantage is specific to biofilm growth and requires production of the Psl polysaccharide. In contrast, *P. aeruginosa* PA14 is better able to invade preformed biofilms and is more inclined to remain surface-associated under starvation conditions. These data together suggest that while P. aeruginosa PAO1 and PA14 are both able to effectively colonize surfaces, they do so in different ways that are advantageous under different environmental settings.

2.2 Introduction

Biofilms are surface-attached microbial communities that mediate long-term growth and persistence on substrates as varied as vegetable produce and indwelling medical devices (1, 2). Biofilms are typically polymicrobial in nature and exhibit an increased tolerance to antimicrobial agents, predation, and reactive oxygen species (3–7). The transition from planktonic to biofilm modes of growth is complex and uses signaling systems initiated by surface engagement that have downstream consequences for biofilm formation (8–10). To form a biofilm, motile bacteria such as *Pseudomonas aeruginosa* use appendages including flagella and pili to mediate early surface engagement (11, 12). Surface colonization and growth during biofilm formation are also linked to extracellular polysaccharide (EPS) production, which provides cell-to-surface and cell-cell adhesion (13). For some species, EPS matrix is crucial for early surface attachment (13); matrix material also strongly influences biofilm architecture and structural integrity (14, 15), collective biophysical properties (16–18), and the population dynamics of different strains and species competing for space and resources (19).

Our understanding of biofilm formation comes in part from the study of the PA14 and PAO1 strains of *P. aeruginosa*, a Gram-negative bacterium that forms prolific biofilms in aquatic environments, soils, and clinical settings (20–23). This species uses two distinct signaling systems to initiate biofilm formation (24, 25): the second messenger c-di-GMP, which is regulated through the Wsp system (26–28), and the second messenger cyclic AMP (cAMP), which is regulated through the Pil-Chp/Vfr system (29, 30). Prior work documenting variation in propensity of PAO1 and PA14 to commit to surface attachment have intimated those different strains of *P. aeruginosa* more heavily rely on different components of the signaling pathways controlling biofilm initiation. PAO1, for example, commits to surface attachment and extracellular matrix secretion relatively quickly via the Wsp system-mediated increases in c-di-GMP production (28, 31, 32). PA14 surface commitment control may instead be dominated by signaling via the Pil-Chp system initiated through type IV pili (TFP) engaging a surface, which in turn transmits this surface signal to the adenylate cyclase, CyaB. The activation of CyaB increases concentrations of

cAMP, resulting in production and secretion of cell surface localized PilY1. The PilY1 protein participates in the activation of diguanylate cyclase SadC by an unknown mechanism to enhance c-di-GMP production (30, 33–36).

P. aeruginosa PAO1 and PA14, both isolated from infected wounds (37, 38), represent two distinct lineages based on whole-genome phylogenetic analysis (39). As noted above, they differ in their pattern for committing to surface attachment; their matrix compositions differ as well: both produce Pel, but PAO1 produces a major matrix polysaccharide, Psl, that PA14 lacks (40–42). The overall result is that these two strains exhibit distinct surface association strategies: PAO1 commits relatively quickly to attachment and matrix production after surface contact, while PA14 shows a nonprocessive mode of surface commitment in which cells frequently disengage from surfaces after initial contact while their progeny are primed for subsequent reattachment through a cAMP-dependent signaling pathway (25, 30, 43, 44).

Although PAO1 and PA14 are both heavily studied as models for biofilm formation, there is relatively little work exploring the adaptive rationale for their distinct surface association and biofilm commitment strategies. Biofilm production is very expensive both in terms of metabolic cost and opportunity cost if poorly timed relative to environmental suitability, and the differences in biofilm production strategy between strains and species may often reflect adaptations to different ecological circumstances (45–47). These niche-specific conditions may include, for example, variation in the typical lifetime of a given location patch for growth, the longevity of important nutrient supplies, and whether encountered surfaces are usually bare or already occupied by other bacteria. On the basis of the mechanistic differences in how PAO1 and PA14 control surface attachment and commitment to matrix production, we explore how these two strains compete against each other in model biofilms, studying in particular their population dynamics and spatial structure with respect to each other in coculture versus monoculture. We find that their distinct biofilm production strategies do indeed have significant consequences for the outcome of competition and that PAO1 and PA14 are best suited for surface occupation under different environmental circumstances.

2.3 Results

PAO1 outcompetes PA14 in dual-strain biofilms.

To test if the colonization strategies used by *P. aeruginosa* PA14 or PAO1 impart an advantage during the initial colonization of a clean surface, we used microfluidic devices in which bacteria can be monitored as they attach and grow on glass substrata. To allow for visualization of each strain by fluorescence microscopy, constitutive fluorescent protein expression constructs were introduced, with GFP and mKO-κ inserted at the att site of PAO1 and PA14, respectively (48).

To assess competition during early biofilm formation, PAO1 and PA14 were inoculated into microfluidic chambers in a 1:1 ratio and imaged over 7 h of flow in a buffered minimal medium containing 1.0 mM K2HPO4, 0.6 mM MgSO4, and 0.4% arginine. We measured the fold change in fluorescence for each strain over time normalized to 0 h; PAO1 showed a significant advantage in biomass accumulation over PA14 as early as 4 h after surface inoculation. After 7 h of incubation, the number of PAO1 cells was ~2-fold greater than that of PA14 (Fig. 1A to C).

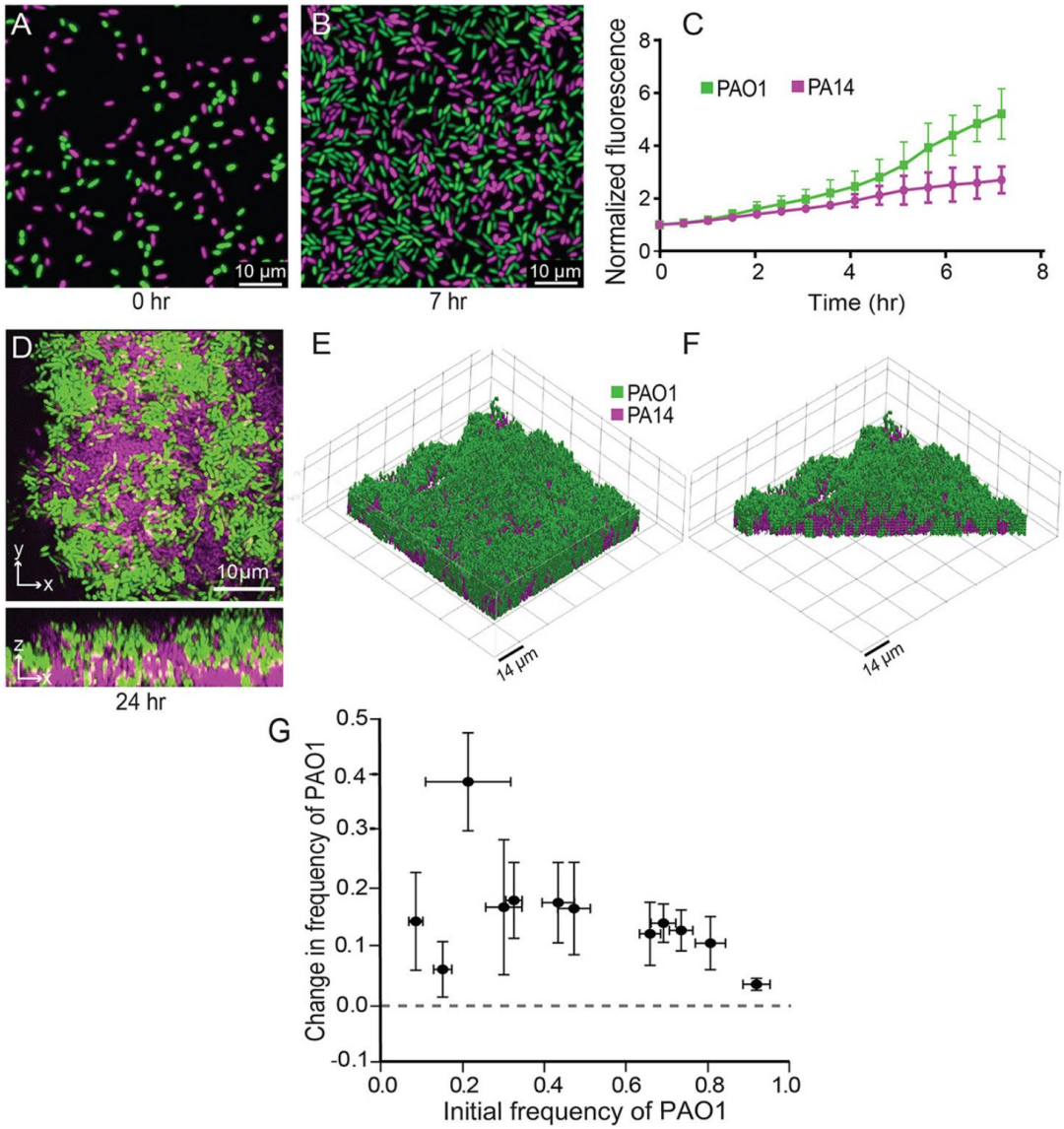

FIG. 1 PA14-PAO1 dual strain biofilm population dynamics. (A, B, and D) Representative widefield fluorescence (A and B) and confocal (D) images of PA14-PAO1 coculture biofilms at the time points indicated under each image. Biofilms were inoculated with a 1:1 mixture of each strain at 0 h. The same color scheme for PAO1 (green) and PA14 (magenta) is used in all panels here and in all figures. (C) Quantification of early surface coverage by each strain (0 to 7 h). $n = 3$, $P < 0.05$ after 5.5 h by 2-way ANOVA with Sidak posttest. (E) 3D rendering of a PA14-PAO1 dual-strain biofilm at 24 h. (F) Cutaway 3D rendering of the same biofilm in panel E, showing its internal structure. (G) Change in frequency of strain WT PAO1 as a function of its initial frequency in dual-strain biofilms with WT PA14. $n = 9$ nonoverlapping image stacks from 4 separate microfluidic devices. Error bars denote the standard deviations

If the observed advantage of PAO1 during biofilm competition was due to enhanced growth rate or antagonistic interactions with PA14 via diffusible secreted factors, one would expect a similar competitive outcome in mixed liquid culture conditions. We tested this possibility by growing planktonic PAO1 and PA14 in glass tubes containing sterile biofilm medium either in monoculture or 1:1 coculture. PAO1 and PA14 grew equally well when cultured separately (see Fig. S1A in the supplemental material), and neither strain outgrew the other in mixed planktonic cultures (Fig. S1B). Notably, the CFU counts of the strains in a coculture were lower by similar measures than their respective CFU counts when grown alone; this indicates neutral competition in which the two strains compete for limited resources in mixed liquid coculture, but neither has an advantage over the other. These results suggest that the advantage in biofilm competition for PAO1 is not due to higher basal growth capacity but rather to other root causes.

Biofilms often exhibit complex architectures that can vary significantly in mixed-strain or mixed-species contexts (49–53); in light of these observations, we next assessed the population dynamics and spatial structure of PAO1 and PA14 allowed to grow for longer periods in biofilm coculture. The two strains were grown together in microfluidic chambers for 24 h and then imaged by confocal microscopy. Consistent with the pattern observed in early-stage biofilms inoculated with a 1:1 ratio of PAO1 and PA14 (Fig. 1A to C), after 24 h PAO1 appeared to overgrow PA14 (Fig. 1D). Z-projections of confocal image stacks revealed that PAO1 grows across the top of the PA14 cell clusters (Fig. 1D to F), consistent with a previous study competing different strains of PAO1 that vary in their matrix production (54).

he above-described data provide evidence that when grown in the biofilm context, PAO1 has an advantage against PA14 during early colonization and 24 h of biofilm growth. Thus far, a 1:1 inoculation ratio of PAO1 to PA14 was used to assess dual-strain population dynamics. This condition does not account for the possibility of frequency-dependent selection, in which the outcome of competition may depend on the initial ratio of the two strains. To test if the competitive advantage of PAO1 was frequency dependent, we varied

the starting PAO1 relative abundance and measured the change in frequency of PAO1 versus PA14 after 24 h. Regardless of the starting conditions, PAO1 consistently increased in frequency over PA14 (Fig. 1G), and PA14 biovolume accumulation was suppressed in coculture with PAO1 relative to when PA14 was cultivated on its own (Fig. S2A and B). The pattern shown in Fig. 1G is characteristic of uniform positive selection that would ultimately lead to complete displacement of PA14 by PAO1 during successive rounds of biofilm competition. We also tested whether changes in initial surface colonization density might affect these population dynamics and found that they did not (Fig. S2C). We conclude from these experiments that under the flow conditions used here, PAO1 outcompetes PA14 in a frequency- and density-independent fashion.

Psl is required for PAO1 to outcompete PA14 in biofilm competition.

We have provided evidence that PAO1 robustly outcompetes PA14 when both are grown together in biofilms under flow. To clarify the mechanism of these dynamics, we attempted to alter the competition outcome by manipulating the biofilm formation capacity of PAO1 or PA14. P. aeruginosa produces three extracellular polysaccharides (EPS) known to facilitate biofilm formation: Pel, Psl, and alginate (55). Alginate is broadly conserved in pseudomonads but only conditionally expressed in PAO1 and PA14 during periods of stress (41, 56, 57) and was shown previously to not contribute to in vitro biofilm formation by these strains (41). PAO1 and PA14 both produce Pel, while Psl is unique to PAO1 (58, 59). Previous work has also shown that Psl is a cooperative resource among secreting cells but that cells that do not produce it are excluded and outcompeted in a PAO1 background (54). We hypothesized that Psl provides an advantage for PAO1 not afforded to PA14 and tested a PAOl mutant with a clean deletion of the psl promoter (referred to as the PAO1 Δpsl mutant here) against PA14 during biofilm growth. Loss of Psl production eliminated the competitive advantage of PAO1 in biofilm coculture with PA14, and indeed the PAO1 Δpsl mutant decreased in relative abundance by over 40% in chambers inoculated with a 1:1 mixed culture (Fig. 2; see Fig. S3A for absolute initial and final frequency data). This result was entirely explained by the dynamics of competition during biofilm growth between PAO1 and the PAO1 Δpsl mutant rather than differences in colonization of the

glass at the start of the experiment (Fig. S3A). As a baseline control, we also competed WT PAO1 against the PAO1 Δpsl strain, which recapitulated earlier work showing that WT PAO1 overgrows and outcompetes its isogenic Δpsl deletion mutant (Fig. S3B and C) (54).

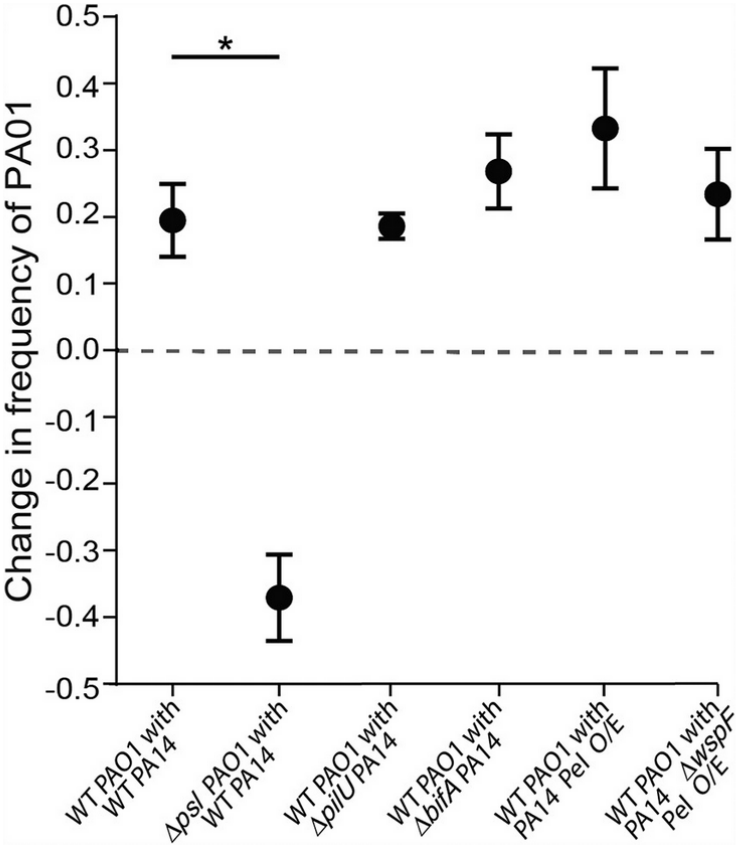

FIG. 2 Competitive dynamics of PAO1 and PA14 with altered piliation or matrix production capacity. This figure reports the change in frequency of WT PAO1 and the PAO1 Δpsl mutant in coculture biofilms with WT PA14 as well as the change in frequency of WT PAO1 in a dual-strain biofilms with PA14ΔpilU, PA14 ΔbifA, and Pel-overproducing strains (Pel O/E) supplemented with arabinose. Biofilms were inoculated with a 1:1 mixture of each strain pair (n = 9 to 18 nonoverlapping image stacks from 4 to 6 separate microfluidic chambers). Error bars denote the standard deviations; Wilcoxon signed-rank tests with Bonferroni correction were used for pairwise comparisons; *, $P < 0.05$; all other comparisons were not significant.

We next explored whether the inverse manipulation of increasing PA14 biofilm production capacity could allow it to better compete against WT PAO1. First, we took advantage of the observation that type 4 pili (T4P) have been shown to mediate initial attachment by P. aeruginosa (12), and recent work showed that manipulation of T4P functions may enhance surface commitment by PA14 (44). Specifically, we tested if the PA14 ΔpilU mutant, which is hyper-piliated, shows high constitutive cAMP signaling, and rapidly colonizes surfaces, would gain a competitive advantage when grown in a biofilm with PAO1. This was not the case; the PA14 ΔpilU mutant was outcompeted by PAO1 by a margin comparable to that of wild-type (WT) PA14 (Fig. 2). Taking note of the absolute initial and final frequency data (Fig. S3A), whereas all other strain pairs initially colonized the chamber glass surfaces at ~1:1, reflecting the 1:1 mixed liquid cultures introduced to the microfluidic chambers to initiate these experiments, the ΔpilU PA14 strain was outcompeted by PAO1 even at this initial colonization stage. Against the ΔpilU PA14 mutant, PAO1 was overrepresented on the surface after the inoculation period from a 1:1 mixed liquid culture and subsequently increased in relative abundance even further (compare red and blue data points in Fig. S3A).

Next, having shown that Psl plays an important role in the PAO1 strain's ability to compete against PA14, we reasoned that PA14 might gain an advantage, or at least mitigate its disadvantage, through hyperinduction of its primary matrix polysaccharide, Pel. To test this hypothesis, we first used a ΔbifA mutant, which we showed previously displays increased c-di-GMP signaling and enhanced Pel polysaccharide production (60), but the PA14 ΔbifA mutant was not any more successful against PAO1 than WT PA14. As an alternative approach, we next used a strain that expresses the pel operon under the control of an arabinose-inducible promoter (designated Pel O/E). Interestingly, while induction of pel expression with 0.2% arabinose increased biofilm accumulation of this strain in monoculture (Fig. S3D), its competitive ability under either arabinose condition was not enhanced relative to that of WT PA14 when grown with PAO1 (Fig. 2). Finally, we used a variant of the Pel O/E strain that also overproduced c-di-GMP due to a mutation in the

wspF gene (designated Pel O/E ΔwspF); again, this strain, when induced with 0.2% arabinose, did not show enhanced fitness against PAO1 compared to the PA14 parent strain (Fig. 2) despite enhanced biomass in monoculture (Fig. S3D). Taken together, these data show that Psl production is a key factor allowing PAO1 to outcompete PA14 and that enhancing PA14 biofilm production via several different strategies does not mitigate PA14's disadvantage against Psl-producing PAO1 during biofilm formation.

PAO1 outcompetes PA14 during dispersal from one patch to another.

Competition for access to space and nutrients in one location is important for evolutionary fitness, as is the ability, when required, to disperse to new locations for future growth (61). Bacteria that commit strongly to biofilm production in a given location may experience a trade-off in their ability to disperse to new locations (45, 62), so we explored whether introduction of a simulated dispersal regime influences the outcome of competition between PA14 and PAO1. We grew a 1:1 mixture of PA14 and PAO1 in microfluidic chambers under flow for 20 h, after which we introduced a dispersal stage. For each such event, the outflow tube from the first microfluidic chamber was attached to a second, clean chamber, and the biofilm effluent was used to seed the downstream chamber for 2 h. The goal was to imitate the natural transition of *P. aeruginosa* from an existing biofilm to a new environment with an intervening planktonic phase (Fig. 3A, top).

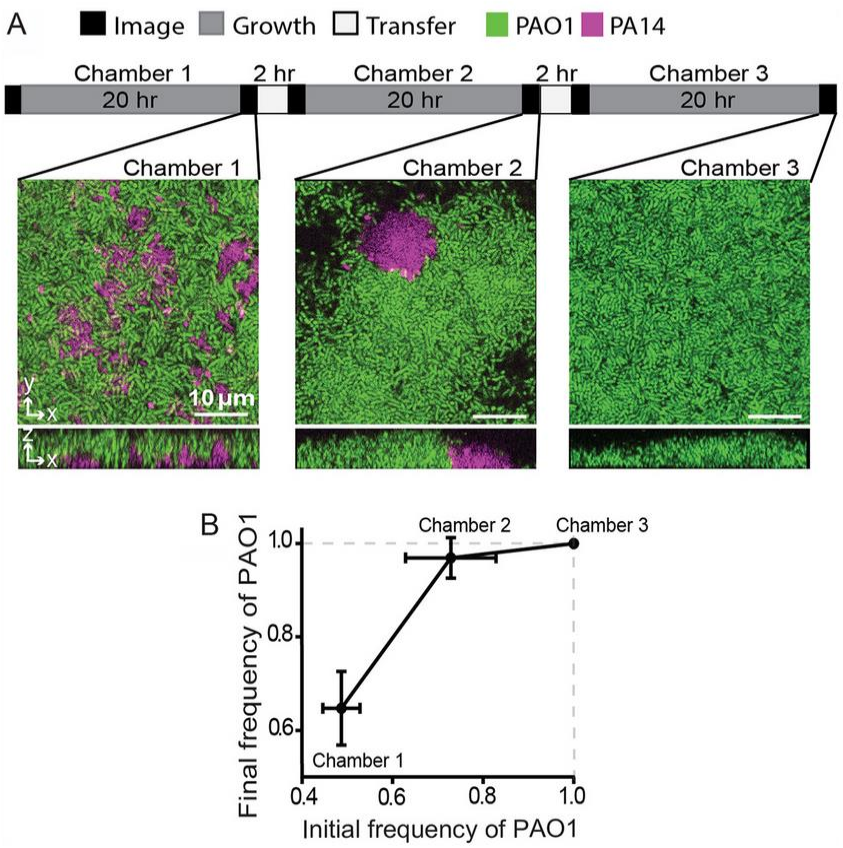

FIG. 3 PAO1 outcompetes PA14 in a dispersal regime. (A) Graphical summary of dispersal experiment regime (top) and representative images of biofilms in serially inoculated chambers (bottom). (B) The frequency of PAO1 in dispersal experiments through serially inoculated chambers with intervening 20-h incubations. All error bars denote standard deviations (n = 9 nonoverlapping image stacks from 4 separate microfluidic chambers).

In biofilms coinoculated 1:1 with PAO1 and PA14, PAO1 accounted for ~70% of the population at the end of the 20-h incubation (Fig. 3A and B), consistent with experiments in the sections described above. Following the first transfer to a new chamber and 20 h of incubation, PAO1 rose in relative abundance to an average of 97% of the total population. After the second transfer and 20 h of incubation, PAO1 had reached fixation; that is, it comprised 100% of the population in all sample image stacks (Fig. 3A and B). These data indicate that PAO1 suffers no disadvantage during dispersal steps and, as predicted by the population dynamics data in Fig. 1H, drives the PA14 strain entirely out of coinoculated biofilms after successive rounds of biofilm competition punctuated by dispersal events.

The results reflect the net outcome of competition during surface colonization, subsequent biofilm growth, dispersal into the effluent liquid phase, recolonization of downstream sites, and new rounds of biofilm growth.

It is possible that in the experiments described above, PA14 dispersal out of biofilms incubated for 20 h was blocked due to PAO1 overgrowing and locking PA14 into place in the lower layers of the cocultured biofilms. We assessed this possibility by repeating the serial chamber inoculation experiment described above, but we allowed for only 3 h of incubation before each dispersal event. We chose 3-h incubations because PAO1 could not overgrow PA14 in this short of an interval. As there were relatively few cells departing the chambers after 3 h of coculture incubation, too few cells were found on the surface of downstream chambers to reliably quantify, so we instead calculated the strain frequencies observed in chambers after 3 h of incubation and then inoculated new chambers with the same strain frequencies but at ~500-fold higher density. With this experimental regimen, PAO1 was again found to increase in frequency from one chamber to the next but had not yet reached 100% of the population by the end of the experiment (Fig. S4). Therefore, shortening the biofilm incubation periods between chamber transfers did not alter the qualitative result that PAO1 consistently displaces PA14, but it did slow the speed at which PAO1 does so.

Differential response of PAO1 and PA14 in biofilms subject to starvation.

The experiments described in the previous section suggest that PAO1 exceeds PA14 in its dispersal during simulated disturbance events in which the cells leaving an existing biofilm under normal flow conditions must colonize a new location. Disturbance events can be more concrete, for example, when nutrient supplies are suddenly cut off at a given location due to depletion or change in flow conditions. Indeed, nutrient supply in many natural environments may more often occur in transient bursts rather than continuously. Considering these factors, we explored how PAO1 and PA14 in coculture biofilms would

react to carbon starvation. We grew dual-strain biofilms for 12 h and then changed the influent flow to a carbon-free (but otherwise equivalent) biofilm medium for 4 h. Following the switch to nutrient-depleted medium flow, PA14's surface coverage reduced by 5%, while that of PAO1 decreased by 40% (Fig. 4A, B, and E). To see if this result would hold for larger biofilms incubated for longer periods prior to starvation, we repeated this experiment after allowing the coinoculated biofilms to grow for 24 h. Once again, the total amount of PA14 remained nearly unchanged following starvation, while that of PAO1 decreased in this case by nearly 60% (Fig. 4C, D, and F).

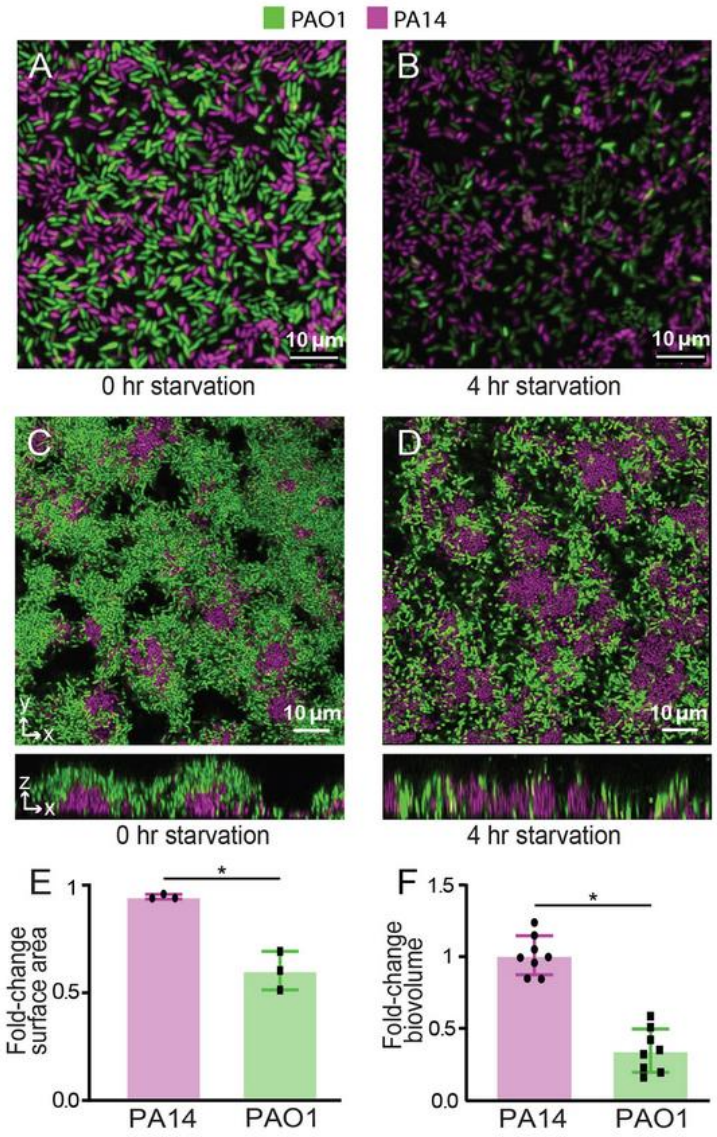

FIG. 4 Responses of biofilm-dwelling PAO1 and PA14 to nutrient depletion. Coculture biofilms of PAO1 and PA14 were grown for 12 h or 24 h and deprived of their carbon source (arginine) for 4 h. The surface area occupied by PAO1 and PA14 in 12-h-old biofilms (coinoculated at 1:1) was measured before (A) and after (B) carbon deprivation. (E) Fold changes in surface area occupied by each strain are shown. The total biovolumes of PAO1 and PA14 in 24-h-old biofilms (coinoculated at 1:1) were assessed before (C) and after (D) carbon deprivation. (F) Fold changes in the biovolume of each strain are shown. Error bars denote standard deviations (n = 3 for panel E; n = 8 nonoverlapping image stacks from 4 separate microfluidic chambers for panel F). Error bars denote the standard deviations. Wilcoxon signed-rank tests with Bonferroni correction were used for pairwise comparisons; *, $P < 0.05$.

To clarify whether cell death was occurring in biofilms following carbon depletion, we repeated these experiments once again, growing 1:1 coculture biofilms of PA14 and PAO1 for 24 h prior to starvation; in this case, the starvation media lacking carbon also contained propidium iodide (PI), whose diffusion into cells is an indicator of compromised membrane integrity and cell death. We found no PI staining until 3 h after the switch to carbon-free media, with somewhat more cell death in PA14 than PAO1 (Fig. S5A). A similar result was reflected in the cells collected from the liquid effluent of the chambers for the full duration of the starvation treatment (Fig. S5B).

These data and those of the previous section suggest that PAO1 is more inclined to disperse from existing cell monolayers and from biofilms several cell layers in depth, during both continual influx of carbon-replete media and following a sudden loss of a carbon source. PA14 is slower to commit to biofilm production but also more inclined to stay in place if nutrient supplies are cut off for short periods.

PA14 is more proficient than PAO1 at invading resident biofilms.

The data described above suggest that PAO1 is proficient at outcompeting PA14 during early surface colonization and subsequent biofilm growth as well as during successive rounds of serially connected new locations to inhabit. Following nutrient deprivation, PA14 mostly retains its occupied surface, while PAO1 is more inclined to disperse. So far,

all experimental regimes in the preceding sections have challenged the two strains to colonize and compete in previously unoccupied locations, but in more natural contexts one might imagine that colonizing bacteria instead encounter surfaces that are already occupied by other strains and species. Our next experiments were designed to assess the relative abilities of PA14 and PAO1 to invade preexisting biofilms of the other strain.

Here, we grew a biofilm of one of the strains in monoculture, which we refer to as the resident strain. After 12 h of growth of the resident strain, we introduced the second strain (the invader) for 4 h to assess its ability to colonize and integrate into the resident biofilm. By visual inspection alone it was evident that PAO1 showed minimal invasion into resident PA14 biofilms (Fig. 5A and B), while PA14 was considerably better able to invade preformed biofilms of PAO1 (Fig. 5C and D). To quantify invasion efficiency by PAO1 and PA14, we measured the fold change in total fluorescence of the invading strain over the 4-h invasion assay. PA14 invades resident PAO1 biofilms rapidly, whereas PAO1 hardly invades resident PA14 biofilms at all (Fig. 5E). In separate experiments that repeated this invasion protocol using resident biofilms that had been incubated for 24 h, we also measured the total biovolume of the invading strain after 4 h. By the end of the assay, PA14 invading biovolume was ~100-fold higher than that of PAO1 invading a resident PA14 biofilm, as measured by confocal microscopy (Fig. 5F).

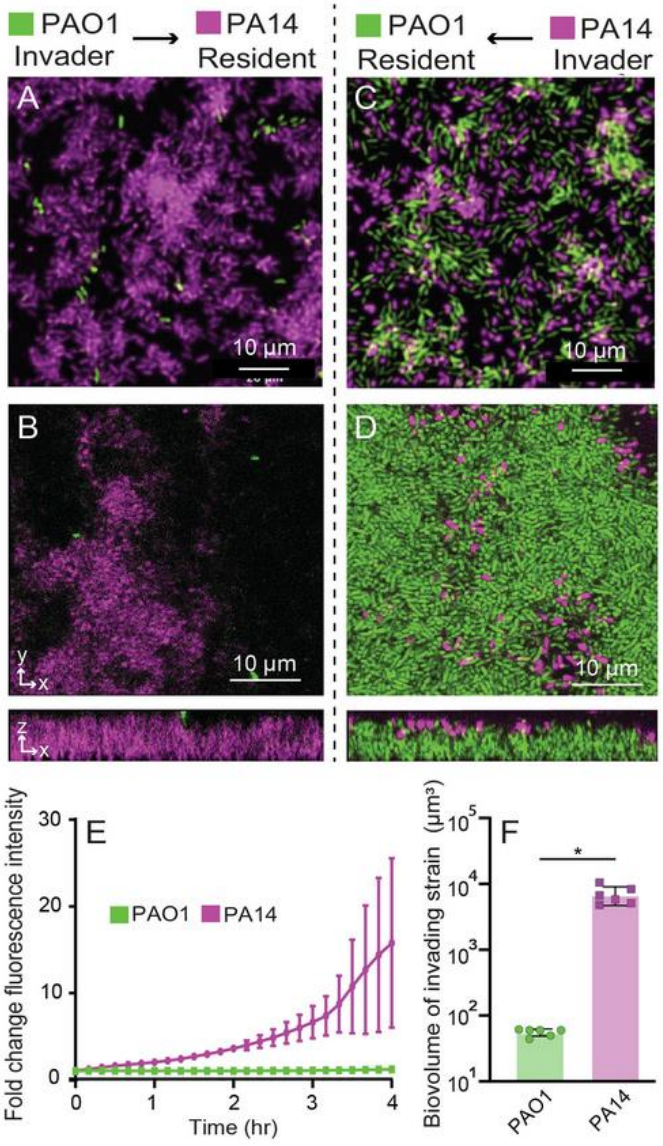

FIG. 5 Reciprocal invasion dynamics of resident biofilms. Resident biofilms of PA14 were grown for 12 h and invaded by PAO1 for 4 h (A, widefield fluorescence image; B, confocal optical section and z-projection). Resident biofilms of PAO1 were grown for 12 h (A, C, and E) or 24 h (B, D, and F) and invaded by PA14 for 4 h (C, widefield fluorescence image; D, confocal optical section and z-projection). (E) The invasion efficiency of PA14 (purple) and PAO1 (green) was measured over time by normalizing the change in fluorescence intensity from the start of the assay through 4 h of invasion. $n = 3$, $P < 0.05$ after 3 h by 2-way ANOVA with Sidak posttest. (F) The total invading strain biovolume of PAO1 and PA14 at the end of the invasion assay ($n = 6$ nonoverlapping image stacks from 4 separate microfluidic chambers). Error bars denote the standard deviations. $P < 0.05$ by Wilcoxon signed-rank test

2.4 Discussion

Biofilms are spatially and physiologically heterogenous environments in which bacteria both cooperate and compete intensely with each other for access to space and resources. Biofilm formation itself is increasingly conceptualized as a core response to ecological competition (19, 63, 64), and here we investigated reference strains *P. aeruginosa* PAO1 and PA14 for their ability to compete with each other in the context of biofilm growth. Long studied as models of biofilm formation, these two strains of *P. aeruginosa* vary substantially in their regulatory mechanisms of surface attachment and compositions of secreted extracellular matrix (16, 25, 42, 44, 65). We show that under microfluidic biofilm culture conditions, PAO1 quickly outcompetes and overgrows PA14 in a density- and frequency-independent manner. PAO1 and PA14 were also found to spatially segregate over 24 h, with PA14 mostly limited to the substratum and PAO1 overgrowing PA14.

That PAO1 begins to outnumber PA14 in the early (2 to 7 h) stages of surface occupation is most likely attributable to the difference in their patterns of surface attachment. Prior work has intimated that PAO1 commits quickly to surface adhesion and extracellular matrix secretion relative to PA14 (25, 44). Following surface colonization, subsequent differences between PAO1 and PA14 in their extracellular matrix begin to contribute to their population dynamics. This interpretation is reinforced by the fact that the competitive advantage of PAO1 is specific to the biofilm mode of growth, during which PAO1 produces matrix containing Pel and Psl, while PA14 only produces Pel. Psl production by PAO1 was essential for its advantage against PA14 under flow and was the dominant controlling factor (of those we examined here) for the outcome of competition; no other physiological manipulation that we tested could alter the outcome of competition between the two.

Others have highlighted Psl production as fundamental to competition in biofilm environments for *P. aeruginosa*, including when isogenic strains are competed against each other (54) and when PAO1 cohabits biofilms with other species, such as *P. protegens* and

Klebsiella pneumoniae (65). Extensive work has explored the relative roles of the Pel and Psl polysaccharides of the P. aeruginosa extracellular matrix (42, 66), indicating that they offer some structural redundancy to one another in strains that can produce both, such as PAO1. There is also evidence that Pel and Psl make different contributions to the viscoelastic properties and spatial structure of Pseudomonas biofilms. Of particular note, Chew *et al.* (16) found that Psl is important for extracellular matrix cross-linking and overall matrix elasticity, strengthening biofilms and promoting microcolony formation extending from basal substrata. Pel, on the other hand, tends to increase biofilm viscosity, encourage streamer formation (67, 68), and facilitate lateral spreading (16). Paralleling the observations we made here, Chew et al. also found that Psl-producing PAO1 formed mixed-species biofilms in which it grew over the top of Staphylococcus aureus, while Psl-deficient PAO1 was less able to overgrow *S. aureus* in coculture (16).

An additional important element of fitness for any biofilm-producing microbe is balancing investment into local competition versus dispersal (69). Previous work has linked relative investment in matrix production to trade-offs in this balance (62). Here, we explored how PAO1 and PA14 disperse in two different ways, measuring the propensity of each to leave biofilms passively during normal flow of nutrient-replete medium and the propensity of each strain to disperse during a starvation event. We found that PAO1 was more prone to dispersal under both conditions. In serially colonized chambers during flow of nutrient-replete medium, PAO1 ultimately displaced the PA14 strain. Under starvation conditions in which we only studied single chambers subjected to nutrient deprivation, we saw that PA14 was far more strongly inclined to stay in place. Thus, PA14 may be more suited to retaining a grip on space it has occupied when nutrients run low, even as some of its population dies under starvation, while PAO1 is more inclined overall to disperse. The relative advantage of staying in place under starvation conditions depends on the prevailing environmental conditions: if local nutrient supply fluctuates, then remaining in place may be the better strategy, but if nutrient supply does not return once depleted, then dispersal will be optimal.

Our final series of experiments showed that PA14 is markedly better able to colonize a previously established biofilm of PAO1 than vice versa, by 2 orders of magnitude, over a relatively short colonization and growth time scale of 4 h. This suggests that PA14 is better suited to exploiting previously colonized environments, while PAO1 is superior in dispersing to and then competing for space and resources on unoccupied surfaces. Recent genomic analysis has found that strains similar to PA14 predominate among CF-derived isolates, while the PAO1-like strains are more likely to be encountered among environmental isolates (70) (noting, though, that the original PA14 and PAO1 isolates both came from wounds). We speculate on the basis of our results that PA14 has evolved a surface occupation strategy best suited to taking advantage of previously colonized surfaces and commitment to staying in place under fluctuating nutrient conditions, while PAO1 is better suited to rapid exploitation of unoccupied surfaces followed by rapid dispersal under nutrient limitation to find new locations for future growth. Due to the enormous diversity of environments in which bacterial biofilms grow, we imagine these are just two among many possible strategies that evolved to optimize surface occupation among Pseudomonas and other bacterial species.

2.5 Material and Methods

Strains and media.

Strains of *P. aeruginosa* are all derivatives of PAO1 or PA14 and were constructed by standard allelic exchange. The biofilm growth substrate was buffered minimal medium containing 1.0 mM K2HPO4, 0.6 mM MgSO4, and 0.4% arginine. Starvation medium omitted arginine and, for the cell death assays, contained propidium iodide at 2 μg/ml.

Microfluidic device assembly.

The microfluidic devices were made by bonding polydimethylsiloxane (PDMS) chamber molds to size number 1.5 cover glass slips (60 mm by 36 mm [length by width]; Thermo-Fisher, Waltham, MA) using standard soft lithography techniques (71). Each PDMS mold contained 4 chambers, each of which measured 3,000 μm by 500 μm by 75 μm (length by width by depth). To establish flow in these chambers, medium was loaded into 1-ml BD

plastic syringes with 25-gauge needles. These syringes were joined to number 30 Cole-Parmer PTFE tubing (inner diameter, 0.3 mm), which was connected to prebored holes in the microfluidic device. Tubing was also placed on the opposite end of the chamber to direct the effluent to a waste container. Syringes were mounted to syringe pumps (Pico plus elite; Harvard Apparatus), and flow was maintained at 0.5 μl/min for all experiments. Note that while this flow rate is 100-fold lower than that used for some other biofilm growth protocols with P. aeruginosa (25), it results in similar average flow velocities through our PDMS microfluidic chambers, which are likewise ~100-fold smaller in cross-sectional area than commercial flow devices like those used in Lee et al. (44).

Biofilm growth.

Overnight cultures of *P. aeruginosa* PAO1 and PA14 were grown at 37°C with shaking in lysogeny broth (LB) prior to the start of biofilm experiments. Cultures were normalized to an optical density at 600 nm (OD600) of 1.0 in KA biofilm medium containing 50 mM Tris-HCl (pH 7.4), 0.6 mM MgSO4, 1.0 K2HPO4, and 0.4% arginine (72). If coculture biofilms were being grown, equal volumes of cultures adjusted to an OD600 of 1.0 were mixed and used as the inoculum for the microfluidic chamber (completely filling its inner volume), and then the bacteria were allowed to rest for 1 h at room temperature to permit cells to attach to the glass surface. For the experiments with varied initial frequencies, after cultures of each strain were adjusted to an OD600 of 1.0, different ratios of the two cultures were added to obtain the desired frequency prior to inoculation. After resting for 1 h to allow surface attachment, the devices were run at 0.5 μl/min at 37°C and imaged by widefield or confocal microscopy (see below) at time intervals that varied per experiment, as noted in Results. At every sampling time point, images were acquired from 3 or more nonoverlapping locations within each biofilm chamber. All experiments were repeated with at least 3 biological replicates with 3 or more technical replicates on different days. Total replicates for each experiment are noted in the figure legends for each data set in the text and supplemental material.

For the serial chamber inoculation experiments, dual-strain biofilms (1:1 initial frequency of PA14 to PAO1) were incubated for 24 h or 3 h (Fig. 3; see also Fig. S4 in the supplemental material), and a 0.5-cm length of tubing was connected to the outlet channel.

At every sampling time point, images were acquired from nonoverlapping locations within each biofilm chamber. The outlet chamber was then allowed to seed a new chamber for 2 h, initiating chamber 2. Chamber 2 was then incubated for 20 h, imaged, and used to seed chamber 3 in a similar manner. The same procedure was performed for the version of this experiment in which biofilms grew for only 3 h prior to being used to seed the next downstream chamber, with one exception. Because very few cells exited chambers incubated for only 3 h, there were too few of them found in the connected downstream chambers to quantify. To compensate for this issue, we quantified the relative abundance of PAO1 and PA14 at the end of chamber 1 after 3 h of incubation and then inoculated a new chamber with the same strain relative abundances, except with about a 500-fold increased density, to allow sufficient biomass to accumulate to determine the relative frequency of each strain at the beginning of biofilm growth in the downstream chamber.

For invasion experiments, we grew the resident biofilm for 12 h at a medium flow rate of 0.5 μl per/min at 37°C, after which we introduced the invading strain (adjusted to an OD600 of 1.0) at the same flow rate for 4 h by switching the chamber inlets to new tubing connected to new syringes containing the invading strain. At every sampling time point, at least 3 images were acquired from nonoverlapping locations within each biofilm chamber. For the version of this experiment for which we used confocal microscopy, we grew resident biofilms for 24 h prior to invasion to ensure that the resident biofilms completely covered the glass substratum before the invading strain was introduced to the chambers.

Microscopy and image analysis.

Biofilms in the microfluidic chambers were imaged using a Zeiss LSM 880 microscope with a 40×/1.2-numeric-aperture (NA) or 10×/0.4 NA water objective (confocal imaging) or a Nikon Eclipse Ti inverted microscope with a Plan Apochromat 100× DM oil objective (widefield imaging). For confocal imaging, a 543-nm laser line was used to excite mKO-κ, and a 488-nm laser line was used to excite GFP; for widefield imaging, mKO-κ and GFP were imaged using standard mCherry and fluorescein isothiocyanate filter sets. All quantitative analysis of confocal microscopy data was performed using BiofilmQ (73). Confocal two-dimensional (2D) sections and Z-projections were generated using Zeiss Zen software, and 3D renderings of biofilms in Fig. 1 were generated using Paraview.

Widefield images were generated using the native Nikon Elements software and analyzed using ImageJ.

Starvation assay.

For the biofilm starvation studies, dual-strain biofilms (1:1 initial frequency of PA14 to PAO1) were incubated for 12 h or 24 h, after which inflow ports were reconnected to new tubing connected to new syringes containing medium identical to the original incubation medium but without the carbon source (arginine). For the version of this experiment with 12-h biofilms, images were taken by widefield microscopy every 10 min for 4 h. For the version of this experiment with 24-h biofilms, images were taken immediately after the start of starvation (0 h) and then once more at the end of the starvation period (4 h). In another version of this experiment for Fig. S5 with 24-h biofilms inoculated with 1:1 PAO1-PA14, propidium iodide was added to the starvation medium (2 μg/ml) that lacked arginine, and images were taken every 1 h for 4 h to monitor propidium iodide uptake by PAO1 and PA14 as a proxy for cell death. Effluent during the course of the 4-h starvation was collected into a 1.5-ml Eppendorf tube on ice (to stop any further cell division). Cells in the effluent were then collected and placed under agar pads for imaging to determine the fraction of dead cells that had dispersed from the biofilm during the starvation treatment.

Statistics.

All statistical analyses were performed in GraphPad Prism. Pairwise comparisons were performed using Wilcoxon signed-rank tests with Bonferroni correction. The comparisons in Fig. 1C and 5E were performed by 2-way analysis of variance (ANOVA) with a Sidak posttest. All error bars indicate standard deviations unless otherwise noted.

2.6 Supplemental figures

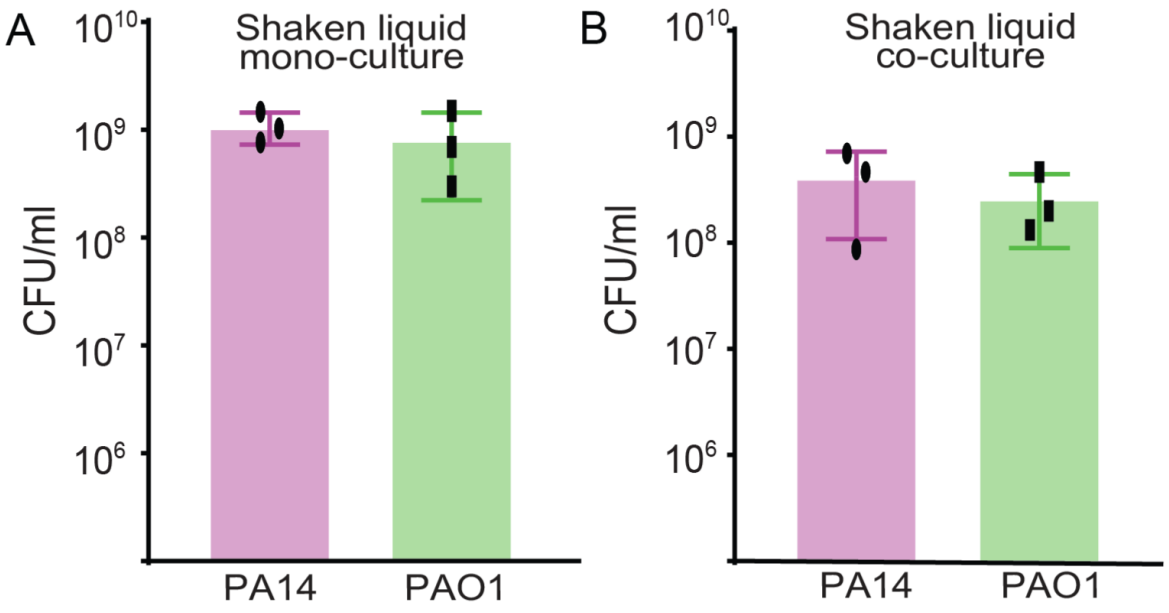

FIG. S1. Well-mixed liquid culture growth comparison of PA14 and PAO1 in monoculture and co-culture. PA14 and PAO1 were back-diluted 1:10 from overnight cultures and allowed to6 regrow into exponential phase for 3 hr prior to being back-diluted once again to OD 600 = 0.057 either on their own (A) or together at a 1:1 starting ratio (B). Population size in stationary phase8 was measured by colony forming unit (CFU) count. n = 3; error bars denote the standard deviation. PAO1 and PA14 were not significantly different from each other in mono-culture or co-culture by10 2-way ANOVA with a Sidak post-test.

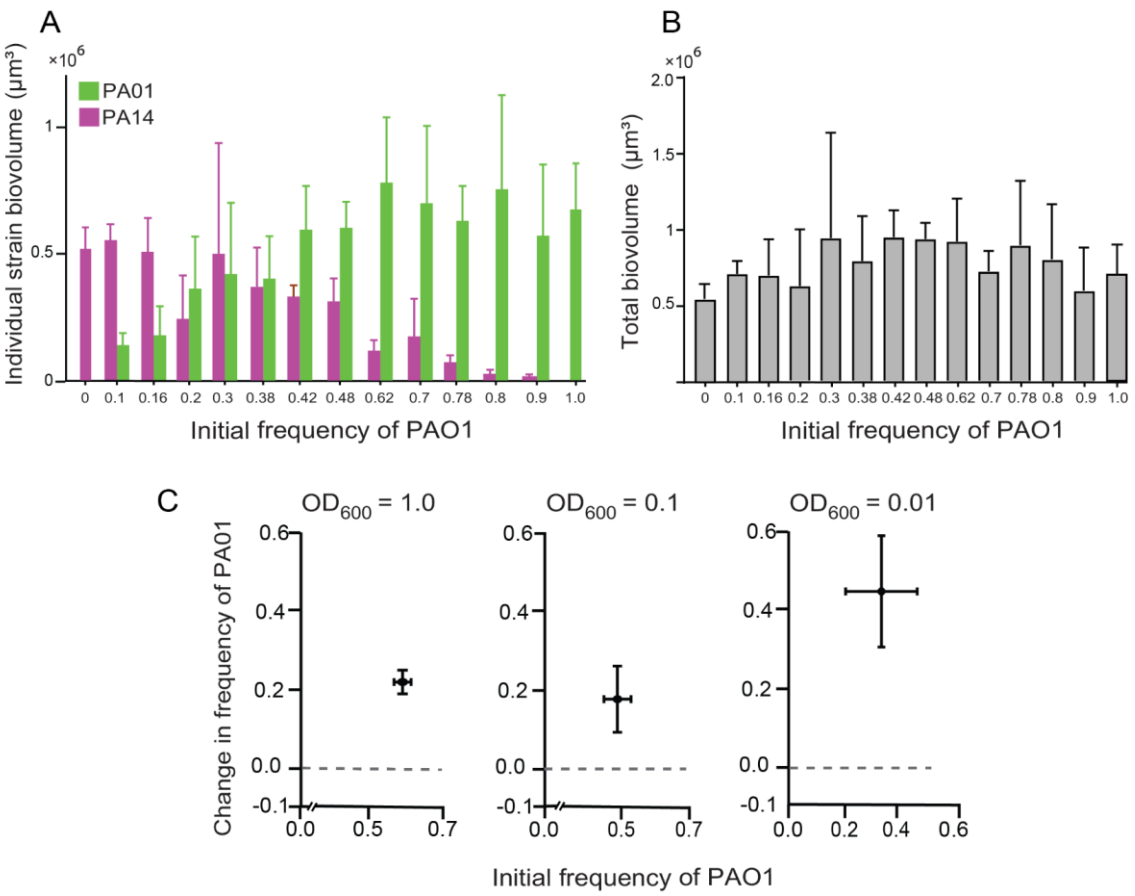

FIG. S2. Absolute growth rate dynamics in biofilm co-cultures of PA14 and PAO1, and tests for density-dependence of the PAO1 biofilm competitive advantage. (A) The biovolume accumulation of PA14 and PAO1 in co-culture from a full spectrum of initial frequencies of the two strains. (B) The total biovolume of both strains from each initial condition in (A). Data from (A) and (B) are the same as those from Figure 1G of the main text, visualized in a different way n = 9 non-overlapping image stacks from 4 separate microfluidic chambers. Error bars denote the standard deviation. (C) Competition between PA14 and PAO1 from approximately 1:1 initial inoculation at three different initial culture densities used for inoculation. For each inoculation density, n = 9 non-overlapping image stacks from 4 separate microfluidic chambers; error bars denote the standard deviation.

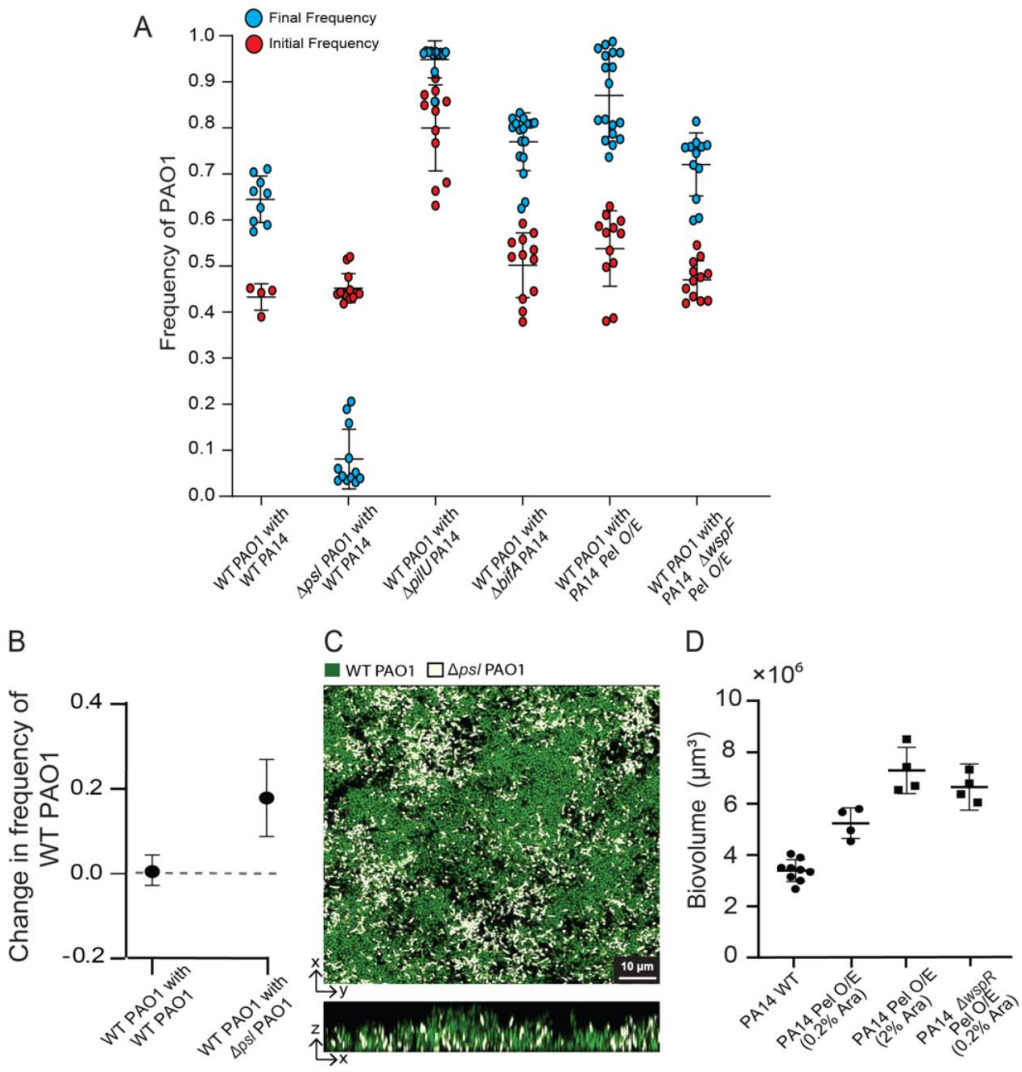

FIG. S3. Control biofilm competition experiments with strain PAO1 and Pel over expression strains of PA14. (A) Absolute initial and final frequencies of PAO1 (and in once case PAO1 Dpsl) against PA14 and isogenic strains with altered piliation or matrix production. The change-in-frequency data in Figure 2 are derived from the final and initial frequencies displayed in this panel. n = 9-18 non-overlapping image stacks from 4-6 separate microfluidic chambers; error bars denote the standard deviation. (B,C) Biofilm competition of PAO1 against itself and against a PAO1 mutant with reduced Psl production. n = 4-9 non-overlapping image stacks from 2-4 separate microfluidic chambers; error bars denote the standard deviation. (D) Biofilm production of PA14 WT in mono-culture and in three strain backgrounds with augmented Pel production by overexpression in trans for Pel, or with the wspR deletion. n = 4-9 non-overlapping image stacks from 2-4 separate microfluidic chambers; error bars denote the standard deviation.

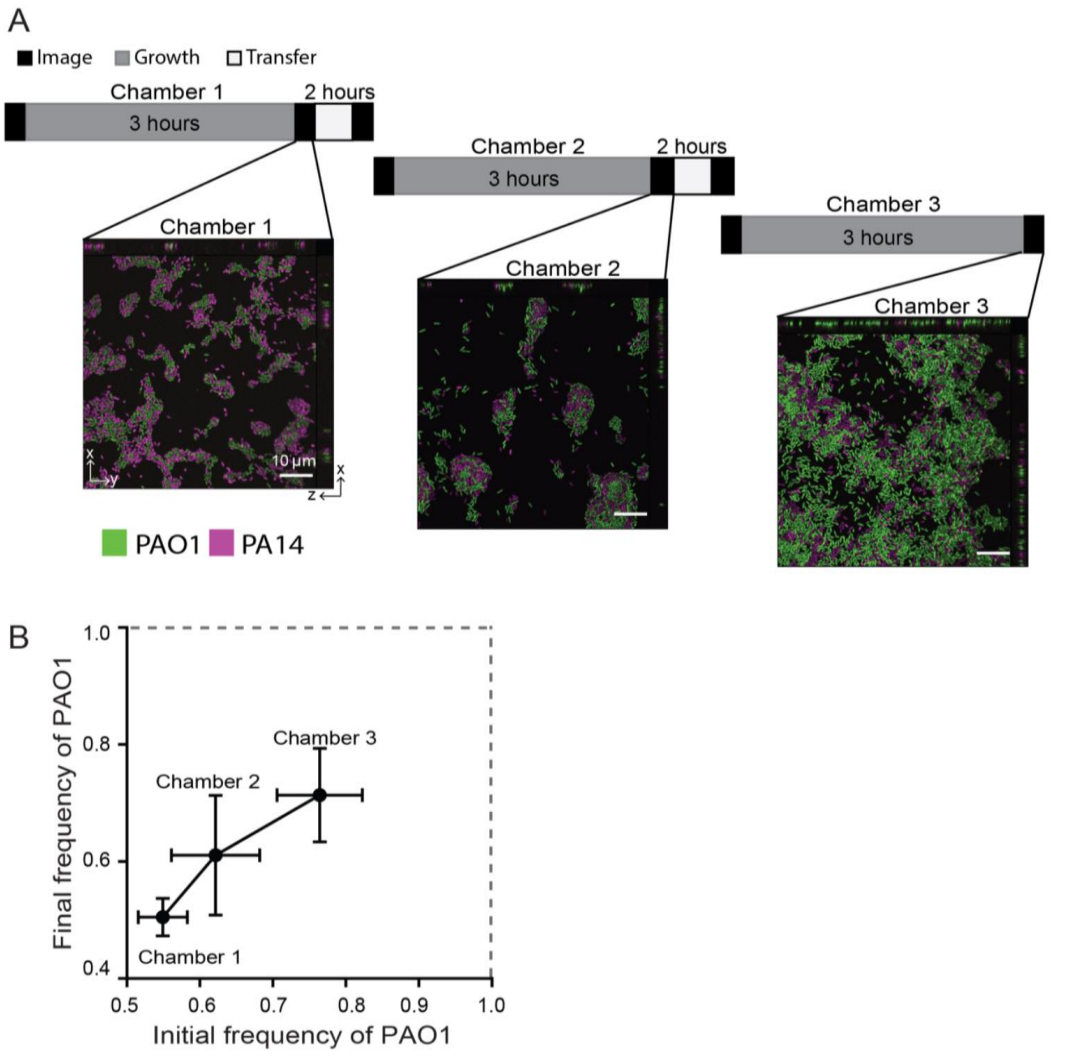

FIG. S4. PAO1 outcompetes PA14 in a high-frequency dispersal regime. (A) Graphical summary of dispersal experiment regime (top) and representative images of biofilms in serially inoculated chambers (bottom). (B) The frequency of PAO1 in dispersal experiments through serially inoculated chambers with intervening 3 hr incubations. All error bars denote standard deviation (n = 9 non-overlapping image stacks from 4 separate microfluidic chambers). Population densities exiting the 3 hr-incubated biofilm chambers were too low to consistently colonize subsequent chambers with sufficient surface coverage. To adjust for this effect, the final frequencies of each strain in chambers following their 3 hr incubation were used to seed downstream chambers, but at higher cell density to obtain sufficient surface coverage for seeding the next chamber's biofilm growth

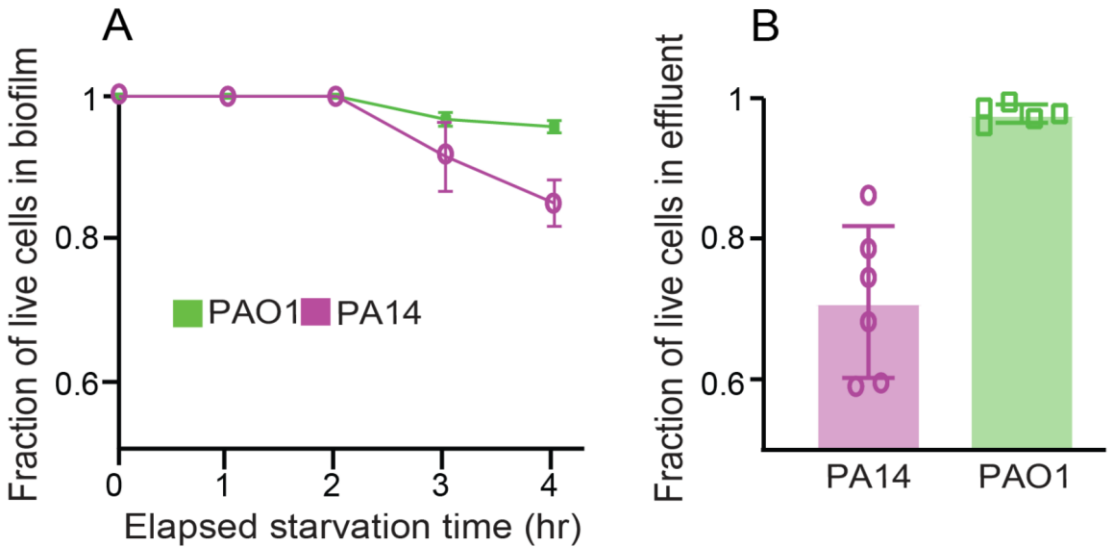

FIG. S5. Tracking cell death following carbon starvation in growing biofilms and dispersed cells in the effluent liquid phase. Biofilms inoculated with a 1:1 mixture of P. aeruginosa PAO1 and PA14 were incubated for 24 h under constant flow, after which the inflow tubing was switched to a new syringe containing carbon-free medium and propidium iodide (2μg/mL) at room temperature. The biofilms were imaged 1/hr for 4 hr, and effluent from these chambers was collected continuously into chilled storage tubes, from which samples were taken for imaging at the end of the experiment. (A) The frequency of living PA14 and PAO1 cells (cell with zero propidium iodide staining) within biofilms undergoing carbon starvation for 4 hr. n = 6 non-overlapping image stacks from 3 separate microfluidic chambers. Error bars denote the standard deviation. (B) The fraction of living PA14 and PAO1 cells in the effluent collected over 4 hr of carbon starvation. Effluent was collected separately for n = 6 independent microfluidic chambers; error bars denote the standard deviation

2.7 References

1.Jahid IK, Ha SD. 2012. A review of microbial biofilms of produce: future challenge to food safety. Food Sci Biotechnol 21:299–316. 10.1007/s10068-012-0041-1.

2.Donlan RM. 2001. Biofilms and device-associated infections. Emerg Infect Dis 7:277–281. 10.3201/eid0702.010226. PubMed.

3.Van Acker H, Van Dijck P, Coenye T. 2014. Molecular mechanisms of antimicrobial tolerance and resistance in bacterial and fungal biofilms. Trends Microbiol 22:326–333. 10.1016/j.tim.2014.02.001. PubMed.

4.Matz C, McDougald D, Moreno AM, Yung PY, Yildiz FH, Kjelleberg S. 2005. Biofilm formation and phenotypic variation enhance predation-driven persistence of Vibrio cholerae. Proc Natl Acad Sci USA 102:16819–16824. 10.1073/pnas.0505350102. PubMed.

5.Gambino M, Cappitelli F. 2016. Mini-review: biofilm responses to oxidative stress. Biofouling 32:167–178. 10.1080/08927014.2015.1134515. PubMed.

6.Vidakovic L, Singh PK, Hartmann R, Nadell CD, Drescher K. 2018. Dynamic biofilm architecture confers individual and collective mechanisms of viral protection. Nat Microbiol 3:26–31. 10.1038/s41564-017-0050-1. PubMed.

7.Wucher BR, Elsayed M, Adelman JS, Kadouri DE, Nadell CD. 2021. Bacterial predation transforms the landscape and community assembly of biofilms. Curr Biol 31:2643–2651. 10.1016/j.cub.2021.03.036. PubMed.

8.Valentini M, Filloux A. 2016. Biofilms and Cyclic di-GMP (c-di-GMP) signaling: lessons from Pseudomonas aeruginosa and other bacteria. J Biol Chem 291:12547–12555. 10.1074/jbc.R115.711507. PubMed.

9.Fong JCN, Yildiz FH. 2008. Interplay between cyclic AMP-cyclic AMP receptor protein and cyclic di-GMP signaling in Vibrio cholerae biofilm formation. J Bacteriol 190:6646–6659. 10.1128/JB.00466-08. PubMed.

10.Passos da Silva D, Schofield MC, Parsek MR, Tseng BS. 2017. An update on the sociomicrobiology of quorum sensing in Gram-negative biofilm development. Pathogens 6:1–9. 10.3390/pathogens6040051.

11.Toutain CM, Caizza NC, Zegans ME, O'Toole GA. 2007. Roles for flagellar stators in biofilm formation by Pseudomonas aeruginosa. Res Microbiol 158:471–477. 10.1016/j.resmic.2007.04.001. PubMed.

12.O'Toole GA, Kolter R. 1998. Flagellar and twitching motility are necessary for Pseudomonas aeruginosa biofilm development. Mol Microbiol 30:295–304. 10.1046/j.1365-2958.1998.01062.x. PubMed.

13.Zhao K, Tseng BS, Beckerman B, Jin F, Gibiansky ML, Harrison JJ, Luijten E, Parsek MR, Wong GCL. 2013. Psl trails guide exploration and microcolony formation in Pseudomonas aeruginosa biofilms. Nature 497:388–391. 10.1038/nature12155. PubMed.

14.Colvin KM, Gordon VD, Murakami K, Borlee BR, Wozniak DJ, Wong GCL, Parsek MR. 2011. The pel polysaccharide can serve a structural and protective role in the biofilm matrix of Pseudomonas aeruginosa. PLoS Pathog 7:e1001264. 10.1371/journal.ppat.1001264. PubMed.

15.Ghafoor A, Hay ID, Rehm BHA. 2011. Role of exopolysaccharides in Pseudomonas aeruginosa biofilm formation and architecture. Appl Environ Microbiol 77:5238–5246. 10.1128/AEM.00637-11. PubMed.

16.Chew SC, Kundukad B, Seviour T, Van der Maarel JRC, Yang L, Rice SA, Doyle P, Kjelleberg S. 2014. Dynamic remodeling of microbial biofilms by functionally distinct exopolysaccharides. mBio 5:e01536-11. 10.1128/mBio.01536-14.

17.Hartmann R, Singh PK, Pearce P, Mok R, Song B, Díaz-Pascual F, Dunkel J, Drescher K. 2019. Emergence of three-dimensional order and structure in growing biofilms. Nat Phys 15:251–256. 10.1038/s41567-018-0356-9. PubMed.

18.Cont A, Rossy T, Al-Mayyah Z, Persat A. 2020. Biofilms deform soft surfaces and disrupt epithelia. Elife 9:1–22. 10.7554/eLife.56533.

19.Nadell CD, Drescher K, Foster KR. 2016. Spatial structure, cooperation and competition in biofilms. Nat Rev Microbiol 14:589–600. 10.1038/nrmicro.2016.84. PubMed.

20.Pellett S, Bigley DV, Grimes DJ. 1983. Distribution of Pseudomonas aeruginosa in a riverine ecosystem. Appl Environ Microbiol 45:328–332. 10.1128/aem.45.1.328-332.1983. PubMed.

21.Green SK, Schroth MN, Cho JJ, Kominos SD, Vitanza-Jack VB. 1974. Agricultural Plants and Soil as a Reservoir for Pseudomonas aeruginosa. Appl Microbiol 28:987–991. 10.1128/am.28.6.987-991.1974. PubMed.

22.Romling U, Wingender J, Muller H, Tummler B. 1994. A major Pseudomonas aeruginosa clone common to patients and aquatic habitats. Appl Environ Microbiol 60:1734–1738. 10.1128/aem.60.6.1734-1738.1994. PubMed.

23.Moreau-Marquis S, Stanton BA, O'Toole GA. 2008. Pseudomonas aeruginosa biofilm formation in the cystic fibrosis airway. Pulm Pharmacol Ther 21:595–599. 10.1016/j.pupt.2007.12.001. PubMed.

24.Armbruster CR, Parsek MR. 2018. New insight into the early stages of biofilm formation. Proc Natl Acad Sci USA 115:4317–4319. 10.1073/pnas.1804084115. PubMed.

25.Pa P, Parsek MR, Toole GAO, Golestanian R, Wong CL. 2020. Social cooperativity of bacteria during reversible surface attachment in young biofilms: a quantitative comparison of Pseudomonas aeruginosa PA14 and PAO1. mBio 11:e02644-19. 10.1128/mBio.02644-19. PubMed.

26.Hengge R. 2009. Principles of c-di-GMP signalling in bacteria. Nat Rev Microbiol 7:263–273. 10.1038/nrmicro2109. PubMed.

27.Jones CJ, Utada A, Davis KR, Thongsomboon W, Zamorano Sanchez D, Banakar V, Cegelski L, Wong GCL, Yildiz FH. 2015. C-di-GMP regulates motile to sessile transition by modulating MshA pili biogenesis and near-surface motility behavior in Vibrio cholerae. PLoS Pathog 11:e1005068. 10.1371/journal.ppat.1005068. PubMed.

28.Güvener ZT, Harwood CS. 2007. Subcellular location characteristics of the Pseudomonas aeruginosa GGDEF protein, WspR, indicate that it produces cyclic-di-GMP in response to growth on surfaces. Mol Microbiol 66:1459–1473. 10.1111/j.1365-2958.2007.06008.x. PubMed.

29.McDonough KA, Rodriguez A. 2011. The myriad roles of cyclic AMP in microbial pathogens: from signal to sword. Nat Rev Microbiol 10:27–38. 10.1038/nrmicro2688. PubMed.

30.Luo Y, Zhao K, Baker AE, Kuchma SL, Coggan KA, Wolfgang MC, Wong GCL, O'Toole GA. 2015. A hierarchical cascade of second messengers regulates Pseudomonas aeruginosa Surface Behaviors. mBio 6:e02456-14. 10.1128/mBio.02456-14. PubMed.

31.O'Connor JR, Kuwada NJ, Huangyutitham V, Wiggins PA, Harwood CS. 2012. Surface sensing and lateral subcellular localization of WspA, the receptor in a chemosensory-like system leading to c-di-GMP production. Mol Microbiol 86:720–729. 10.1111/mmi.12013. PubMed.

32.Hickman JW, Tifrea DF, Harwood CS. 2005. A chemosensory system that regulates biofilm formation through modulation of cyclic diguanylate levels. Proc Natl Acad Sci USA 102:14422–14427. 10.1073/pnas.0507170102. PubMed.

33.Treuner-Lange A, Chang YW, Glatter T, Herfurth M, Lindow S, Chreifi G, Jensen GJ, Søgaard-Andersen L. 2020. PilY1 and minor pilins form a complex priming the type IVa pilus in Myxococcus xanthus. Nat Commun 11:5054. 10.1038/s41467-020-18803-z. PubMed.

34.Kuchma SL, Ballok AE, Merritt JH, Hammond JH, Lu W, Rabinowitz JD, O'Toole GA. 2010. Cyclic-di-GMP-mediated repression of swarming motility by Pseudomonas aeruginosa: the pilY1 gene and its impact on surface-associated behaviors. J Bacteriol 192:2950–2964. 10.1128/JB.01642-09. PubMed.

35.Webster SS, Lee CK, Schmidt WC, Wong GCL. 2020. Fine tuning cyclic-di-GMP signaling in Pseudomonas aeruginosa using the type 4 pili alignment complex. bioRxiv 10.1101/2020.10.17.343988.

36.Persat A, Inclan YF, Engel JN, Stone HA, Gitai Z. 2015. Type IV pili mechanochemically regulate virulence factors in Pseudomonas aeruginosa. Proc Natl Acad Sci USA 112:7563–7568. 10.1073/pnas.1502025112. PubMed.

37.Holloway BW. 1955. Genetic recombination in Pseudomonas aeruginosa. J Gen Microbiol 13:572–581. 10.1099/00221287-13-3-572. PubMed.

38.Holloway BW, Morgan AF. 1986. Genome organization in Pseudomonas. Annu Rev Microbiol 40:79–105. 10.1146/annurev.mi.40.100186.000455. PubMed.

39.Freschi L, Vincent AT, Jeukens J, Emond-Rheault JG, Kukavica-Ibrulj I, Dupont MJ, Charette SJ, Boyle B, Levesque RC. 2019. The Pseudomonas aeruginosa pan-genome provides new insights on its population structure, horizontal gene transfer, and pathogenicity. Genome Biol Evol 11:109–120. 10.1093/gbe/evy259. PubMed.

40.Ryder C, Byrd M, Wozniak DJ. 2007. Role of polysaccharides in Pseudomonas aeruginosa biofilm development. Curr Opin Microbiol 10:644–648. 10.1016/j.mib.2007.09.010. PubMed.

41.Wozniak DJ, Wyckoff TJO, Starkey M, Keyser R, Azadi P, O'Toole GA, Parsek MR. 2003. Alginate is not a significant component of the extracellular polysaccharide matrix of PA14 and PAO1 Pseudomonas aeruginosa biofilms. Proc Natl Acad Sci USA 100:7907–7912. 10.1073/pnas.1231792100. PubMed.

42.Colvin KM, Irie Y, Tart CS, Urbano R, Whitney JC, Ryder C, Howell PL, Wozniak DJ, Parsek MR. 2012. The Pel and Psl polysaccharides provide Pseudomonas aeruginosa structural redundancy within the biofilm matrix. Environ Microbiol 14:1913–1928. 10.1111/j.1462-2920.2011.02657.x. PubMed.

43.Armbruster CR, Lee CK, Parker-Gilham J, de Anda J, Xia A, Tseng BS, Hoffman LR, Jin F, Harwood CS, Wong GCL, Parsek MR. 2019. Heterogeneity in surface sensing produces a division of labor in Pseudomonas aeruginosa populations. Elife 8:1–29. 10.7554/eLife.45084.

44.Lee CK, De Anda J, Baker AE, Bennett RR, Luo Y, Lee EY, Keefe JA, Helali JS, Ma J, Zhao K, Golestanian R, O'Toole GA, Wong GCL. 2018. Multigenerational memory and

adaptive adhesion in early bacterial biofilm communities. Proc Natl Acad Sci USA 115:4471–4476. 10.1073/pnas.1720071115. PubMed.

45.Yan J, Nadell CD, Bassler BL. 2017. Environmental fluctuation governs selection for plasticity in biofilm production. ISME J 11:1569–1577. 10.1038/ismej.2017.33. PubMed.

46.Yawata Y, Nguyen J, Stocker R, Rusconi R. 2016. Microfluidic studies of biofilm formation in dynamic environments. J Bacteriol 198:2589–2595. 10.1128/JB.00118-16. PubMed.

47.Grinberg M, Orevi T, Kashtan N. 2019. Bacterial surface colonization, preferential attachment and fitness under periodic stress. PLoS Comput Biol 15:e1006815. 10.1371/journal.pcbi.1006815. PubMed.

48.Choi KH, Schweizer HP. 2006. mini-Tn7 insertion in bacteria with single attTn7 sites: example Pseudomonas aeruginosa. Nat Protoc 1:153–161. 10.1038/nprot.2006.24. PubMed.

49.Parsek MR, Tolker-Nielsen T. 2008. Pattern formation in Pseudomonas aeruginosa biofilms. Curr Opin Microbiol 11:560–566. 10.1016/j.mib.2008.09.015. PubMed.

50.Teal TK, Lies DP, Wold BJ, Newman DK. 2006. Spatiometabolic stratification of Shewanella oneidensis biofilms. Appl Environ Microbiol 72:7324–7330. 10.1128/AEM.01163-06. PubMed.

51.Burmølle M, Ren D, Bjarnsholt T, Sørensen SJ. 2014. Interactions in multispecies biofilms: do they actually matter? Trends Microbiol 22:84–91. 10.1016/j.tim.2013.12.004. PubMed.

52.Liu W, Jacquiod S, Brejnrod A, Russel J, Burmølle M, Sørensen SJ. 2019. Deciphering links between bacterial interactions and spatial organization in multispecies biofilms. ISME J 13:3054–3066. 10.1038/s41396-019-0494-9. PubMed.

53.Mitri S, Xavier JB, Foster KR. 2011. Social evolution in multispecies biofilms. Proc Natl Acad Sci USA 108(Suppl 2):10839–10846. 10.1073/pnas.1100292108. PubMed.

54.Irie Y, Roberts AEL, Kragh KN, Gordon VD, Hutchison J, Allen RJ, Melaugh G, Bjarnsholt T, West SA, Diggle SP. 2017. The Pseudomonas aeruginosa PSL polysaccharide is a social but noncheatable trait in biofilms. mBio 8:e00374-17. 10.1128/mBio.00374-17. PubMed.

55.Franklin MJ, Nivens DE, Weadge JT, Lynne Howell P. 2011. Biosynthesis of the Pseudomonas aeruginosa extracellular polysaccharides, alginate, Pel, and Psl. Front Microbiol 2:167–176. Crossref. PubMed.

56.Goldberg JB, Gorman WL, Flynn JL, Ohman DE. 1993. A mutation in algN permits trans activation of alginate production by algT in Pseudomonas species. J Bacteriol 175:1303–1308. 10.1128/jb.175.5.1303-1308.1993. PubMed.

57.Sabra W, Kim EJ, Zeng AP. 2002. Physiological responses of Pseudomonas aeruginosa PAO1 to oxidative stress in controlled microaerobic and aerobic cultures. Microbiology (Reading) 148:3195–3202. 10.1099/00221287-148-10-3195. PubMed.

58.Friedman L, Kolter R. 2004. Two genetic loci produce distinct carbohydrate-rich structural components of the Pseudomonas aeruginosa biofilm matrix. J Bacteriol 186:4457–4465. 10.1128/JB.186.14.4457-4465.2004. PubMed.

59.Friedman L, Kolter R. 2004. Genes involved in matrix formation in Pseudomonas aeruginosa PA14 biofilms. Mol Microbiol 51:675–690. 10.1046/j.1365-2958.2003.03877.x. PubMed.

60.Kuchma SL, Brothers KM, Merritt JH, Liberati NT, Ausubel FM, O'Toole GA. 2007. BifA, a cyclic-di-GMP phosphodiesterase, inversely regulates biofilm formation and swarming motility by Pseudomonas aeruginosa PA14. J Bacteriol 189:8165–8178. 10.1128/JB.00586-07. PubMed.

61.McDougald D, Rice SA, Barraud N, Steinberg PD, Kjelleberg S. 2011. Should we stay or should we go: mechanisms and ecological consequences for biofilm dispersal. Nat Rev Microbiol 10:39–50. 10.1038/nrmicro2695. PubMed.

62.Nadell CD, Bassler BL. 2011. A fitness trade-off between local competition and dispersal in Vibrio cholerae biofilms. Proc Natl Acad Sci USA 108:14181–14185. 10.1073/pnas.1111147108. PubMed.

63.Oliveira NM, Oliveria NM, Martinez-Garcia E, Xavier J, Durham WM, Kolter R, Kim W, Foster KR. 2015. Biofilm formation as a response to ecological competition. PLoS Biol 13:e1002191. 10.1371/journal.pbio.1002191. PubMed.

64.Hibbing ME, Fuqua C, Parsek MR, Peterson SB. 2010. Bacterial competition: surviving and thriving in the microbial jungle. Nat Rev Microbiol 8:15–25. 10.1038/nrmicro2259. PubMed.

65.Periasamy S, Nair HAS, Lee KWK, Ong J, Goh JQJ, Kjelleberg S, Rice SA. 2015. Pseudomonas aeruginosa PAO1 exopolysaccharides are important for mixed species biofilm community development and stress tolerance. Front Microbiol 6:851. 10.3389/fmicb.2015.00851. PubMed.

66.Mann EE, Wozniak DJ. 2012. Pseudomonas biofilm matrix composition and niche biology. FEMS Microbiol Rev 36:893–916. 10.1111/j.1574-6976.2011.00322.x. PubMed.

67.Rusconi R, Lecuyer S, Guglielmini L, Stone HA. 2010. Laminar flow around corners triggers the formation of biofilm streamers. J R Soc Interface 7:1293–1299. 10.1098/rsif.2010.0096. PubMed.

68.Drescher K, Shen Y, Bassler BL, Stone HA. 2013. Biofilm streamers cause catastrophic disruption of flow with consequences for environmental and medical systems. Proc Natl Acad Sci USA 110:4345–4350. 10.1073/pnas.1300321110. PubMed.

69.Yawata Y, Cordero OX, Menolascina F, Hehemann J-H, Polz MF, Stocker R. 2014. Competition–dispersal tradeoff ecologically differentiates recently speciated marine bacterioplankton populations. Proc Natl Acad Sci USA 111:5622–5627. 10.1073/pnas.1318943111. PubMed.

70.Ozer EA, Nnah E, DIdelot X, Whitaker RJ, Hauser AR, Ochman H. 2019. The population structure of Pseudomonas aeruginosa Is characterized by genetic isolation of

exoU+ and exoS+ lineages. Genome Biol Evol 11:1780–1796. 10.1093/gbe/evz119. PubMed.

71.Ng JMK, Gitlin I, Stroock AD, Whitesides GM. 2002. Review components for integrated poly (dimethylsiloxane) microfluidic systems. Electrophoresis 23:3461–3473. 10.1002/1522-2683(200210)23:20<3461::AID-ELPS3461>3.0.CO;2-8. PubMed.

72.Collins AJ, Pastora AB, Jarrod Smith T, Dahlstrom K, O'Toole GA. 2020. MapA, a second large RTX adhesin, contributes to biofilm formation by Pseudomonas fluorescens. J Bacteriol 202:e00277-20. 10.1128/JB.00277-20.

73.Hartmann R, Jeckel H, Jelli E, Singh PK, Vaidya S, Bayer M, Rode DKH, Vidakovic L, Díaz-Pascual F, Fong JCN, Dragoš A, Lamprecht O, Thöming JG, Netter N, Häussler S, Nadell CD, Sourjik V, Kovács ÁT, Yildiz FH, Drescher K. 2021. Quantitative image analysis of microbial communities with BiofilmQ. Nat Microbiol 6:151–156. 10.1038/s41564-020-00817-4. PubMed.

Chapter 3

Microscale Biofilm Architecture of *Candida albicans* Biofilms

Swetha Kasetty[1], Jacob Holt[1], David Andes[2], Deborah A. Hogan[3], Carey D. Nadell[1, *]

[1]Department of Biological Sciences, Dartmouth College, Hanover, NH

[2]Division of Infectious Diseases, Departments of Medicine, Microbiology and Immunology School of Medicine and Public Health and School of Pharmacy, University of Wisconsin, Madison, Wisconsin

[3]Department of Microbiology and Immunology, Geisel School of Medicine at Dartmouth, Hanover, NH

Author contributions

C.D.N. and S.K. conceived the project. C.D.N. supervised the project. S.K., and C.D.N. designed experiments. D.A.H. and D.A. provided critical input on experimental design and data interpretation. S.K. performed experiments and image analysis. J.H. provided modeling expertise for Figure 3. S.K. and C.D.N. finalized figures. S.K. and C.D.N. wrote the paper

3.1 Abstract

C. albicans is an opportunistic pathogen found in diverse human niches, including human gut, skin, and medical devices, and can form robust biofilms in all these chemically variable clinical sites. We studied *C. albicans* biofilm characteristics in three distinct nutritional niches – one synthetic and two host niche mimic media. We found that biofilm architecture and properties like morphology, biovolume accumulation, strength of attachment and local biovolume packing were distinct in each nutritional niche. Finally, in experimental methods novel to fungal biofilms, we explored the ability of C. *albicans* cell's ability to integrate into existing biofilms and found that it was dependent of a combination of local biovolume packing and total biovolume.

3.2 Introduction

Candida albicans is a fungal commensal and a common member of the healthy human microbiome [1]. In individuals with a healthy immune system, *C. albicans* can be found in gastrointestinal tract, reproductive tract, oral cavity, and skin, often kept in balance with the surrounding microbial communities. However, changes in the microbiota, host immune system or local environment can enable pathogenic switch in *C. albicans* causing it to overgrow and cause infection [2]. Reversible morphological plasticity between yeast, pseudo hyphal and true hyphal forms is an important virulence factor that facilitates disease establishment and proliferation [3]. In fact, non-filamentous *C. albicans* has been shown

to be avirulent [4]. *C. albicans* can grow as biofilms which are highly structured groups composed of these multiple cell types encased in a self-secreted matrix. These *C. albicans* biofilms are intrinsically resistant to conventional antifungal therapies, host immune defenses, and environmental perturbations, making them a significant clinical challenge [5].

The majority of *C. albicans* infections are associated with its ability to form biofilms. Studies have shown biofilm development to occur in a series of sequential steps. The initial step consists of the attachment of unicellular yeast cells onto a surface forming a foundation of a basal yeast. This is followed by cell proliferation across the surface and filamentation. Filamentation is accompanied by the accumulation of an extracellular polysaccharide matrix [5]. Finally, yeast cells bud off the tips of hyphal cells and are released from the biofilm into the surroundings where they can colonize other surfaces [6]. Dispersion of biofilm-associated cells carries great clinical significance as released cells can initiate formation of new and more virulent biofilms [7].

C. albicans can form robust biofilms in several host nutritional niches during its pathogenic lifestyle. It is most often identified in nosocomial infections capable of invading several host sites from deep tissues and organs to superficial sites [8]. More significantly, *C. albicans* is adept at adhering to catheters and various indwelling medical implants and is also a commonly isolated bloodstream pathogen in hospitalized patients [9]–[11]. The fungus has vast nutritional flexibility allowing it to adapt readily to the nutritional milieu that it encounters. It has an uncommon capability to simultaneously use different carbon sources. This nutritional flexibility is essential for colonization of diverse and complex host niches [12].

C. albicans metabolism in response to nutrient availability has been shown to impact its pathogenic behavior. Metabolic adaptation can impact changes in nutrient assimilation, cell wall remodeling, expression of virulence factors and immune surveillance [13]. There has

been growing evidence of differing degrees of stress resistance and virulence with differing nutrient availability at the molecular scale [14]. However, if and how biofilm architecture and characteristics – an important virulence mechanism in *C. albicans* – vary with respect to available nutrients is not well understood. Further, how external factors like flow and sheer stress effect biofilms in variable nutrient niches affect *C. albicans* biofilms have not been explored.

Using fluorescently labelled *C. albicans* and microfluidic techniques we explore *C. albicans* biofilm formation and architecture in synthetic and biologically relevant mimic media. We show that *C. albicans* biofilm characteristics like morphology, biovolume and strength of attachment are dependent on nutritional environment. We show that the ability of planktonic cells to integrate into existing biofilms was dependent on local biovolume packing and total biovolume. There was greater degree of integration of new strain into existing biofilm in natural human host niches, a potential novel recorded behavior of *C. albicans* virulence that could be the cause of clinically challenging *C. albicans* infection outcomes.

3.3 Results

Biofilm description in synthetic media and host niche mimic media

We aimed to characterize the architecture and properties of *C. albicans* biofilms in the presence of different nutrient profiles. We used RPMI, a synthetic nutrient rich media used for growing and studying *C. albicans* across labs. We compared this with a cystic fibrosis lung environment mimic media – artificial sputum media for confocal imaging (ASMi) [15] – a modified version of the artificial sputum media developed by the Whiteley group [16]- and artificial urine media – two nutritional mimic media of natural host sites where

C. albicans biofilms have been shown to be present and prevalent[17-18]. *C. albicans* was modified by allelic exchange to contain a chromosomal construct for constitutive expression of GFP or mKate2 under the control of pACT promoter[15], [19]. GFP and mKate2 were selected for these studies for their brightness and because they could be easily distinguished by fluorescence microscopy.

To investigate *C. albicans* biofilm growth under flow of RPMI, ASMi and urine media, we inoculated derivatives of strain CAI4 in microfluidic devices (see Materials and Methods). First, the extent of attachment in each media was documented. For this *C. albicans* was grown at 30^{o}C overnight to ensure yeast cell morphology [20], after which OD normalized cells were suspended in the respective media and inoculated into microfluidic chambers. The cells were allowed to attach to the glass cover slip for an hour at 37^{o}C. Confocal images after 1h incubation showed that the amount of biovolume on glass were comparable across the three media (Fig. 1A). Following this flow of media was initiated in the chambers and biofilms were allowed to grow for 24h. Confocal imaging and biovolume quantification showed that there was most biovolume accumulation in RPMI followed by ASMi and the least in urine (Fig. 1B). Interestingly we saw variability in biovolume accumulation and biofilm architecture especially in natural host niche mimic media (Fig. 1B Sup. 1). We hypothesize this type of heterogeneity in total biovolume accumulation and architecture could be characteristic of naturally found *C. albicans* biofilms because of the variability of nutrient profiles in host niches.

Confocal images showed that the RPMI chambers contained highly filamentous and dense biofilms, *C. albicans* looked to contain true hyphae with extensive knitting (Fig. 1Di). ASMi chambers in contract contained majority pseudo hyphae as its filamentous morphology and relatively reduced amount of biovolume (Fig. 1Dii). The biofilms grown in artificial urine had the least amount of biovolume and were also in majority in their true hyphal form, however, the hyphae looked shorter in comparison to those that grew in RPMI (Fig. 1Diii).

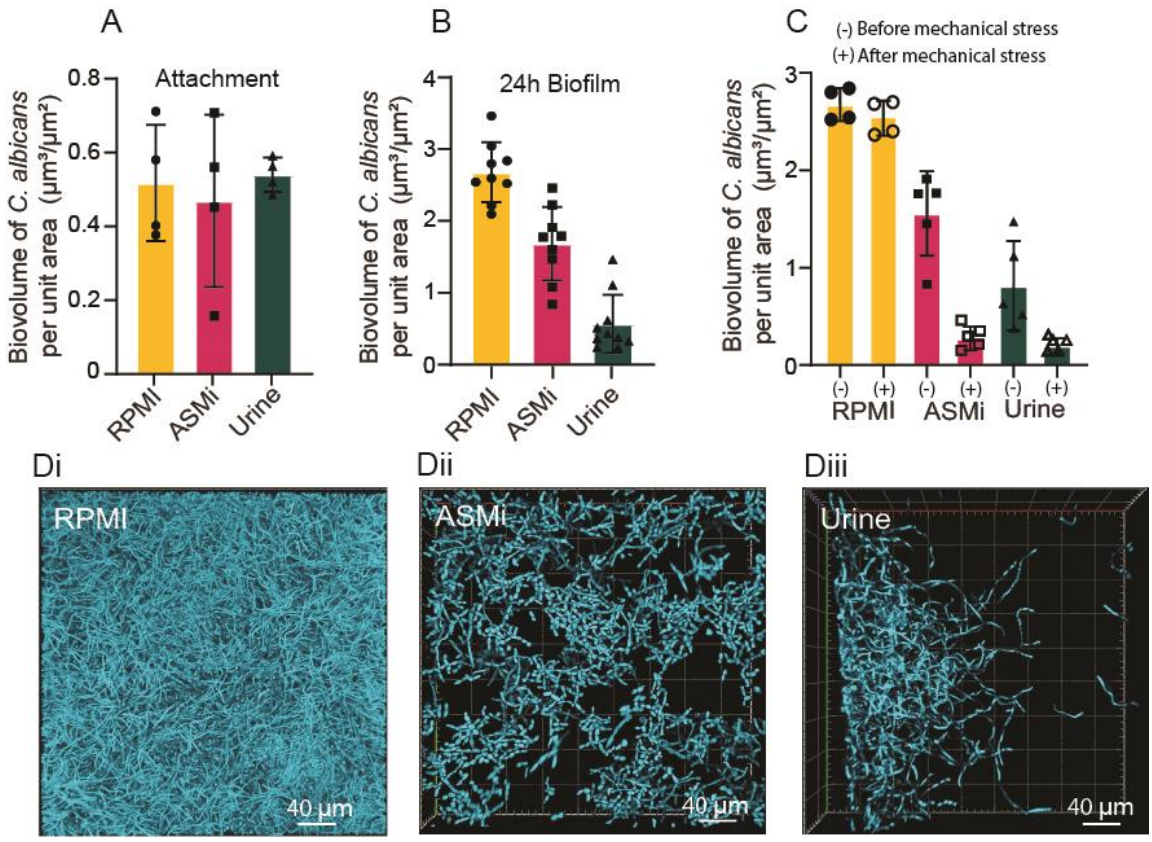

FIG. 1: *C. albicans* biofilms in different nutrient environments. (A) Biovolume per unit area of glass cover slip of attached *C. albicans* cells after 1h incubation at 37ºC in three different media (n=4) (B) Biovolume of *C. albicans* biofilms grown under flow at 37ºC for 24h per unit area of glass in three different media (n=9) (C) Biovolume per unit of *C. albicans* biofilms before and after flow rate was increased to 5000 times the original for 3mins – mechanical stress (n=4-5) (D)Representative 3D confocal renderings of *C. albicans* biofilms grown in (i) RPMI media (ii) ASMi media (iii) Urine media.

C. albicans biofilms have not only been shown to be resistant to treatment by antifungal but are also resistant to mechanical forces [12], [21-23]. Biofilms formed especially on catheters are very hard to remove and usually results in replacement of the entire medical device [21]. We were curious to see if and to what extent nutrient media played a role in strength of attachment and resistance to mechanical stress. We grew *C. albicans* biofilms in the three media underflow for 24h and then increased the flow rate to 5000 times the original for 3mins to stimulate exposure to high mechanical stress. We show that strength

of attachment is growth media dependent, the biofilms grown in RPMI showed no change in biovolume after application of mechanical stress, whereas the biofilms in ASMi and urine showed 60-80% reduction in total biovolume (Fig. 1C). Though there is reduction in biovolume in ASMi and urine, impressively there is still biovolume left at the end of the mechanical stress treatment (Fig. 1C Sup. 2) that could potentially lead to recolonization of that space pointing to the ability of *C. albicans* biofilms to overcome mechanical clearance in host niches.

Frequency distribution of local biovolume packing in *C. albicans* biofilms

The microscale architecture of a biofilm is the result of a combination of external factors like shear stress and nutrient availability and internal factors like matrix composition and microbial interactions. Cellular scale architecture in turn can affect the biofilm characteristics like strength of attachment to a surface or resistance to mechanical forces. Cellular ordering and structural adaptations can additionally inform us about the potential expression of genes across the biofilm.

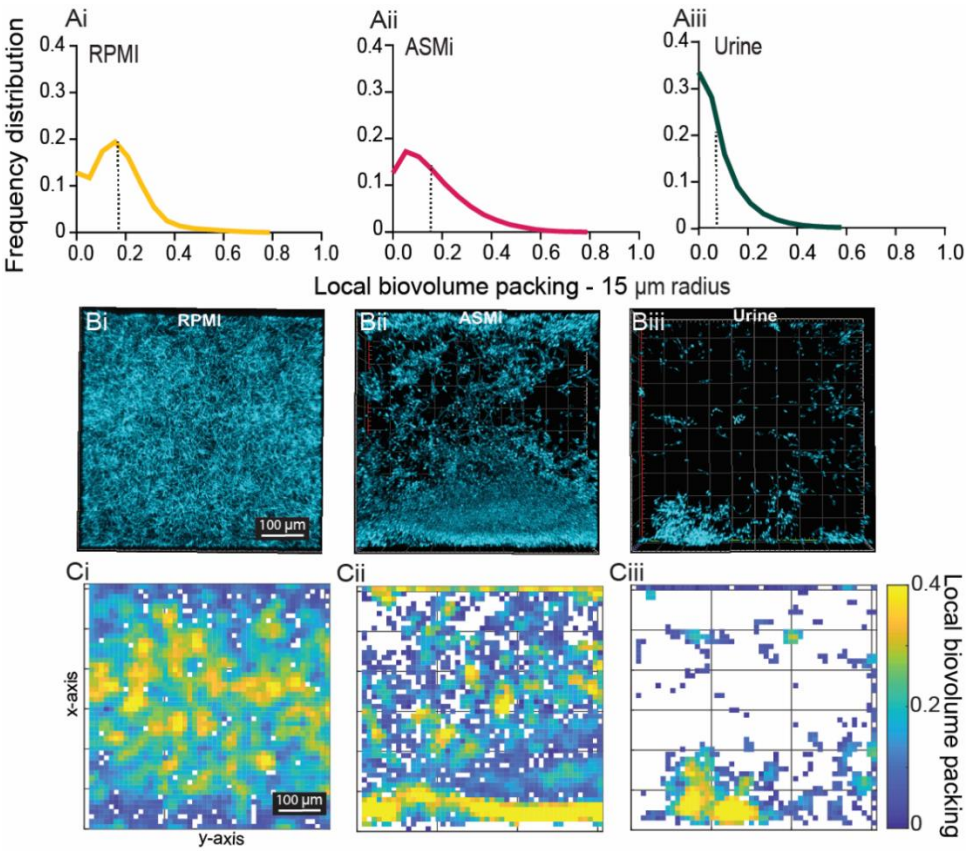

FIG. 2: *C. albicans* biofilms local biovolume packing. (A) The frequency distribution of local biovolume packing at 15 µm radius of 24h old *C. albicans* biofilms grown at 37^{O}C under flow in (n =9) (i) RPMI (ii) ASMi (iii) urine. The lines represent the median (B) Representative 3D confocal images showing local packing in biofilms grown in (i) RPMI (ii) ASMi (iii) Urine. (C) Heat map of local biovolume packing for representative images of biofilms grown in (i) RPMI (ii) ASMi (iii) urine.

Given the heterogeneity of biofilms formed in the three different media across the entire microfluidic chamber (Sup. 1) we looked at biofilm at a smaller scale. BiofilmQ segments the confocal image into cubes of a given length to acquire spatial data. For each segmented *C. albicans* biovolume, we looked at the biovolume packing in a 15µm radius which quantifies the biovolume of *C. albicans* that occupies space around each segmented *C. albicans* in a radius of 15µm. The frequency distribution of local biovolume packing was plotted across samples (Fig. 2A). The frequency distribution of biovolume packing was similar between RPMI and ASMi relative to that of *C. albicans* biofilm grown in urine

media. In *C. albicans* biofilms grown in RPMI, we see more normal distribution of frequency distribution of biovolume packing with a peak at about 0.19 (Fig. 2Ai). This suggests an even density packing across the biofilm, this can be visualized in both the representative image and heat map of biovolume packing (Fig 2. Bi and Ci). For biofilms grown in ASMi, the peak of the distribution is one sided (Fig. 2Aii) suggesting denser areas in some parts of the biofilm. This is illustrated in the representative confocal image and heat map of biovolume packing (Fig 2. Bi and Ci). Finally, in the biofilms in urine media we see a large fraction of samples closer to zero biovolume packing (Fig. 2Aii) suggesting a very sparsely populated biofilm. This is evident in representative confocal image and heat map (Fig. 2 Biii and Ciii).

We observed that biofilms grown in RPMI, and urine were both filamentous, however their frequency distribution of local biovolume packing were very different. Differences in metabolism could be resulting in changes in matrix composition and quantity of components produced. Interestingly, we see similar areas of local density packing in biofilms grown in RPMI and ASMi even though the first is in hyphal morphology and the later in pseudo hyphal morphology. From the previous section we also saw that the strength of attachment is not dependent on local biovolume packing suggesting to us again the matrix composition could potentially be altered between biofilms grown in these two media. An interesting area for future work is to explore adhesion proteins and matrix of *C. albicans* grown in these different media under flow.

Combination of frequency distribution of local biovolume packing and resident biovolume in *C. albicans* biofilm determines invisibility

So far, in the preceding sections we have explored *C. albicans* ability to colonize and grow in previously unoccupied locations. Another natural context one might imagine is that the colonizing microbe could instead encounter surfaces that are already occupied by other

strains and species. Our next experiments were designed to assess the relative abilities of *C. albicans* to invade preexisting biofilms grown in different nutritional media.

Here, we first grew biofilms of *C. albicans* in the three media, which we refer to as the resident strain. After 24h of growth of the resident strain, we introduced the second strain (the invader) for 2h to assess its ability to colonize and integrate into the resident biofilm. By visual inspection alone it was evident there was minimal invasion into resident biofilms grown in RPMI (Fig. 3A Sup. 4A), while there was considerably higher invasion into biofilms grown in ASMi and urine (Fig 3A Sup. 3B 3C). To quantify invasion efficiency, we first quantified the frequency of invading strain 2h post invasion (Fig. 3A). Next, we plotted biovolume of the invading strain 2h post invasion as a function of resident biofilm packing density (Fig 3B). We found in the case of biofilms grown in RPMI with more even distribution of local biovolume packing shown in the previous section, the invading cells were not able to establish themselves in the resident biofilm. In the case of ASMi biofilms, the invading cells were able to establish themselves in a local biovolume packing dependent manner with high invader biovolume in low density packing (Fig. 3B). The differences in combination of local biovolume packing and total biovolume results in changes in invisibility of *C. albicans* biofilms grown in RPMI versus ASMi. Finally, in the urine media resident biofilms were so sparely packed that the invader was able to establish themselves at relatively high biovolume throughout the entire resident biofilm as is evident in high frequency of invading strain (Fig. 3A and 3B)

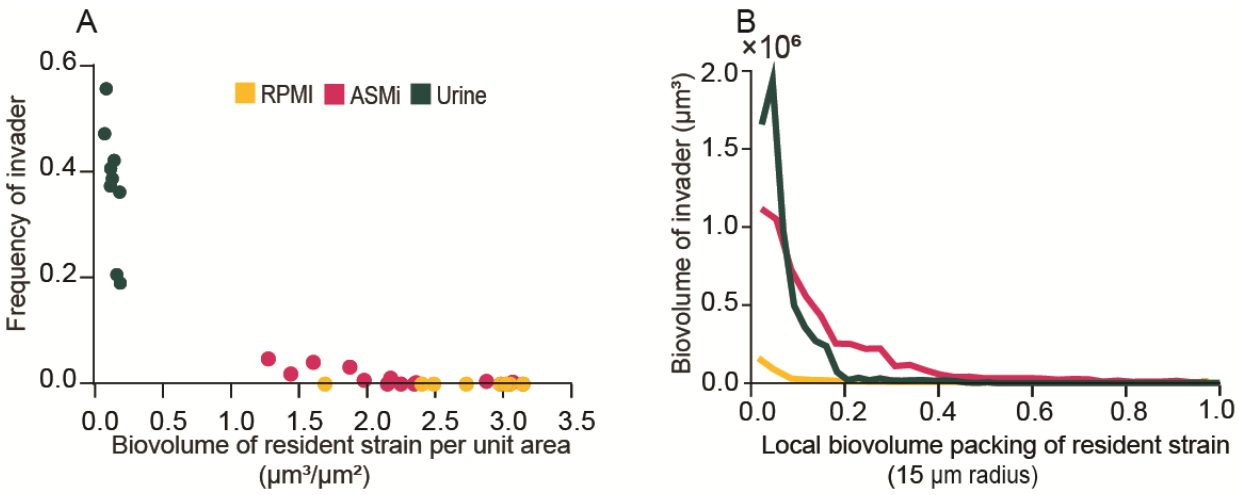

FIG. 3: ***C. albicans* biofilms invasion dynamics**. (A) The frequency or the relative fraction of invader in a biofilm with both invader and resident strains are plotted as a function of the C. albicans resident strain biovolume per unit area of glass (n=9) (B) Biovolume of invader strain in a total area imaging of 250000μm^3 was plotted as a function of the local biovolume packing of the resident *C. albicans* strain (n=9).

Invading *C. albicans* can displace resident *C. albicans* and integrate into resident biofilms grown in artificial urine media

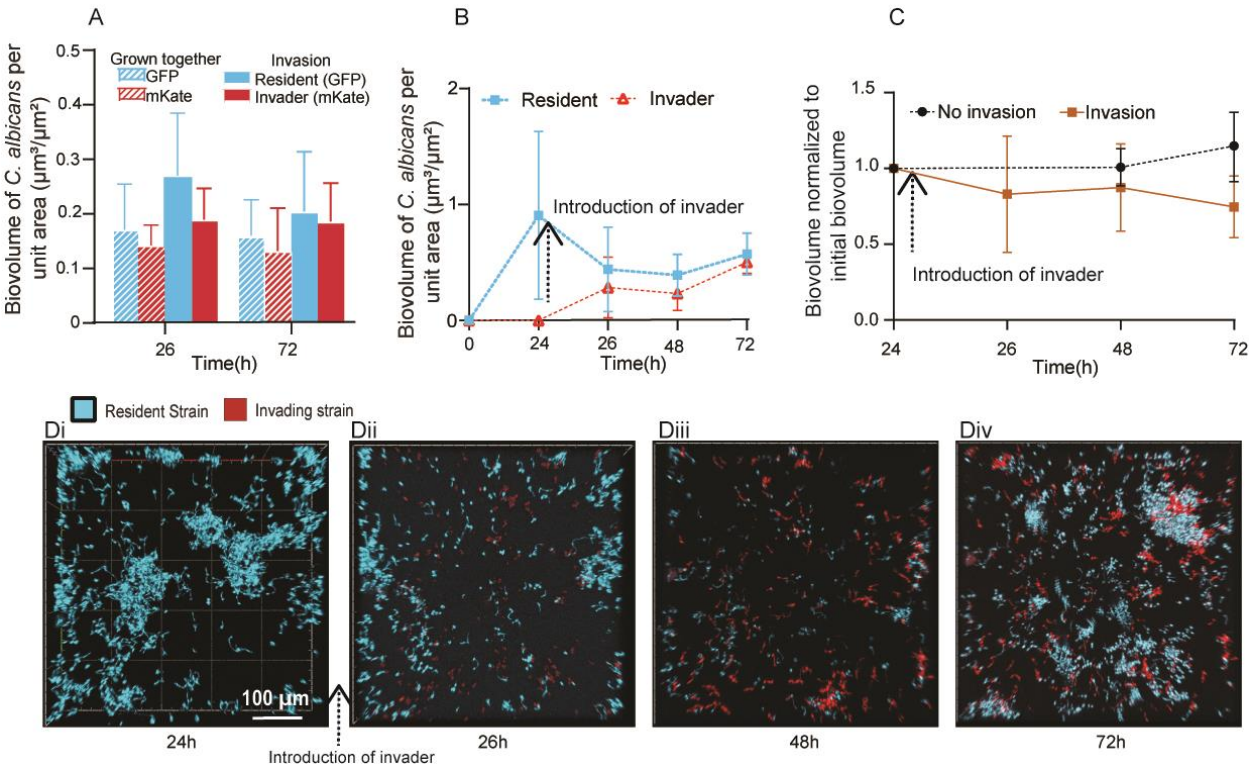

FIG. 4: Biofilm invasion dynamics in urine media. (A) Biovolume of isogenic strains at 26h and 72h in together and invasion experiments (n=3) (B) Biovolume of invading and resident *C. albicans* strains during the course of invasion experiments (n=6) (C) The total biovolume in invasion and no invasion experiments normalized to initial biovolume at 24h biofilm growth (n=3-6) (D) Representative 3D confocal images through the course of an invasion experiment)

We conducted two sets of experiments. The first in which two isogenic strains of *C. albicans* were introduced into the chamber at the same time and allowed to grow; this set of experiments will be referred to as together. Next, we grew one isogenic strain which we refer to as resident strain for 24h under flow and then introduce the second strain called invader strain for two hours; these experiments will be referred to as invasion. We noticed that in urine media the biovolume of two isogenic strains of *C. albicans* grown together and in invasion experiments had comparable biovolumes at 26 and 72 hours after the start of the experiments (Fig. 4A). This observation was very interesting and suggested that the final composition of a dual strain *C. albicans* biofilm was not dependent on its initial

inoculation conditions, irrespective of when in the lifecycle of the biofilm two *C. albicans* come in contact, it seemed to lead to a well-mixed biofilm.

We found that the introduction of the invader strain caused a decrease in resident strain followed by an increase in invader strain (Fig. 4B 4D). The decrease in invader biovolume was from the tubing change performed to introduce the invading strain, in the control the resident strain was able to regrow to its original biovolume at 24h before the tubing change (Sup. 4). However, in the case of the invasion experiment, the invader replaced the resident and integrate into the resident biofilm and increase in total biovolume (Fig 4B). It is possible this kind of behavior is common in natural niches associated with urine and *C. albicans* infections. Cells dispersing from the top of a urinary catheter could interact with a downstream biofilm in this manner. Alternately disseminating cells from the blood could encounter existing biofilms in the urinary tract. The integration of a more virulent strain into an existing resident biofilm could lead to worse disease outcomes. This brings to light yet another feature of robustness of a *C. albicans* biofilm characteristic and consequently another challenge we face for its removal.

Lastly, when the biovolume is normalized to resident strain biovolume at 24h just before the start of the invasion experiment, the total biovolume (invader + resident) in the chambers through the experiment seemed to be regulated and hovered around the original biovolume at 24h (Fig 4C). This regulation of biovolume was also seen in single strain biofilm growth over time. This kind of regulation of biovolume or stable biovolume despite accesses to nutrition and space has been implicated in commensal to pathogenic switch in *C. albicans* [22]. Interestingly that study showed that *C. albicans* was present primarily in its yeast morphology during this regulation. In contrast we see that *C. albicans* in filamenting and in a biofilm. This novel behavior of biovolume regulation could have important ecological functions. For example, it could be a potential mechanism to evade immune system detection. Further work is necessary to understand the functions of such behavior.

3.4 Materials and Methods

Strains and media

C. albicans strains are derivatives of strain CAI4. All strains were grown on YPD (10 g yeast extract, 20 g peptone, and 20 g dextrose [all amounts per liter]), RPMI 1640 (Sigma – Aldrich), ASMi [15] and artificial Urine (Pickering Laboratories - 1700-0018). RPMi and RPMI was bought from the commercial sources as mentioned.

The fluorescently labelled strains of *C. albicans* GPF and mKate2 were obtained from Barelle et al., 2004 [19] and Kasetty et al., 2021 [15] respectively.

Microfluidic device assembly

The microfluidic devices were made by bonding polydimethylsiloxane (PDMS) chamber molds to size #1.5 cover glass slips (60 mm 36 mm) [length L width W], Thermo-Fisher, Waltham, MA) using standard soft lithography techniques (96). Each PDMS mold contained four chambers, each of which measured 10000µm 500µm 70µm (L W depth D). To establish flow in these chambers, medium was loaded into 1-ml BRANDZIG syringe with 25-gauge needles. These syringes were joined to #30 Cole-Parmer polytetrafluoroethylene (PTFE) tubing (inner diameter, 0.3 mm), which was connected to pre-bored holes in the microfluidic device. Tubing was also placed on the opposite end of the chamber to direct the effluent to a waste container. Syringes were mounted to syringe pumps (Pico Plus Elite, Harvard Apparatus), and flow was maintained at 0.1 µl per min for all experiments.

Biofilm growth

Overnight cultures of *C. albicans* were grown at 30°C with shaking in YPD prior to the start of biofilm experiments. Cultures were normalized to an OD 600 of 0.5 in RPMI, ASMi

or Urine medium. Cells were inoculated into a microfluidic chamber (completely filling its inner volume), and then allowed to rest for 1h at 37°C to permit cells to attach to the glass surface. The devices were then run at 0.1 µl per min at 37°C and imaged by confocal microscopy (see below) at time intervals that varied per experiment as noted in each figure.

To measure strength of attachment of biofilms, biofilms were grown in three media for 24h. The flow rate was increased to 500 µl per min for three mins. Confocal images were taken before and after the mechanical stress treatment.

For invasion experiments, we grew the resident biofilm for 24 h at a flow rate of 0.1 µl per/min at 37°C, after which we introduced the invading strain (adjusted to an OD_{600} of 1.0) at the same flow rate for 2h by switching the chamber inlets to new tubing connected to new syringes containing the invading strain. Confocal images were taken before invasion, 2h and 24h after invasion protocol.

Microscopy and image analysis

Biofilms inside microfluidic chambers were imaged using a Zeiss LSM 880 confocal microscope with a 40/1.2 numerical aperture (NA) or 10/0.4 NA water objective. A 488-nm laser line was used to excite GFP, and a 594-nm laser line was used to excite mKate2. All quantitative analysis of microscopy data was performed using BiofilmQ [23].

To calculate the volume of invader around the resident, a custom python script was built. For each replicate image stack, the corresponding BiofilmQ generated data was loaded into the python script. The BiofilmQ data is composed of cubes from each laser channel-invader or resident – and every cube contains volume and 3D location data. To find the volume of invader around each resident, the script looped through the resident cubes and found the invader cubes with centroids (center of mass of a cube) within a range of 15

μm from the centroid of the focal resident. The volumes of these invader cubes were then summed and stored in a .cvs file.

3.5 Conclusions

The incidence of *C. albicans* infections have been increasing in recent years and clearing these infections have become a significant medical challenge [5]. Biofilms particularly are very robust and resistant to a variety of treatment methods. Here, we sought to study *C. albicans* biofilms grown in different nutrient environments and characterize their biofilm properties. Given *C. albicans's* metabolic flexibility we were curious to see to what extant their biofilm characteristics would differ in variable nutrient niches. We demonstrated that the biofilm architecture and biovolume accumulation under flow were distinct across three nutritional environments. Finally, we show that new *C. albicans* cells can invade an existing biofilm in a density packing dependent manner. The identification of this novel characteristic could shed light into *C. albicans* biofilm dynamics especially in filamentous biofilms.

Few studies have looked at metabolic flexibility of *C. albicans*, especially its effect on biofilm characteristics. We show that growth and morphology but not attachment in a flow system is dependent on the available nutrients. We speculate that the metabolic pathway *C. albicans* chooses as result of available nutrients ultimately effects its growth dynamics. In a nutrient rich environment like RPMI, it can quickly accumulate biomass and form a robust biofilm. These biofilms are also very strongly attached to their surface in comparison to biofilms grown in ASMi or urine. The precise pathway that is chosen by *C. albicans* and the extent of its effect on biofilm dynamics is an important area for future work.

Our final series of experiments showed that *C. albicans* can colonize a previously established *C. albicans* biofilm, in a combination of local biovolume density and total biovolume dependent manner, over a relatively short colonization time of 2h. We also saw that in urine media the new *C. albicans* is able to completely integrate into the existing *C. albicans* biofilm. This suggests that *C. albicans* is suited to exploiting previously colonized regions. We know that medical devices like catheters are colonized by *C. albicans* and clearing these infections can be demanding [24]. On this basis we speculate that in less densely packed biofilms, like those found in urine environments, *C. albicans* has evolved surface occupation strategy best suited to taking advantage of previously colonized surfaces.

Flow has shown to have effects on biofilm formation. In bacterial biofilms, surface residence time [25], upstream surface motility in addition to the formation of biofilm aggregates [26] have been shown to be affected by flow. There has been less investigation of the effects of flow dynamics and shear on *C. albicans* biofilms. Some existing work showed that biofilms formed under shear are more highly compacted and physically robust relative to those grown in static conditions [27]. However, the combined effect of flow and available nutrients have not been explored. We infer from our results that nutrient availability plays a critical role in addition to shear stress. Understanding the precise molecular mechanisms responsible for shear stress regulation and metabolic flexibility and the interconnectedness between the two is an important for future study.

3.6 Supplemental figures

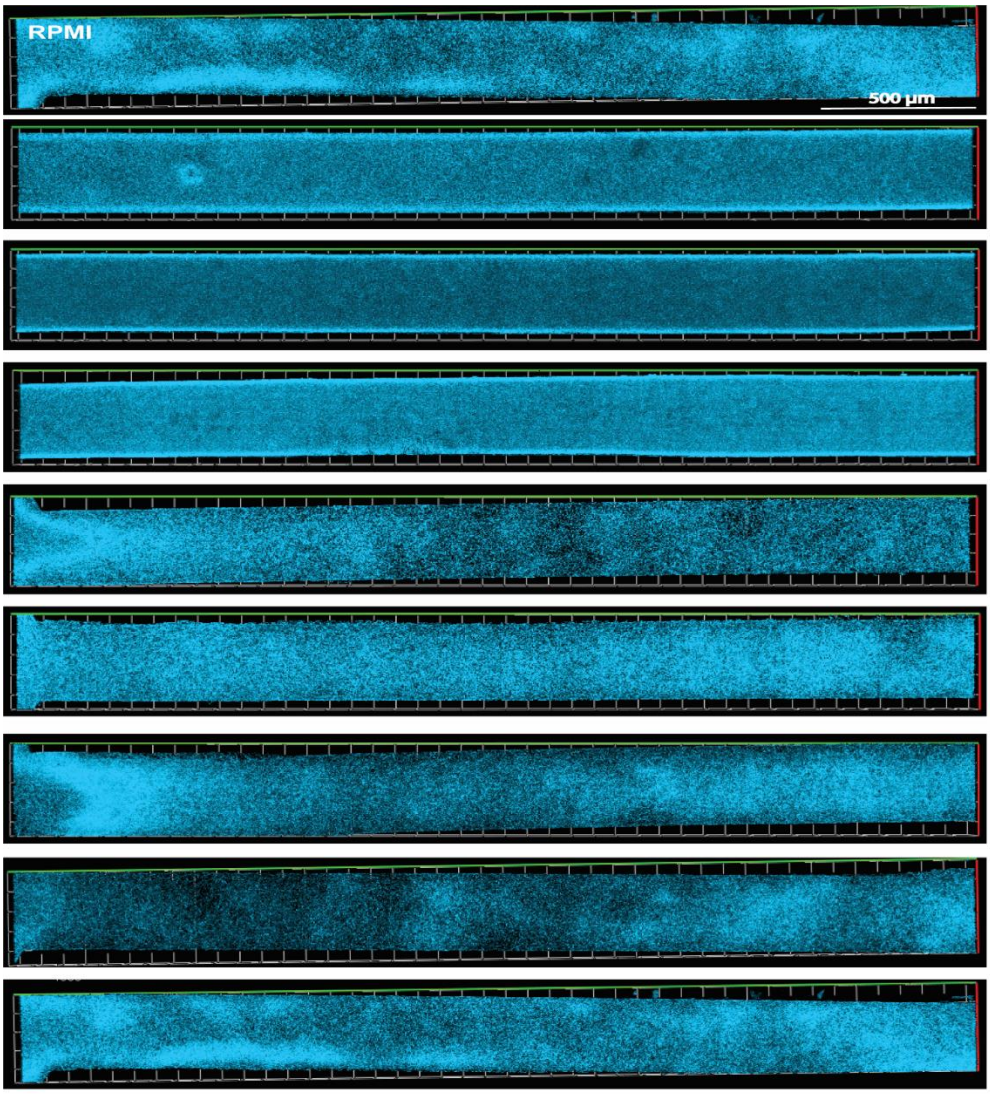

FIG. S1a: *C. albicans* biofilms in RPMI media. Confocal 3D renderings of entire microfluidic chambers with *C. albicans* biofilms grown under flow for 24h at 37ºC

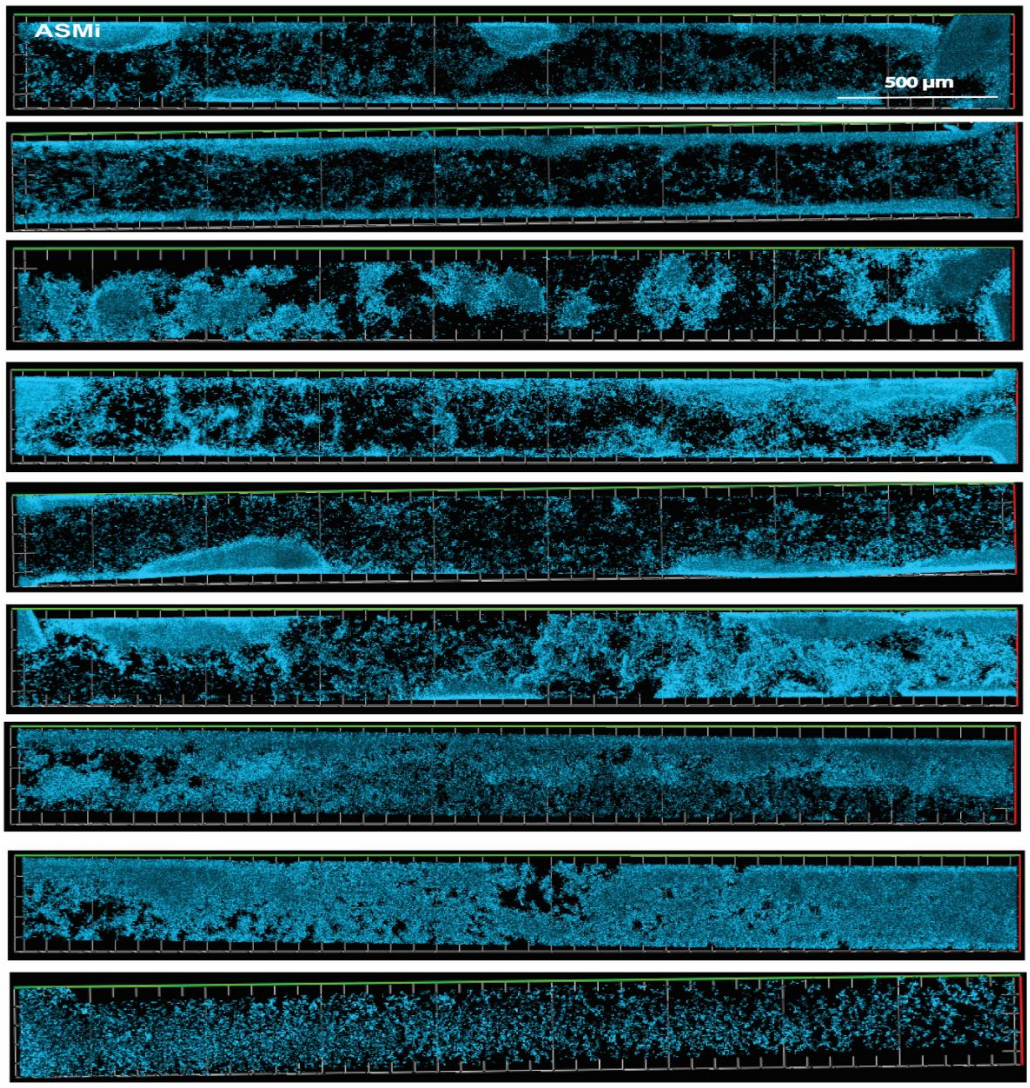

FIG. S1b: *C. albicans* biofilms in ASMi media. Confocal 3D renderings of entire microfluidic chambers with *C. albicans* biofilms grown under flow for 24h at 37ºC

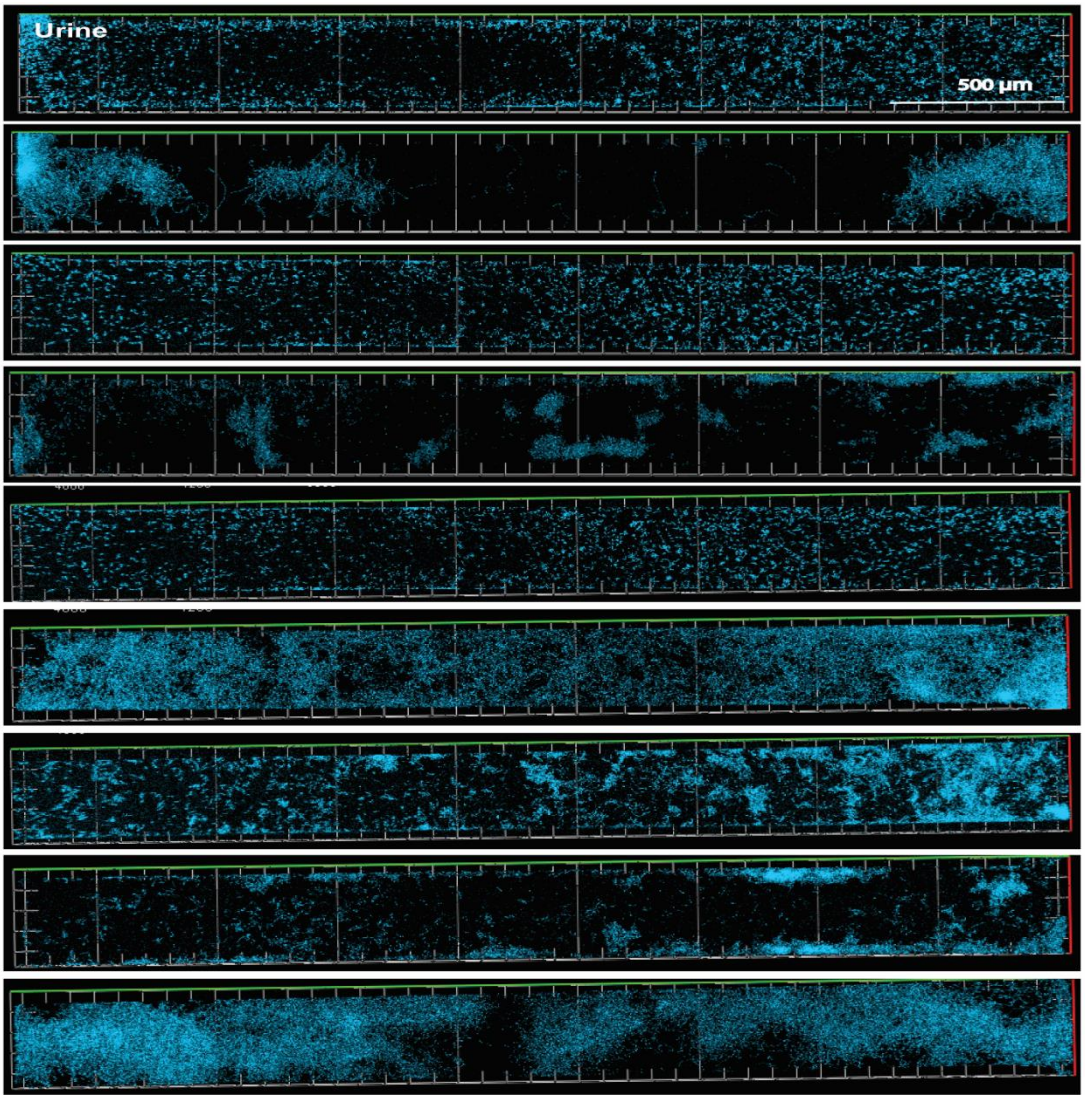

FIG. S1c: ***C. albicans*** **biofilms in urine media**. Confocal 3D renderings of entire microfluidic chambers with *C. albicans* biofilms grown under flow for 24h at 37ºC

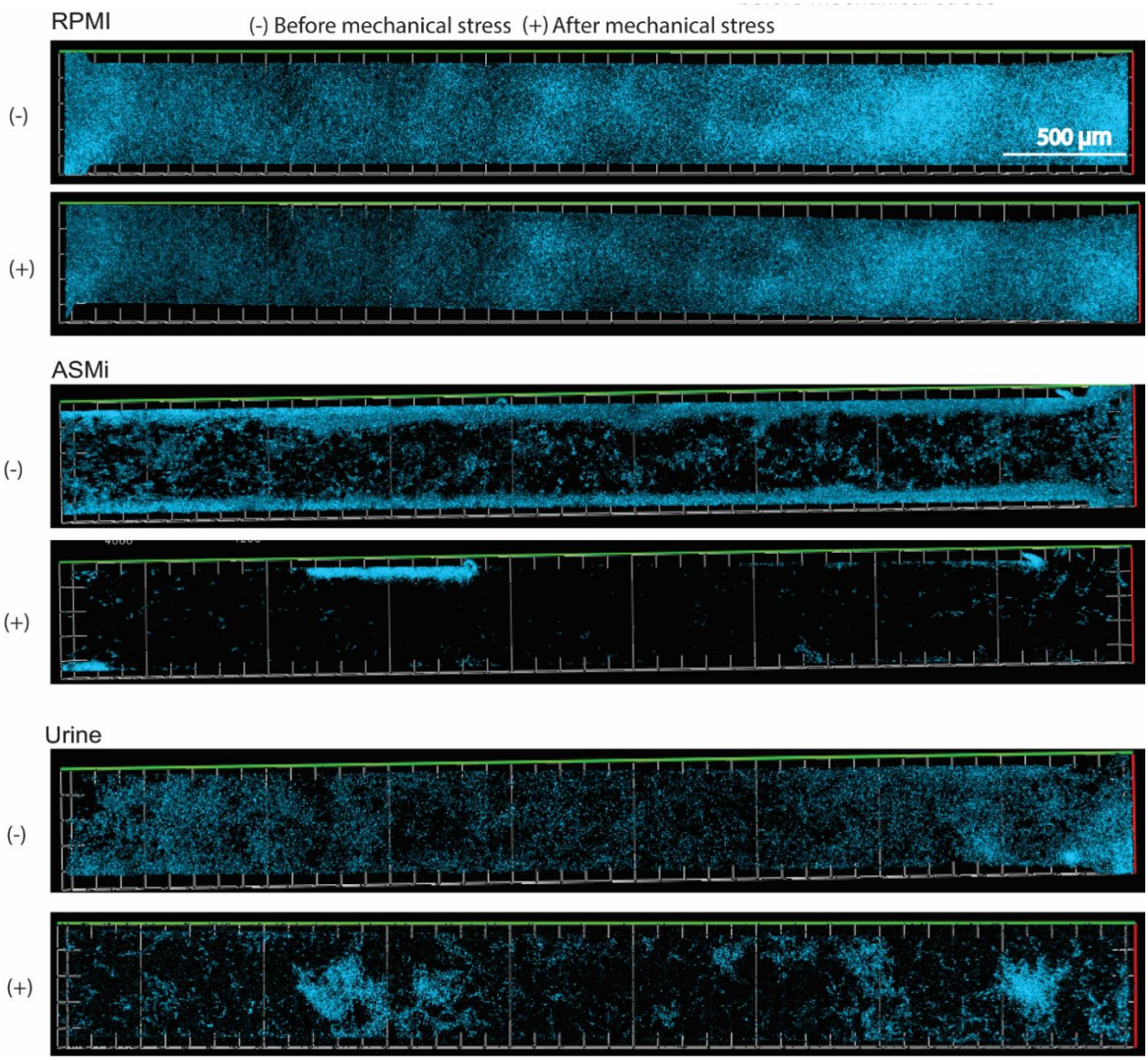

FIG. S2: *C. albicans* biofilms and mechanical stress. Representative confocal 3D renderings of entire microfluidic chambers with 24h *C. albicans* biofilms in three different nutritional media before and after simulation of mechanical stress – 5000 times flow rate increase for 3mins

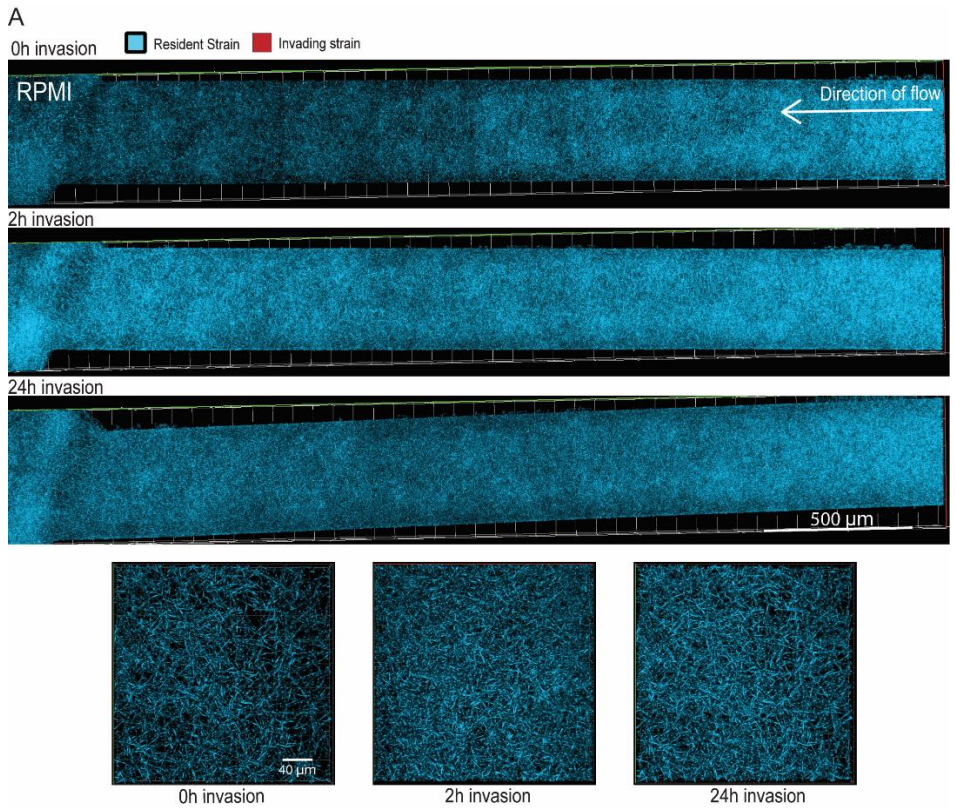
A
0h invasion
Resident Strain
Invading strain
RPMI
Direction of flow
2h invasion
24h invasion
500 µm
40 µm
0h invasion
2h invasion
24h invasion

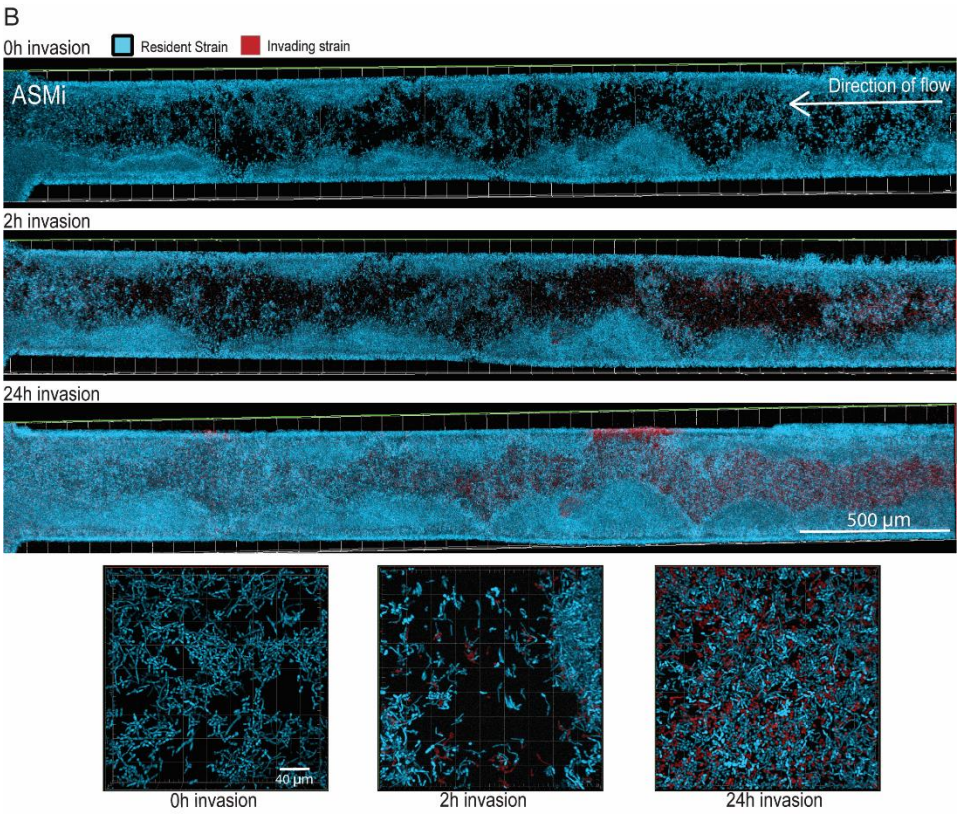
B
0h invasion
Resident Strain
Invading strain
ASMi
Direction of flow
2h invasion
24h invasion
500 µm
40 µm
0h invasion
2h invasion
24h invasion

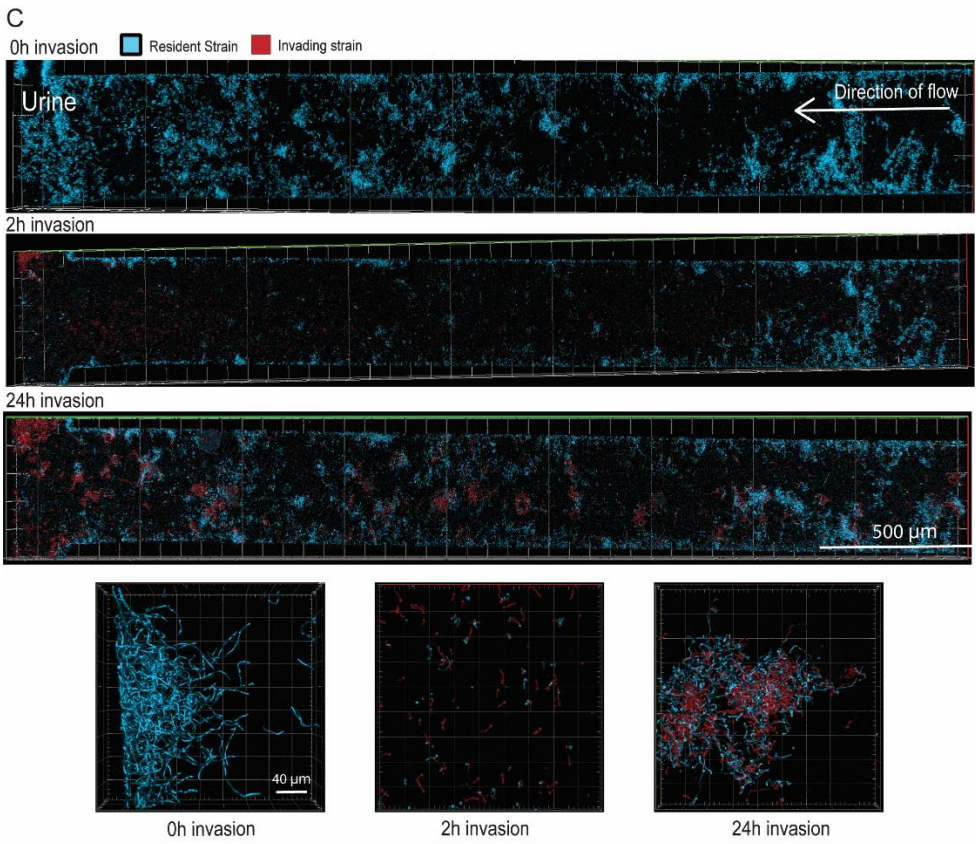

FIG. S3: Invasion dynamics. Representative 3D Confocal images of *C. albicans* invasion dynamics at different time points in (A)RPMI (B) ASMi (C) Urine media.

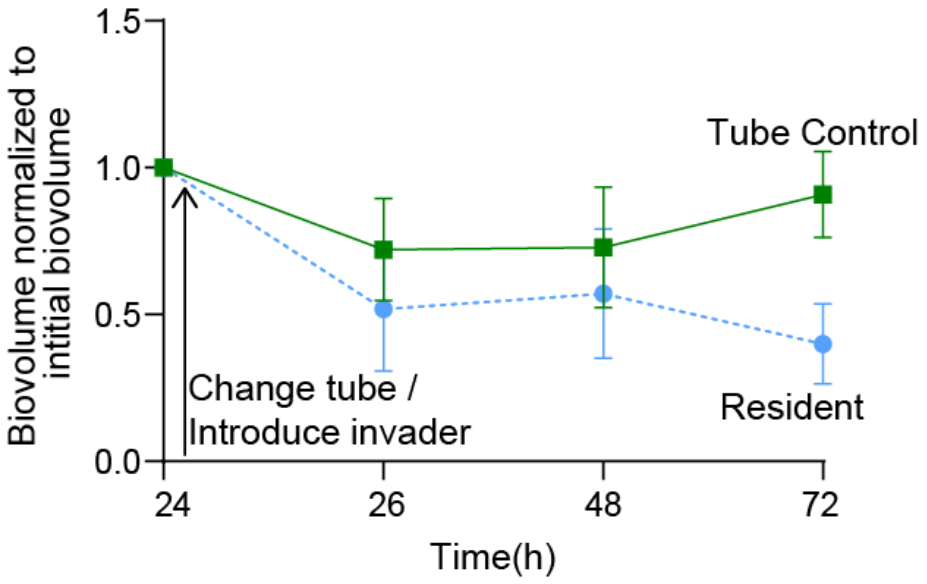

FIG. S4: Invasion experimental control. The total biovolume of resident strain in invasion and tubing control experiments normalized to initial biovolume at 24h biofilm growth (n=3)

3.7 Appendix 1

Filamentation affects spatial distribution of genotypes in *C. albicans* biofilms

It has been well established biofilm function, characteristics and evolution are strongly influenced by spatial arrangement of members with them [22]. Spatially constrained interactions are well known to be important in ecology, for example, the occurrence of diffusible goods is more common in spatially constrained populations. Additionally, many phenotypes associated with biofilm formation and the pathogenesis of bacterial infections like secreted factors such as digestive enzymes and nutrient chelating molecules occur in higher frequency when certain genotypes are spatially close to one another [16], [23]. Recently, the spatiotemporal distributions of different genotypes and how they originate have been explored in bacterial biofilms [24], however, such studies and characterization in their fungal counterparts are still lacking.

We characterized the patterns of spatial arrangement of two isogenic *C. albicans* strains in a biofilm. The two strains are genetically identical but for the florescent protein they express. We calculated autocorrelation length for biofilms grown in different media; Autocorrelation length is a good measurement of lineage segregation because smaller lengths indicate a more mixed population. Autocorrelation length of biofilms grown in YPD where the *C. albicans* cells are majority in yeast morphology was used for comparison Autocorrelation length of *C. albicans* grown in YPD was about double that of biofilms with isogenic strains grown in RPMI, ASMi and Urine (Fig. 2A). This indicates that there is more intermixing of isogenic strains when in filamentous morphology in comparison to yeast morphology (Fig. 2B Sup. 3).

The *C. albicans* matrix – an integral component of *C. albicans* biofilms – assembly occurs extracellularly making matrix assembly a cooperative community mechanism [25]. This matrix sharing could potentially be responsible for intermixing of genotypes in filamentous *C. albicans* biofilms. The secreted matrix components of yeast cells are not well recorded and is likely they are different from its filamentous counterpart. Further investigation and comparison of extracellular matrix and adhesion components produced by yeast and filamenting *C. albicans* cells may help decipher the causes for their respective genetic biofilm structures.

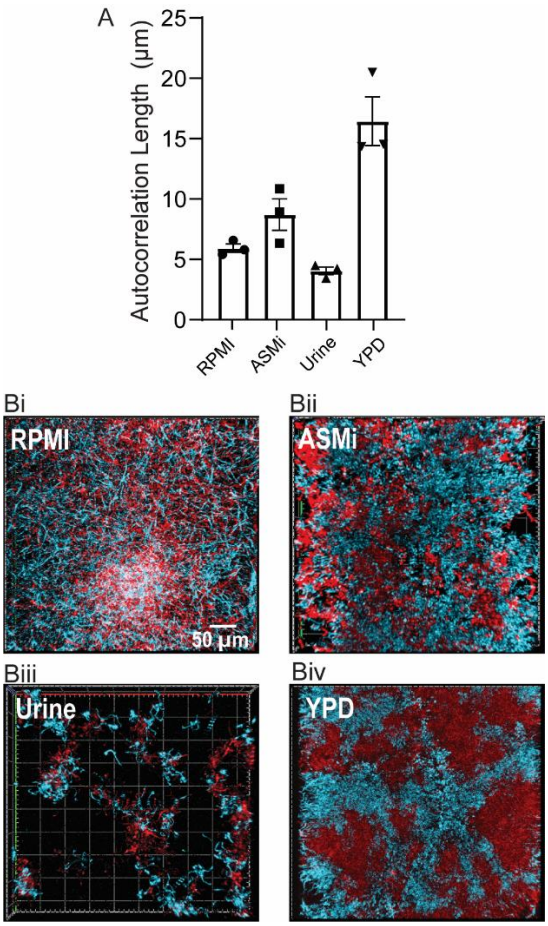

FIG. A1: Spatial genetic structure within *C. albicans* biofilms. (A) Autocorrelation length – proxy for degree of intermixing - for *C. albicans* biofilms with two isogenic strains grown in four different nutritional media (n=3) (B) Representative 3D confocal renderings of isogenic *C. albicans* strain biofilms grown in (i) RPMI media (ii) ASMi media (iii) urine media (iv) YPD media

3.8 References

[1] J. J. Limon, J. H. Skalski, and D. M. Underhill, "Commensal Fungi in Health and Disease," *Cell Host Microbe*, vol. 22, no. 2, pp. 156–165, Aug. 2017, doi: 10.1016/j.chom.2017.07.002.

[2] J. A. Romo and C. A. Kumamoto, "On Commensalism of Candida," *J. Fungi*, vol. 6, no. 1, p. 16, Jan. 2020, doi: 10.3390/jof6010016.

[3] S. M. Noble, B. A. Gianetti, and J. N. Witchley, "Candida albicans cell-type switching and functional plasticity in the mammalian host," *Nat. Rev. Microbiol.*, vol. 15, no. 2, pp. 96–108, Feb. 2017, doi: 10.1038/nrmicro.2016.157.

[4] H.-J. Lo, J. R. Köhler, B. DiDomenico, D. Loebenberg, A. Cacciapuoti, and G. R. Fink, "Nonfilamentous C. albicans Mutants Are Avirulent," *Cell*, vol. 90, no. 5, pp. 939–949, Sep. 1997, doi: 10.1016/S0092-8674(00)80358-X.

[5] M. Gulati and C. J. Nobile, "Candida albicans biofilms: development, regulation, and molecular mechanisms," *Microbes Infect.*, vol. 18, no. 5, pp. 310–321, May 2016, doi: 10.1016/j.micinf.2016.01.002.

[6] J. S. Finkel and A. P. Mitchell, "Genetic control of Candida albicans biofilm development," *Nat. Rev. Microbiol.*, vol. 9, no. 2, pp. 109–118, Feb. 2011, doi: 10.1038/nrmicro2475.

[7] P. Uppuluri *et al.*, "Dispersion as an Important Step in the Candida albicans Biofilm Developmental Cycle," *PLoS Pathog.*, vol. 6, no. 3, p. e1000828, Mar. 2010, doi: 10.1371/journal.ppat.1000828.

[8] S. E. Herwald and C. A. Kumamoto, "Candida albicans Niche Specialization: Features That Distinguish Biofilm Cells from Commensal Cells," *Curr. Fungal Infect. Rep.*, vol. 8, no. 2, pp. 179–184, Jun. 2014, doi: 10.1007/s12281-014-0178-x.

[9] D. Andes, J. Nett, P. Oschel, R. Albrecht, K. Marchillo, and A. Pitula, "Development and Characterization of an In Vivo Central Venous Catheter Candida albicans Biofilm Model," *Infect. Immun.*, vol. 72, no. 10, pp. 6023–6031, Oct. 2004, doi: 10.1128/IAI.72.10.6023-6031.2004.

[10] S. P. Hawser and L. J. Douglas, “Biofilm formation by Candida species on the surface of catheter materials in vitro.,” *Infect. Immun.*, vol. 62, no. 3, pp. 915–921, 1994, doi: 10.1128/IAI.62.3.915-921.1994.

[11] K. D. Mandakhalikar, J. N. Rahmat, E. Chiong, K. G. Neoh, L. Shen, and P. A. Tambyah, “Extraction and quantification of biofilm bacteria: Method optimized for urinary catheters,” *Sci. Rep.*, vol. 8, no. 1, p. 8069, Dec. 2018, doi: 10.1038/s41598-018-26342-3.

[12] F. L. Mayer, D. Wilson, and B. Hube, “*Candida albicans* pathogenicity mechanisms,” *Virulence*, vol. 4, no. 2, pp. 119–128, Feb. 2013, doi: 10.4161/viru.22913.

[13] A. J. P. Brown, G. D. Brown, M. G. Netea, and N. A. R. Gow, “Metabolism impacts upon Candida immunogenicity and pathogenicity at multiple levels,” *Trends Microbiol.*, vol. 22, no. 11, pp. 614–622, Nov. 2014, doi: 10.1016/j.tim.2014.07.001.

[14] R. B. Williams and M. C. Lorenz, “Multiple Alternative Carbon Pathways Combine To Promote Candida albicans Stress Resistance, Immune Interactions, and Virulence,” *mBio*, vol. 11, no. 1, pp. e03070-19, Feb. 2020, doi: 10.1128/mBio.03070-19.

[15] S. Kasetty, D. L. Mould, D. A. Hogan, and C. D. Nadell, “Both Pseudomonas aeruginosa and Candida albicans Accumulate Greater Biomass in Dual-Species Biofilms under Flow,” *mSphere*, vol. 6, no. 3, pp. e00416-21, Jun. 2021, doi: 10.1128/mSphere.00416-21.

[16] S. E. Darch *et al.*, “Spatial determinants of quorum signaling in a *Pseudomonas aeruginosa* infection model,” *Proc. Natl. Acad. Sci.*, vol. 115, no. 18, pp. 4779–4784, May 2018, doi: 10.1073/pnas.1719317115.

[17] N. Grahl *et al.*, “Profiling of Bacterial and Fungal Microbial Communities in Cystic Fibrosis Sputum Using RNA,” *mSphere*, vol. 3, no. 4, pp. e00292-18, Aug. 2018, doi: 10.1128/mSphere.00292-18.

[18] P. Uppuluri, H. Dinakaran, D. P. Thomas, A. K. Chaturvedi, and J. L. Lopez-Ribot, “Characteristics of Candida albicans Biofilms Grown in a Synthetic Urine Medium,” *J. Clin. Microbiol.*, vol. 47, no. 12, pp. 4078–4083, Dec. 2009, doi: 10.1128/JCM.01377-09.

[19] C. J. Barelle, C. L. Manson, D. M. MacCallum, F. C. Odds, N. A. R. Gow, and A. J. P. Brown, “GFP as a quantitative reporter of gene regulation inCandida albicans,” *Yeast*, vol. 21, no. 4, pp. 333–340, Mar. 2004, doi: 10.1002/yea.1099.

[20] L. Mukaremera, K. K. Lee, H. M. Mora-Montes, and N. A. R. Gow, “Candida albicans Yeast, Pseudohyphal, and Hyphal Morphogenesis Differentially Affects Immune Recognition,” *Front. Immunol.*, vol. 8, p. 629, Jun. 2017, doi: 10.3389/fimmu.2017.00629.

[21] E. M. Kojic and R. O. Darouiche, “*Candida* Infections of Medical Devices,” *Clin. Microbiol. Rev.*, vol. 17, no. 2, pp. 255–267, Apr. 2004, doi: 10.1128/CMR.17.2.255-267.2004.

[22] S. J. White *et al.*, “Self-Regulation of Candida albicans Population Size during GI Colonization,” *PLoS Pathog.*, vol. 3, no. 12, p. e184, Dec. 2007, doi: 10.1371/journal.ppat.0030184.

[23] R. Hartmann *et al.*, “BiofilmQ, a software tool for quantitative image analysis of microbial biofilm communities,” Microbiology, preprint, Aug. 2019. doi: 10.1101/735423.

[24] X. Wang, H. Lünsdorf, I. Ehrén, A. Brauner, and U. Römling, “Characteristics of Biofilms from Urinary Tract Catheters and Presence of Biofilm-Related Components in Escherichia coli,” *Curr. Microbiol.*, vol. 60, no. 6, pp. 446–453, Jun. 2010, doi: 10.1007/s00284-009-9563-z.

[25] S. Lecuyer, “Shear Stress Increases the Residence Time of Adhesion of Pseudomonas aeruginosa,” *Biophys. J.*, p. 10.

[26] “Colonization, Competition, and Dispersal of Pathogens in Fluid Flow Networks | Elsevier Enhanced Reader.” https://reader.elsevier.com/reader/sd/pii/S0960982215002766?token=A854DE04C99B9646E0D

[27] P. K. Mukherjee, D. V. Chand, J. Chandra, J. M. Anderson, and M. A. Ghannoum, “Shear stress modulates the thickness and architecture of Candida albicans biofilms in a phase-dependent manner,” *Mycoses*, vol. 52, no. 5, pp. 440–446, 2009, doi: 10.1111/j.1439-0507.2008.01632.x.

Chapter 4

Both *Pseudomonas aeruginosa* and *Candida albicans* Accumulate Greater Biomass in Dual Species Biofilms under Flow

Swetha Kasetty, [a] Dallas L. Mould, [b] Deborah A. Hogan, [b] Carey D. Nadell [a]

a Department of Biological Sciences, Dartmouth, Hanover, New Hampshire, USA
b Department of Microbiology and Immunology, Geisel School of Medicine at Dartmouth, Hanover, New Hampshire, USA

Published in *mSphere* 2021; https://doi.org/10.1128/mSphere.00416-21

Author contributions

C.D.N. and D.A.H. conceived and supervised the project. S.K., D.L.M., D.A.H., and C.D.N. designed experiments. S.K. performed experiments and image analysis. S.K. and C.D.N. finalized figures. D.L.M. and D.A.H. contributed critical reagents. S.K., D.L.M., D.A.H., and C.D.N. wrote the paper.

4.1 Abstract

Microbe-microbe interactions can strongly influence growth and biofilm formation kinetics. For *Pseudomonas aeruginosa* and *Candida albicans*, which are found together in diverse clinical sites, including urinary and intravenous catheters and the lungs of individuals with cystic fibrosis (CF), we compared the kinetics of biofilm formation by each species in dual-species and single-species biofilms. We engineered fluorescent protein constructs for *P. aeruginosa* (producing *mKO-κ*) and *C. albicans* (producing *mKate2*) that did not alter growth and enabled single-cell resolution imaging by live sample microscopy. Using these strains in an optically clear derivative of synthetic CF sputum medium, we found that both *P. aeruginosa* and *C. albicans* displayed increased biovolume accumulation—by three- and sixfold, respectively—in dual-species biofilms relative to single-species biofilms. This result was specific to the biofilm environment, as enhanced growth was not observed in planktonic cocultures. Stimulation of *C. albicans* biofilm formation occurred regardless of whether *P. aeruginosa* was added at the time of fungal inoculation or 24 h after the initiation of biofilm development. *P. aeruginosa* biofilm increases in cocultures did not require the Pel extracellular polysaccharide, phenazines, and siderophores known to influence *C. albicans*. *P. aeruginosa* mutants lacking Anr, LasR, and BapA were not significantly stimulated by *C. albicans*, but they still promoted a significant enhancement of biofilm development of the fungus, suggesting a fungal response to the presence of bacteria. Last, we showed that a set of *P. aeruginosa* clinical isolates also prompted an increase of biovolume by *C. albicans* in coculture.

4.2 Introduction

Microbial biofilm growth, even in monospecies contexts, involves the interplay of many biological and physical factors that are dynamic in space and time (1–3). In many natural environments, including numerous chronic infections, biofilms are multispecies mixtures whose collective properties and dynamics may be difficult to predict from those of each constituent's monospecies biofilm growth. In the context of infection, the extent and kind of interactions among different biofilm-dwelling microbes also govern clinically relevant factors, such as drug resistance and virulence (4). For example, multispecies biofilm growth has been implicated in conjunctivitis (5), tooth decay (6), prosthesis and wound infections (7, 8), and respiratory diseases (9, 10). Clinical microbiologists are just starting to consider the multispecies nature of pathogenic biofilms and its implications for prevention and treatment (11).

Exemplars of chronic, multispecies biofilm infections are those that occur consistently in the lungs of patients with cystic fibrosis (CF), a genetic disorder in humans as a result of mutations in the cystic fibrosis transmembrane conductance regulator. Disruption of this protein's function results in pathologies throughout the body including the accumulation of highly viscous mucus in the lungs, which hinders normal mucociliary clearance. As a result, bacterial and fungal pathogens that would otherwise be easily removed from healthy lungs instead accumulate and lead to chronic infections (12). Chronic CF lung infections are caused by diverse and metabolically flexible populations and consortia, and they are extremely recalcitrant to antibiotic and phagocytic clearance (13). While the ecology of the infecting species shapes the community and potentially has a profound influence on disease severity in the CF lung, it remains poorly understood (9). Given that the spatial interactions of pathogens can strongly affect disease outcome (14), we aimed to create an experimental model in vitro to investigate the biofilm formation kinetics of one or more species in coculture. Studies of multispecies biofilm formation and biofilm dynamics in general benefit tremendously from high-resolution imaging, which allows for studying the cell-length-scale behaviors and higher-order structures that contribute to the community's cumulative

growth, organization, and function. However, imaging live biofilms in situ is often difficult, if not impossible, in many natural contexts. A helpful strategy to mitigate this problem is to reconstitute key features of the *in-situ* environment using an in vitro system that is more amenable to imaging.

Here, we chose to study *Pseudomonas aeruginosa* and *Candida albicans* as representatives of potentially interacting species in a polymicrobial CF infection, as both these species are commonly isolated from CF lung infections and believed to be important co-pathogens in patients (15). They are also thought to cooccur in other infection environments, including trauma wounds and surrounding urinary catheters (16). *C. albicans* is a polymorphic and opportunistic pathogen with the ability to form invasive hyphal filaments and drug-resistant biofilms (17). *P. aeruginosa* is another opportunistic pathogen with diverse virulence mechanisms, to which biofilm formation contributes directly and indirectly (18). *P. aeruginosa-C. albicans* interactions are well studied in liquid and agar colony models. Among the primary findings from this literature, *P. aeruginosa* has been shown to preferentially attach to and form biofilms on *C. albicans* hyphae in static culture, eventually killing them (19), but *P. aeruginosa* also inhibits the yeast-to-hyphal switch of *C. albicans* in liquid and agar colony cultures, enhancing *C. albicans* survival (20). Prior work has intimated a feedback loop whereby *C. albicans* produces ethanol, which increases biofilm formation, inhibits swarming motility, and enhances the production of antifungal phenazines on the part of *P. aeruginosa* (21, 22). These phenotypes in turn cause downregulation of the central pathway that induces hyphal growth and inhibit mitochondrial activity, stimulating further ethanol production by *C. albicans* (23). On the other hand, some in vivo experiments using a zebrafish model have indicated mutually enhanced virulence of the two species, suggesting that environmental shifts may have strong impacts on the properties of cocultures of these microbes (24). As local concentrations of metabolic products involved in interspecies interactions are determined by the relative and absolute abundances, it is critical to understand the dynamics of biofilm formation for each species in mixed culture.

Using engineered strains with novel fluorescent protein constructs and microfluidic culture with a modified synthetic sputum medium allowing for high-resolution imaging of *C. albicans* and *P. aeruginosa*, we show that their biofilm architecture, rates of biovolume accumulation, and total biovolume is higher for each species in coculture versus monococulture. Growth stimulation for either species was not observed in planktonic coculture conditions. This result is robust to different clinical strains of *P. aeruginosa* and a variety of deletion mutants lacking factors known to participate in *P. aeruginosa*-*C. albicans* interactions.

4.3 Results

Biofilm profiles in mono- and dual-species culture

We aimed to characterize the architecture of monospecies and dual-species biofilms of *P. aeruginosa* and *C. albicans* under flow in a medium that represents the chemical composition of CF sputum. Synthetic cystic fibrosis medium (SCFM2), developed and refined by the Whiteley group (25, 26), is a field standard for this purpose, but this medium is not optically clear due to the presence of reconstituted mucins. To generate an optically clear medium for imaging—and supported by data showing that *P. aeruginosa* does not degrade mucins itself (27)—we made a modified version of SCFM in which the major mucin glycans were substituted for mucin; we term this modified medium artificial sputum medium for imaging, or ASMi (see Materials and Methods). Each species' growth profile was the same SCFM2 as it was in ASMi (see Fig. S1 in the supplemental material).

P. aeruginosa and *C. albicans* were modified by allelic exchange to contain a chromosomal construct for constitutive expression of tandem, codon-optimized copies of mKO-κ (*P. aeruginosa*) or a single copy of mKate2 (*C. albicans*) (see Materials and Methods). mKO-κ or mKate2 was selected for these studies for their brightness and because they could be easily distinguished by fluorescence microscopy. The fluorescent protein expression constructs did not alter the growth rate of either species (Fig. S2).

To investigate mono- and dual-culture biofilm growth under flow of ASMi, we inoculated derivatives of *P. aeruginosa* strain PA14 and *C. albicans* strains CAI4 either alone or together in microfluidic devices (see Materials and Methods). Monococulture *P. aeruginosa* chambers contained small biofilms with compact microcolonies on the order of 10 μm in height (Fig. 1A). Monococulture biofilms of *C. albicans* contained scattered clusters of groups of elongated yeast, many pseudohyphae, and some true hyphae that spanned the height of the chamber (Fig. 1B). By visual inspection of confocal images, it was quickly clear that the architecture and total accumulation of both species were quite different in dual-inoculated conditions compared to the monococulture biofilms. In coculture, *C. albicans* had largely formed true hyphae (Fig. 1C). Quantification of *C. albicans* biovolume found a higher biovolume density near the base of the biofilm in coculture conditions (Fig. 1D). In coculture, *P. aeruginosa* biofilms localized to the hyphae of the highly filamentous *C. albicans* biofilms (Fig. 1C). The biovolume accumulation of *P. aeruginosa* in coculture appeared greater, particularly in the regions also colonized by *C. albicans* (0 to 12μm from the glass substratum) (Fig. 1D).

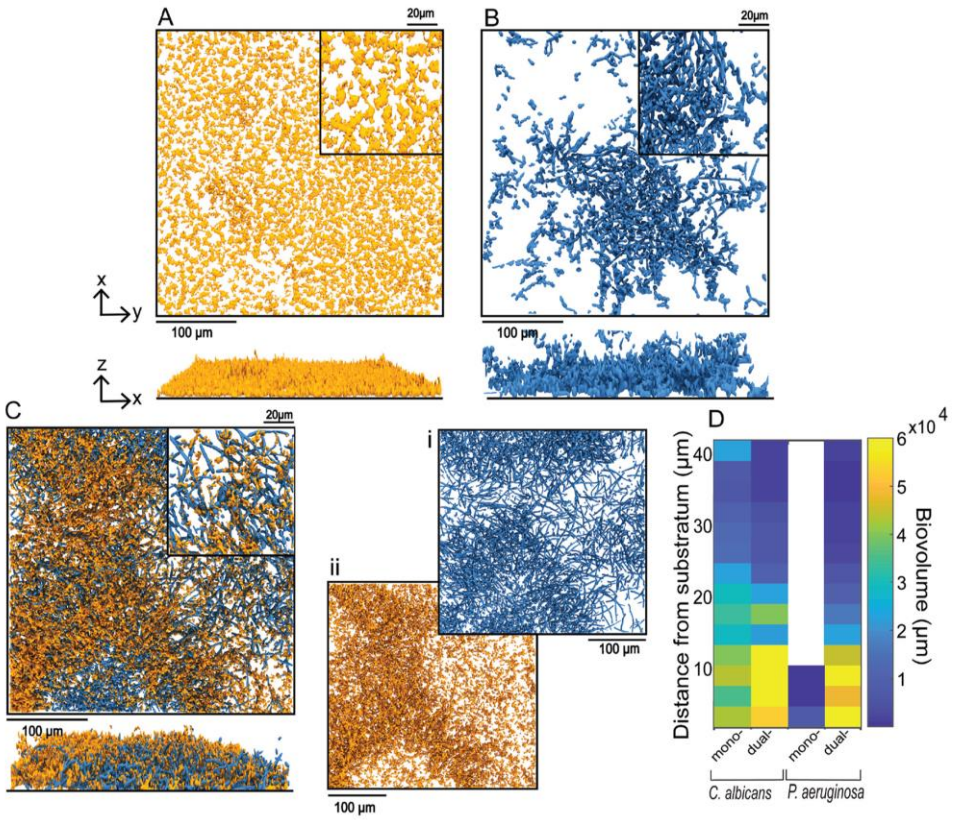

FIG 1. Representative images of mono- and dual-species biofilms of *P. aeruginosa* and *C. albicans*. Three-dimensional (3-D) renderings of 24-h-old monospecies biofilms of *P. aeruginosa* (A) and *C. albicans* (B). Bottom panels show side views of the same images as those above them. (C) *P. aeruginosa*-*C. albicans* dual-species biofilm at 24 h. Split channel of *C. albicans* biofilm (i) and *P. aeruginosa* biofilm (ii) from the *P. aeruginosa*-*C. albicans* dual-species biofilm. (D) Heat maps of *C. albicans* and *P. aeruginosa* biovolume as a function of height from the base substratum in mono- and dual-species biofilms from panels A to C.

Quantitative analysis of image stacks from replicate biofilms collected from independent experiments found that the total biovolume of both species increased substantially in coculture relative to monococulture (Fig. 2A and B). The increase in biofilm biovolume in coculture was significant by 24 h for *C. albicans* (Fig. 2A) and for *P. aeruginosa* (Fig. 2B). In order to determine whether the increase in biovolume required the presence of *P. aeruginosa* at the time of initial colonization, we added *P. aeruginosa* or a medium-only control to *C. albicans* 24-h-old biofilms. In these experiments, the *P. aeruginosa* cells were spiked into the chambers for 1 h, followed by a return to sterile ASMi medium. In

control experiments, the same spiking procedure was performed but with sterile ASMi medium. While *C. albicans* biofilm accumulation followed its normal monococulture profile in the control condition, *C. albicans* biofilm development significantly increased over the subsequent 12 h after the introduction of *P. aeruginosa* (Fig. 2C). To determine whether any mechanical disturbance was sufficient to induce the increase in *C. albicans* biomass accumulation, we introduced 1-μm-diameter inert fluorescent beads to the chambers containing *C. albica* , but we saw no change in biofilm architecture or biomass (Fig. S3).

The enhancement of *C. albicans* biofilm volume by the presence of *P. aeruginosa* was not likely due to an overall improvement in growth when both species are present. In comparison experiments in which both organisms were cultivated planktonically in shaking liquid ASMi medium, the reverse pattern was seen for *C. albicans*: its population density was substantially lower in the presence of *P. aeruginosa* than in its absence (Fig. 2D), recapitulating previously established antagonistic *C. albicans -P. aeruginosa* interaction in liquid growth conditions (19, 28, 29). The population density of *P. aeruginosa* did not change in the presence of *C. albicans* in liquid culture (Fig. 2E). We infer from this outcome that the increase in accumulation of both species in microfluidic coculture is specific to the biofilm environment. Because increased rate of biovolume increase can result from higher retention of cells in the chambers due to decreases in active dispersal or disruption by fluid flow, we quantified the cells in the effluent collected from the outlet of the microfluidic chambers (see Materials and Methods). Significantly fewer *C. albicans* cells were found in the effluent from dual-species biofilms (Fig. 2F). *P. aeruginosa* cell concentration in effluent stayed the same in absolute terms (Fig. 2F) but was lower upon normalization to the amount of biovolume in the biofilm chamber (Fig. S4).

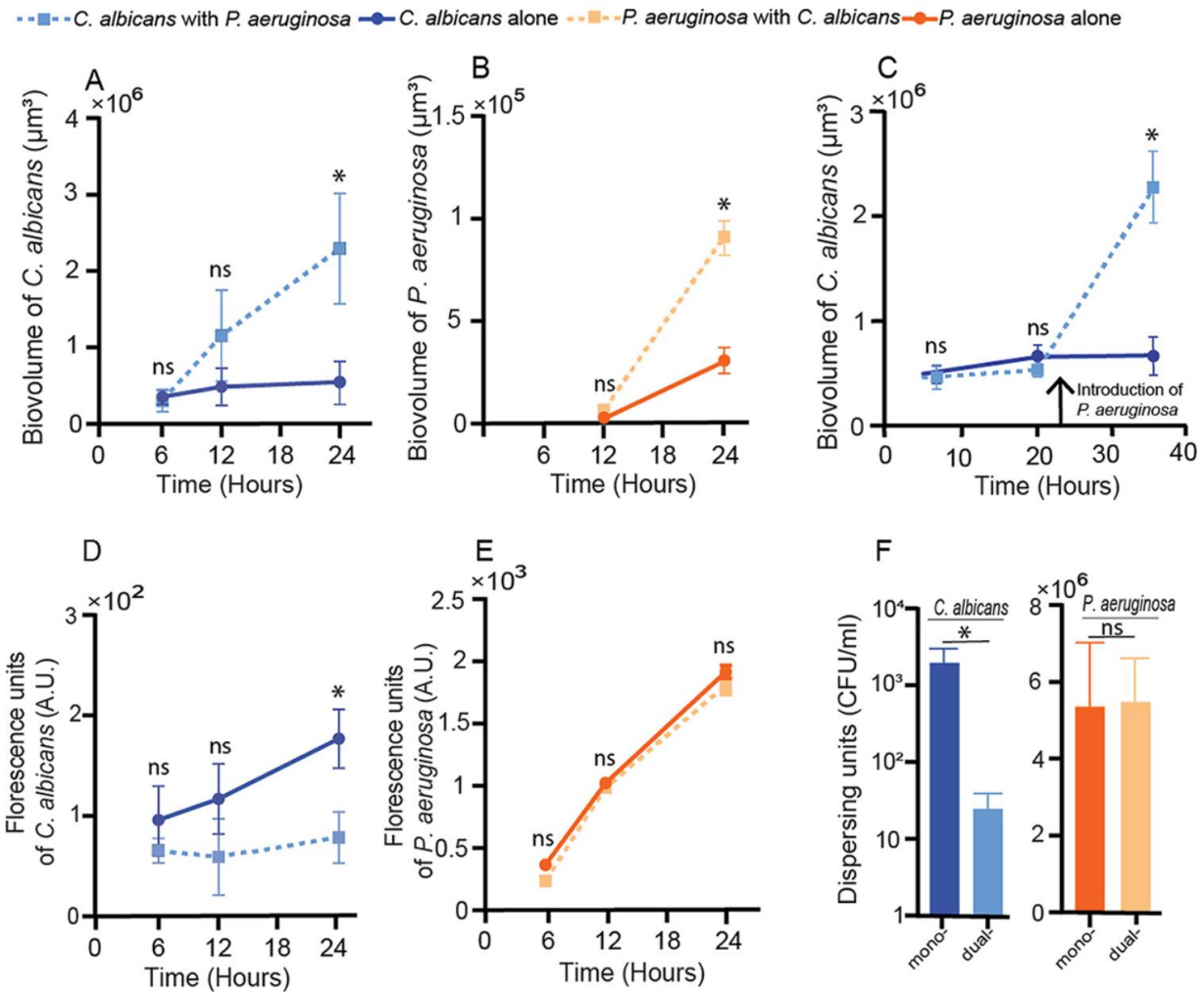

FIG 2. *P. aeruginosa* and *C. albicans* in mono- and dual-species culture. (A) Biovolume of *C. albicans* in mono- and dual-species biofilms (n= 24). (B) Biovolume of *P. aeruginosa* in mono- and dual-species biofilms (n= 24). (C) Biovolume of *C. albicans* biofilms initially grown in mono and coculture, with the addition of *P. aeruginosa* at the time point indicated by the vertical arrow. For the control, sterile medium was added in place of *P. aeruginosa* (n= 18). (D) Fluorescence counts of *C. albicans* in mono-and dual-species shaking liquid cultures (n= 10). (E) Fluorescence counts of *P. aeruginosa* (in arbitrary units [A.U.]) in mono- and dual-species shaking liquid cultures (n= 10). (F) Dispersing cells of *P. aeruginosa* and *C. albicans* in mono- and dual-species biofilms (n= 11). Error bars in panels A to E denote standard deviations; error bars in panel F denote standard errors. *, P,0.05 by Wilcoxon signed-rank test with Bonferroni correction, ns, not significant.

Exploration of *P. aeruginosa* genes potentially involved in augmenting *C. albicans* biofilms in coculture.

We repeated the mono- and coculture experiments above with mutants of *P. aeruginosa* that have been implicated in altered biofilm morphology or interspecies interaction in prior work. Analyses included mutants defective in the Pel exopolysaccharide production (ΔpelA [30, 31] and ΔwspR[32]), metabolic regulators and products important for biofilm formation (Δanr[33] and Δphz[34]),extracellular adhesins (ΔbapA[35], ΔpilY1[36]), quorum sensing (ΔlasR[37]), and siderophore production (ΔpvdApchE[38]). *C. albicans* increased its accumulation by an order of magnitude or higher in biofilms with any of these mutants, maintaining the trend seen with wild-type *P. aeruginosa* PA14 (Fig. 3A and Fig. S5). In contrast, not all *P. aeruginosa* mutants were equal in their capacity for biofilm formation or for stimulation of biofilm biovolume in the presence of *C. albicans* (Fig. 3B). The ΔpelA and ΔwspR mutants were not defective in biofilm biovolume compared to the wild type, which is consistent with the low detection of Pel extracellular matrix carbohydrate (Fig. S6). Thus, the increased biovolume of *P. aeruginosa* was not due to increased *P. aeruginosa* matrix production. Previously characterized mutants defective in secreted phenazine toxins and pyochelin and pyoverdine siderophores also caused the stimulation of *C. albicans* biofilm accumulation. *P. aeruginosa* mutants with lower levels of monospecies biofilm (Δanr, ΔlasR, ΔbapA, and ΔpilY1) were less stimulated by *C. albicans* at the 24-htime point. It is interesting to note that the amount of *P. aeruginosa* biofilm biomass present did not correlate with the degree of biomass increase in *C. albicans* (Fig. 3C); that is, any addition of *P. aeruginosa*, regardless of its native biofilm-producing capacity, was sufficient to produce a similar increase in accumulation of *C. albicans*.

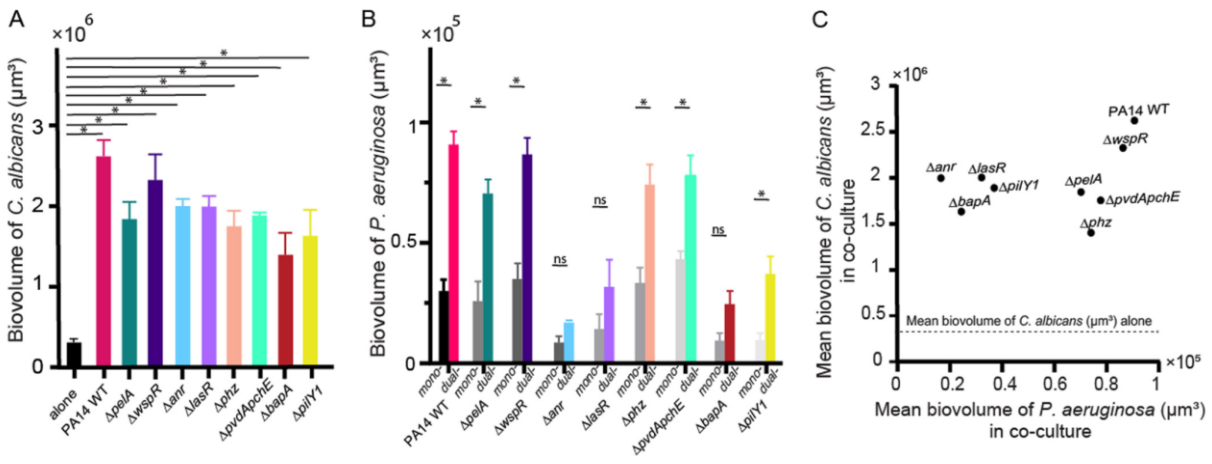

FIG. 3 Deletion mutant assays and medium influent assays to explore the causes of mutual enhancement between *P. aeruginosa* and *C. albicans* in biofilms. (A) Biovolume of *C. albicans* grown in dual-species biofilms with *P. aeruginosa* deletion mutants at 24 h (see main text for mutant descriptions, n= 9 to 24). (B) Biovolumes of mono- and dual-species *P. aeruginosa* biofilms at 24 h (n= 9 to 24). All error bars indicated are standard errors. (C) The mean values of *C. albicans* biovolume are plotted against the corresponding mean value of wild-type (WT) *P. aeruginosa* PA14 and mutant biovolume from their respective dual-species biofilms. There is no significant correlation between the two (linear correlation analysis; P= 0.391; r2= 0.107). *, P,0.05 by Wilcoxon signed-rank test with Bonferroni correction.

P. aeruginosa-C. albicans interaction is robust to CF isolate variation.

After documenting that wild-type PA14 could induce an increase in biofilm biomass accumulation of *C. albicans*, we were curious to see whether this effect was consistent across recent CF clinical isolates of *P. aeruginosa* as well. To explore this question, we obtained *P. aeruginosa* clinical isolates from a patient who was infected with both *P. aeruginosa* and *C. albicans*, and we grew them in mono- or coculture with *C. albicans* in our microfluidic model underflow of ASMi. We found that *C. albicans* biofilm increased significantly in coculture with all clinical isolates, consistent with the results reported above for wild-type PA14 (Fig. 4A). Likewise, for all but one isolate, the biofilm growth of *P. aeruginosa* was greater in coculture with *C. albicans* than it was in mono coculture (Fig. 4B). Though all clinical *P. aeruginosa* isolates prompted an increase in *C. albicans* biofilm accumulation, there was some variance in the degree to which this was the case

(Fig. 4A). This variation made us wonder whether the spatial association between *C. albicans* and different clinical isolates of *P. aeruginosa* might differ as well. To assess this possibility, we grew the different clinical isolates together with *C. albicans*, acquired high-resolution images of coculture biofilms, and quantified the spatial cooccurrence of the two species via their density correlation (39). When averaged across all image replicates, the spatial correlations between *C. albicans* and clinical isolates of *P. aeruginosa* generally were not different from that between *C. albicans* and wild-typePA14 (Fig. 4C). After visualizing the density correlation measurement at high spatial resolution, on the other hand (Fig. 4D), it was clear that for some clinical P. aeruginosa isolates, the spatial association with *C. albicans* was homogenous, while for others it was patchy. Previous work has suggested that heterogeneity within a strain population—here, with respect to spatial cooccurrence with *P. aeruginosa* and *C. albicans* —can impact survival in variable environmental conditions (40–42). The significance of this result for the infection ecology of these two species is not yet clear, but it is notable that among isolates of *P. aeruginosa* from the same patient, the architecture of joint biofilms with *C. albicans* can differ substantially at the micrometer scale (Fig. 4D) even when they appear to be the same or similar when averaged on a larger spatial scale (Fig. 4C).

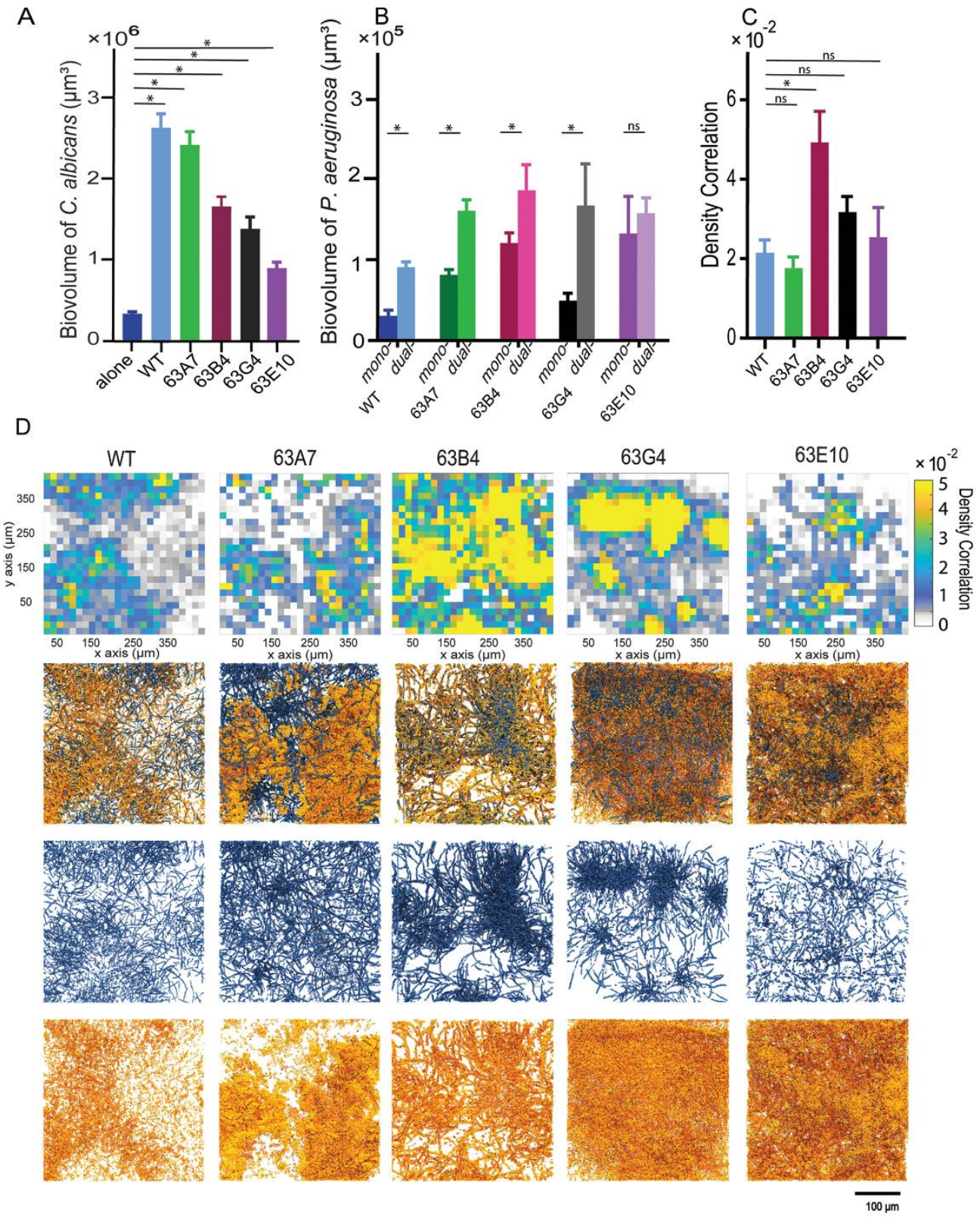
A
Biovolume of C. albicans (µm³)
×10⁶
alone
WT
63A7
63B4
63G4
63E10
B
Biovolume of P. aeruginosa (µm³)
×10⁵
mono
dual
C
Density Correlation
× 10⁻²
ns
D
WT
63A7
63B4
63G4
63E10
y axis (µm)
x axis (µm)
Density Correlation
100 µm

FIG. 4 Biomass accumulation, density correlation analysis, and visualization of *C. albicans* in coculture with different CF clinical isolates of *P. aeruginosa*. (A) Biovolume of *C. albicans* grown as dual-species biofilms with *P. aeruginosa* clinical isolates along with wild-type (WT) PA14 for comparison at 24 h (n = 18). (Biovolumes of *P. aeruginosa* clinical isolates in mono and coculture and dual culture with *C. albicans* at 24 h (n = 18). (C) Global density correlation measurements of WT P. aeruginosa and clinical isolates and *C. albicans* biofilms (n = 6). *, P, 0.05. (D) Visualization of dual-species biofilms of *P. aeruginosa* and *C. albicans*. From top to bottom, spatially resolved density correlation, 3-D renderings of dual-species biofilms, *C. albicans* channel split, and *P. aeruginosa* channel split.

4.4 Discussion

Interest in multispecies biofilms including microbes from different domains of life has been intensifying in recent years, as it is increasingly appreciated that many microbial communities—both inside and outside host organisms—are polymicrobial (43). One of the most highly referenced examples of polymicrobial infections are those within the lungs of patients with CF, and two of the common members of these communities are the opportunistic pathogens *P. aeruginosa* and *C. albicans* (12). Here, we sought to compare the kinetics of biovolume accumulation in mono- and dual biofilms of these two organisms using a new model of biofilm growth under flow of optically clear artificial sputum medium. We demonstrated a marked increase of biofilm biomass accumulation as well as a decrease in cells in biofilm effluent in dual-species culture relative to mono and coculture. These results were robust to a variety of mutant and clinical strain backgrounds of *P. aeruginosa*, and they contrast with the findings of some previous studies of these two organisms in static liquid or agar colony culture (44, 45). We identify an important element driving the increase in biomass accumulation as fluid flow in the dual species biofilm milieu, which is a key novelty of this experimental approach for the study of *P. aeruginosa*-*C. albicans* interactions.

Extensive prior work has shown that *P. aeruginosa* and *C. albicans* interact with each other

through a complex web of secreted factors, including phenazines, siderophores, ethanol, and quorum-sensing autoinducers, which altogether alter environmental iron availability, pH, and oxygen tension. Under static culture conditions (i.e., liquid batch culture or agar colonies), the net result of these interactions is usually antagonism of *P. aeruginosa* against *C. albicans*. It is important to note as well that secreted factors from each species have different and sometimes opposite effects on each other's propensity to produce biofilms or to remain in a dispersive, planktonic state (28, 46). As noted above, when flow - known to impact microbial physiology and surface interaction - is introduced into the two-species system, we see increased filamentation of *C. albicans* and increased biofilm biomass accumulation by both species, accompanied by a decrease in cells exiting the chamber.

While at first glance this may give the impression of mutual benefit, it is also possible that the two species are simply competing for access to space and resources by upregulating adhesion factors (47–49). But why is *P. aeruginosa* no longer able to directly antagonize and kill *C. albicans*, as has been shown previously in static culture? We speculate that introduction of flow fundamentally changes the secreted solute environment created by the two organisms, perhaps with some secreted factors more strongly retained in the biofilm matrix than others, and that this change in solute environment relative to static culture shifts the ecological pattern of biomass accumulation to one in which both species are augmented. It is also possible that over time the dual-species biofilms become densely packed enough to block flow within some regions, allowing secreted products and variation in iron/oxygen availability to accumulate in a patchy manner that contributes to induction of biofilm production by both species.
The precise spatial patterns of exoproduct accumulation in relation to cells and the highly complex matrix that Candida secretes is an important area for future work (50–52).

Our deletion mutant analysis included all the major classes of behavior in *P. aeruginosa* currently known to mediate solute-based interactions with *C. albicans*, but in all cases, the presence of *P. aeruginosa* caused qualitatively the same increase in *C. albicans* biofilm. This suggests that there may be other factors in addition to flow-mediated changes in solute

environment contributing to our results. For example, the introduction of shear stress under flow is an entirely new environmental stimulus relative to static culture, and one which is known via extensive work to be crucial to microbial ecology and evolution (53–58). The flow regime can dramatically alter the morphology and resilience of bacterial biofilms down to their cellular resolution architecture (59, 60), with important implications for pathogenesis in the case of infections (61). Adaptation to the challenges of flow at submillimeter spatial scales has influenced the evolution of bacterial surface motility (2), optimal growth rate in porous media (62), surface colonization mechanisms (63–65), extracellular matrix secretion (66, 67), bacterial cell shape (64, 68–70), planktonic aggregate formation (71), and biofilm community assembly and function (62, 72–75), among many other examples.

The range of spatial structures of *P. aeruginosa* clinical isolates that we observed in dual-species biofilms with *C. albicans* suggests the possibility of between-strain variance in spatial occupation strategy within the CF lung. Since the clinical isolates come from a single CF patient, this variation in biofilm morphology could be the outcome of selection in different spatial locations in the lung, which may have variable *C. albicans* abundance or exposure to antibiotics, toxins, mutagens, nutrient availability, or host immune attack (40, 41). Although the increase in biovolume of both species in dual *P. aeruginosa*-*C. albicans* biofilms varied to an extent, increase of *C. albicans* accumulation was consistent across *P. aeruginosa* isolates. This result prompts us to speculate that the chance encounter of *C. albicans* with *P. aeruginosa* in the CF environment could ultimately lead to changes in disease progression by altering the tendency of the fungus to locally accumulate.

In light of our results, it is important to note that the flow regime has documented effects on biofilm formation for both *P. aeruginosa* and *C. albicans*. The surface residence time of *P. aeruginosa*, for example, increases linearly as shear stress increases (76), and flow promotes upstream surface motility in addition to the formation of bio- film aggregates (77). *P. aeruginosa* has also recently been shown to be highly responsive to mechanical stress induced by flow, with downstream effects on biofilm formation that have yet to be

fully clarified (36, 78). There has been less investigation of the effects of shear flow on *C. albicans* biofilms: existing work does not agree completely on whether shear stress increases total biomass of *C. albicans* biofilms but does agree that biofilms formed under shear are more highly compacted and physically robust relative to those grown in static conditions (79). Importantly, given that dual-species culture produced substantial biomass accumulation for both species relative to mono- coculture under the same flow conditions, flow-induced shear cannot on its own explain our results. Rather we infer that a combination of physical forces resulting from flow in addition to biological interaction between the two species must be responsible for the results obtained here. Dissecting the precise molecular mechanisms of these interspecies interactions is an important area for future study that may bear directly on the outcome of multispecies biofilm growth in the context of infection.

Beyond their prevalence in lung infections among patients with CF, *P. aeruginosa* and *C. albicans* individually are among the most common agents of nosocomial infection currently known (16). They are both frequently isolated from device-related infections, including implanted medical devices, prosthetic implants in wounds and joint replacements, and urinary catheters (16). Both species participate in multispecies infections, for example, with Staphylococcus spp. (80–82), with Streptococcus spp. (83, 84), and with each other (85). Reports of dual isolation of *P. aeruginosa* and *C. albicans* are increasingly reported in the clinical literature in sites such as ventilator tubing (86), and our results of biofilm dual-species culture in microfluidic devices suggest that dual Pseudomonas-Candida biofilms may be especially problematic in this setting because they tend to accumulate more biofilm biomass together than alone. Such rapidly accumulating biofilms can potentially clog catheter flow environments and seed systemic infections as cells disperse from the device-attached biofilm into the bloodstream.

Though recent studies have made tremendous strides in imaging microbiomes within in situ samples that have been fixed (87–90), dissecting live microbial community structure in space and time within native environments remains a challenging task and one of the important frontiers of modern microbiology. Here, we use an in vitro model with medium

tuned to the CF sputum environment to assess live biofilm population dynamics for both members and find that this step toward environmental realism has a strong impact on the ecology of dual-species biofilms of *P. aeruginosa* and *C. albicans*. Many native factors are still missing, however: the mucosal environment is quite different in the native lung, for example, and recent work has suggested that mucus has a strong impact on *P. aeruginosa* physiology, including reducing its propensity toward virulence and biofilm formation (91, 92). Though not an exact match to the in-situ infection environment, our system nevertheless suggests that modest changes to the environmental context in which multispecies interactions are studied can have a large impact on the observed outcome, namely, in this case, a shift toward far higher accumulation of biofilm on the part of *P. aeruginosa* and *C. albicans* when they are together versus when they are alone. On the basis of this observation, we specula pushing toward realism and high-resolution image analysis of biofilm communities will yield important and unexpected insights for many other microbial systems.

4.5 Materials and Methods

Strains and media.

Table 1 includes a full list of strains and plasmids used in this study. Strains of *P. aeruginosa* are either derivatives of strain PA14 or clinical isolates. *C. albicans* strains are derivatives of strain CAI4. All strains were grown on LB (10 g tryptone, 5 g NaCl, 5 g yeast extract [all amounts per liter]) and artificial sputum medium for imaging (ASMi) (*P. aeruginosa*) or YPD (10 g yeast extract, 20 g peptone, and 20 g dextrose [all amounts per liter]) and ASMi (*C. albicans*). The medium recipes and concentrations of reagents used for ASMi are listed below at the end of Materials and Methods. All chemicals and reagents were purchased from Millipore Sigma unless otherwise stated.

Table 1: Strains and plasmids used in this study

Species and strain	Relevant marker(s) or genotype(s)	Reference or source
E. coli		
S17-1	*λpir*	Lorenzo and Timmis (100)
P. aeruginosa PA14		
CNP17	Wild type (WT)	Hogan lab
CNP26	WT with mKO-κ	This study
CNP12	Δ*pelA*	Friedman and Kolter (30)
CNP27	Δ*pelA* with mKO-κ	This study
CNP18	Δ*wspR*	Chen et al. (21)
CNP28	Δ*wspR* with mKO-κ	This study
CNP70	Δ*bapA*	Hogan lab
CNP77	Δ*bapA* with mKO-κ	This study
CNP65	Δ*pilY1*	Hogan lab
CNP67	Δ*pilY1* with mKO-κ	This study
CNP21	Δ*anr*	Hogan lab
CNP50	Δ*anr* with mKO-κ	This study
CNP69	Δ*pchEpvdA*	Hogan lab
CNP76	Δ*pchEpvdA* with mKO-κ	This study
CNP22	Δ*lasR*	Hogan lab
CNP56	Δ*lasR* with mKO-κ	This study
CNP41	Δ*phz*	Hogan lab
CNP54	Δ*phz* with mKO-κ	This study
CNP43	63LB4 clinical CF isolate	Hogan lab
CNP44	63LG4 clinical CF isolate	Hogan lab
CNP45	63RA7 clinical CF isolate	Hogan lab
CNP46	63RE10 clinical CF isolate	Hogan lab
CNP59	63LB4 clinical CF isolate with mKO-κ	This study
CNP57	63LG4 clinical CF isolate with mKO-κ	This study
CNP60	63RA7 clinical CF isolate with mKO-κ	This study
CNP58	63RE10 clinical CF isolate with mKO-κ	This study
C. albicans CAI4		
CNC1	WT with pACT-GFP	Hogan lab
CNC11	WT with pACT mKATE2	This study

Plasmid and strain construction.

All restriction enzymes and ligase were purchased from New England Biolabs, and PCR reagents were purchased from Bio-Rad. The *P. aeruginosa* tandem codon-optimized

version of mKO-κ was custom synthesized by Invitrogen. The construct contains two copies of mKO-κ in tandem, each with its own ribosome binding site, and with different codon composition to prevent excision by recombination. Fluorescent *P. aeruginosa* derivatives were constructed by amplification of the flanking regions upstream and downstream of the Tn7 att site and fusion of the custom fluorescent protein construct to a synthetic tac promoter for high expression from a single chromosomal locus. This fused construct was cloned into the pMQ30 plasmid used for allelic exchange in *P. aeruginosa* (93). This plasmid was then introduced into Escherichia coli S17-lpir by electroporation and conjugated into *P. aeruginosa*, and recombinants were obtained using selection on gentamicin and sucrose counter-selection for loss of the integrated plasmid backbone. For *C. albicans*, a single codon-optimized version of mKate2 was custom synthesized by Invitrogen. The RP10 integrative plasmid, pACT-GFP (94), has been shown to have constant expression levels through *C. albicans* growth cycle. We replaced the green fluorescent protein (GFP) in pACT-GFP (94) with mKate2. For transformation into *C. albican*, the mKate2- containing plasmid was linearized by BglII restriction digestion and concentrated using the Zymo Research DNA Clean & Concentrator-5 kit (catalog no. 11-303), and 1mg was electroporated into electrocompetent *C. albicans* CAI4 prepared as previously described (95). Prototrophic recombinants were selected for on uracil drop-out medium.

Liquid growth curve and fluorescence measurements.

P. aeruginosa strains were grown at 37°C shaking in LB overnight prior to growth curve experiments. The following morning, cultures were back- diluted to an optical density at 600 nm (OD600) of 0.01 in ASMi in 10-ml glass tubes with 2 ml medium (for fluorescence growth curves) or 50-ml Falcon tubes with 30 ml of medium (optical density growth curves), rotating at 250 rpm on an incubated orbital shaker at 37°C. *C. albicans* strains were grown at 30°C shaking in YPD overnight prior to growth curve experiments. They were cultivated overnight at 30°C to maintain cells in yeast form prior to the start of growth curve or biofilm experiments (see below).
The following morning, cultures were back-diluted to an OD 600 of 0.01 in ASMi in 10-

ml glass tubes with 2 ml medium (for fluorescence growth curves) or 50-ml Falcon tubes with 30 ml of medium (optical density growth curves), rotating at 250 rpm on an incubated orbital shaker at 37°C. Fluorescence measurements were made using a Synergy Neo2 every 6 h. A 543-nm excitation source was used to excite mKO-κ, and a 594-nm excitation source was used to excite mKate2. Optical density measurements were made every hour using a benchtop spectrophotometer (CWA Biowave CO8000 cell density meter).

Microfluidic device assembly.

The microfluidic devices were made by bonding polydimethylsiloxane (PDMS) chamber molds to size #1.5 cover glass slips (60 mm X 36 mm [length L X width W], Thermo-Fisher, Waltham, MA) using standard soft lithography techniques (96). Each PDMS mold contained four chambers, each of which measured 3,000µm X 500 µm X 75 µm (L X W X Depth D). To establish flow in these chambers, medium was loaded into 1-ml BD plastic syringes with 25-gauge needles. These syringes were joined to #30 Cole-Parmer polytetrafluoroethylene (PTFE) tubing (inner diameter,0.3 mm), which was connected to prebored holes in the microfluidic device. Tubing was also placed on the opposite end of the chamber to direct the effluent to a waste container. Syringes were mounted to syringe pumps (Pico Plus Elite, Harvard Apparatus), and flow was maintained at 0.1 ml per min for all experiments.

Biofilm growth, matrix staining, and CFU counts.

Overnight cultures of *P. aeruginosa* were grown at 37°C with shaking in LB, and overnight cultures of *C. albicans* were grown at 30°C with shaking in YPD prior to the start of biofilm experiments. Cultures of both strains were normalized to an OD 600 of 0.05 in ASMi medium. If dual species biofilms were to be started, equal volumes of OD-equalized strains were mixed, inoculated into a microfluidic chamber (completely filling its inner volume), and then allowed to rest for 1 h at 37°C to permit cells to attach to the glass sur- face. The devices were then run at 0.1 ml per min at 37°C and imaged by confocal microscopy (see below) at time intervals that varied per experiment as noted in each figure. All experiments

were repeated with at least five biological replicates with three or more technical replicates on different days. Total replicates for each experiment are noted in the figure legends for each data set in the text and supplemental material.

Wisteria floribunda lectin stain (Vector Labs) conjugated to fluorescein dye was used to visualize Pel polysaccharide produced by *P. aeruginosa* (31). The lectin was added to the medium in syringes for these experiments such that biofilms would be exposed to the lectin-dye conjugate for the entire period of biofilm growth (20ml stock lectin solution per ml of medium, per the manufacturer's protocol recommendation from a stock solution of 2-mg/ml dye conjugate). Biofilms were inoculated as noted above for these experiments and grown for 24 h prior to imaging.

To compare growth rates of *P. aeruginosa* and *C. albicans* in turbid synthetic cystic fibrosis medium (SCFM) (25) and optically clear ASMi, both species were grown overnight, *P. aeruginosa* in LB at 37°C and *C. albicans* in YPD at 30°C in 10-ml glass tubes with 2 ml of medium. The following morning, the cultures were back-diluted to an OD600 of 0.01 in either SCFM or ASMi in 50-ml Falcon tubes with 30 ml of medium, rotating at 250 rpm in an orbital shaker at 37°C. One milliliter of culture was taken from the Falcon tube at different time points, and serial dilution was performed and plated on LB agar for *P. aeruginosa* and YPD agar for *C. albicans*. The number of CFU from each plate was recorded and used to calculate growth rates measured by CFU per milliliter per time.

To measure passive dispersal from biofilms as a result of exposure to fluid shear, biofilms of both species were grown as noted above in ASMi medium for 24 h, after which the outlet tubing of the micro- fluidic device was changed to ensure we were measuring dispersal only from the biofilms within the chambers themselves. The flow rate was increased to 500ml per min, and outflow was collected. Serial dilutions were performed and plated on LB agar for *P. aeruginosa* and YPD containing 50 mg/ml chloramphenicol for *C. albicans*. The number of CFU from each plate was recorded and used to calculate the CFU/milliliter culture density emerging from the chambers. This experiment was repeated for 11 biological replicates with independent overnight cultures.

Microscopy and image analysis.

Biofilms inside microfluidic chambers were imaged using a Zeiss LSM 880 confocal microscope with a 40 X /1.2 numerical aperture (NA) or 10 X /0.4 NA water objective. A 543-nm laser line was used to excite mKO-κ, and a 594-nm laser line was used to excite mKate2. A 458-nm laser line was used to excite Wisteria floribunda lectin stain in the case of Pel quantification experiments. All quantitative analysis of microscopy data was performed using BiofilmQ (39). Three-dimensional (3-D) renderings of biofilms in Fig. 1 and 4 were made using Paraview.

Statistics.

All statistical analyses were performed in GraphPad Prism. All reported pairwise comparisons were performed using Wilcoxon signed-rank tests, and multiple comparisons were performed by Wilcoxon signed-rank tests with Bonferroni correction. All error bars indicated standard errors unless otherwise noted.

Artificial sputum media for imaging (ASMi).

The stocks for the base were Na2 HPO4 (0.2 M, 0.69 g/ 25 ml), NaH2PO 4 (0.2 M, 0.71 g/25 ml), KNO 3 (1 M, 2.53 g/25 ml), K2 SO4 (0.25 M, 1.09 g/25 ml). Additional stocks were glucose (20% [wt/vol]) autoclave, L -lactic acid (1 M) (adjust pH to 7 with NaOH), CaCl2·2H2O (1 M, 3.68 g/25 ml), MgCl2·6H2O (1 M, 5.08 g/25 ml), FeSO4·7H2O (1 mg/1 ml) syringe, N-acetylglucosamine (0.25 M, 1.383 g/25 ml), tryptophan (0.1 M, 1.021 g/50 ml). Reagents were DNA (herring sperm DNA), fucose, GalNAc, galactose, choline chloride, sodium octanoate, yeast synthetic dropout excluding Trp, NaCl, morpholinepropanesulfonic acid (MOPS), KCl, NH4Cl, and NaOH. Preparation of ASMi (500 ml) (2 in 250 ml) was as follows: 1) add 400 ml distilled H 2O (diH2 O) and stir bar to a clean beaker; 2) while stirring add 3.250 ml Na 2HPO 4 stock, 3.126 ml NaH2PO4 stock, 174 ml KNO 3 stock, 542 ml K 2SO4 stock, 2 g yeast synthetic dropout – Trp, 1.516 g NaCl, 1.046 g morpholinepropanesulfonic acid (MOPS), 558 mg KCl, 62 mg NH4Cl,

4.65 ml L-lactic acid stock, 1.365 ml glucose stock, 875 ml CaCl2·2H2O stock, 600 ml N acetylglucosamine, 500 ml FeSO4·7H2O, 330 ml tryptophan stock, 303 ml MgCl2·6H2 O, 300 mg DNA, 0.007 g choline chloride, 0.022 g sodium octanoate (replacement 1,2-dipalmitoyl-sn-glycero-3-phosphocholine [DPPC]), 400 mg fucose, 125 mg GalNAc, 90 mg galactose, (replacement for mucin; these are mucin sugars); 3) adjust pH to 6.8 with HCl or NaOH and add distilled H2O to 500 ml; 4) filter sterilize.

Considerations and references.

Considerations follow. (i) It lacks sphingolipids and surfactant proteins, which are moderately abundant. (ii) Mucin sugars are used instead of mucin (97). (iii) Reports of some concentrations vary from source to source. References follow: DPPC (98) (octanoate and choline are used instead at the same concentrations; 2:1 octanoate-choline, since DPPC has two lipid chains per choline. DPPC molarity for choline and 2 that for octanoate), DNA (98), and mucin (98).

4.6 Supplemental figures

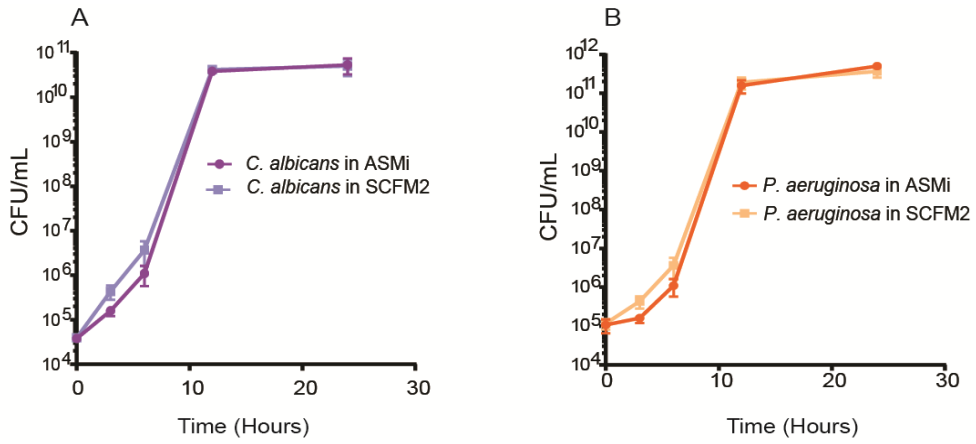

FIG. S1 Growth curves of (A) *C. albicans* and (B) *P. aeruginosa* in standard SCFM2 medium with reconstituted mucin and in ASMi medium containing only mucin sugars without full length mucin polymers ($n = 6$). All error bars indicated are standard errors.

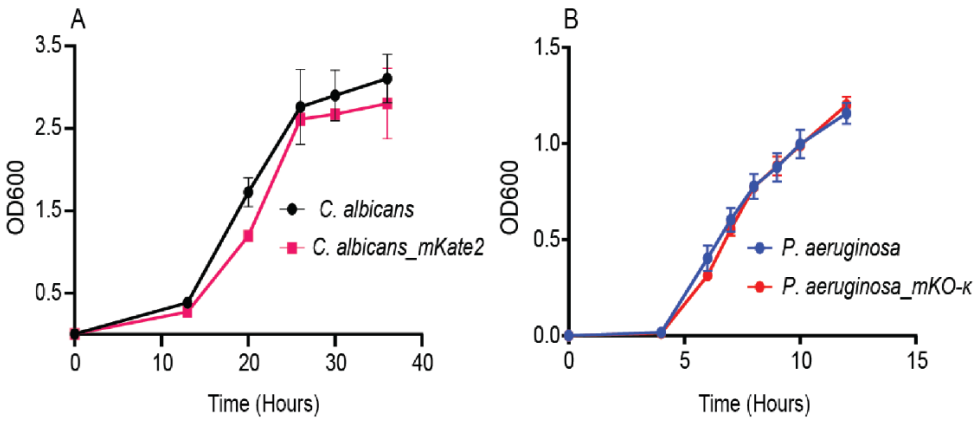

FIG. S2 Growth curves in ASMi medium of (A) wild-type *C. albicans* CAI4 *or C. albicans_ mKate2* and (B) wild type *P. aeruginosa PA14* or *P. aeruginosa_ mKO-κ* ($n = 6$). All error bars indicated are standard errors.

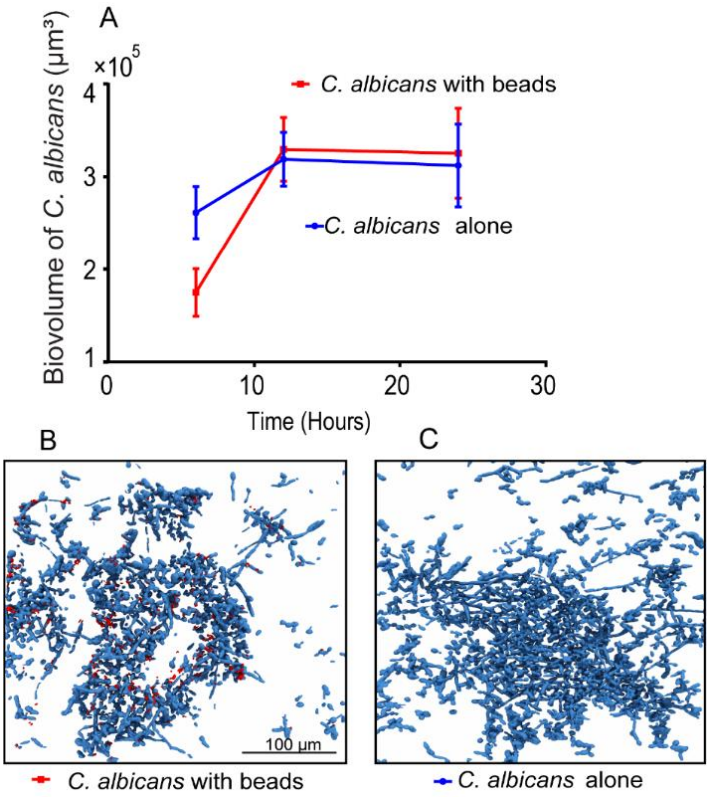

FIG. S3 Inert fluorescent beads were introduced to *C. albicans* expressing *mKate2* biofilms to test for the effect of mechanical disturbance on *C. albicans* biofilm growth. (A) Biovolume of C. albicans with and without fluorescently labeled beads added to the influent medium ($n = 6$). (B) Representative image of C. albicans biofilms grown with fluorescently labeled beads shown in red at the 24-h time point (C) Representative image of C. albicans biofilm in the absence of fluorescent beads in influent medium at 24-h time point. All error bars indicated are standard error.

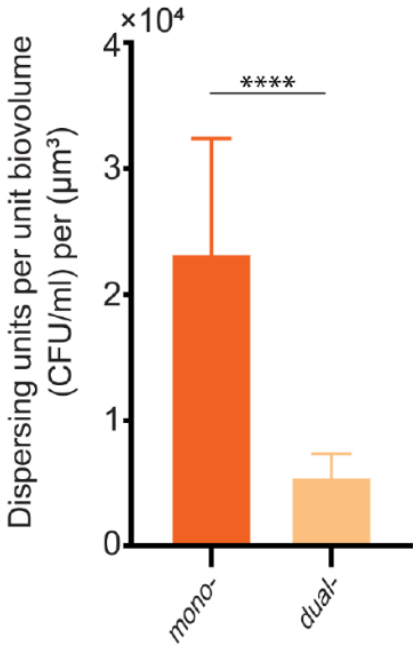

FIG. S4 Passive dispersing *P. aeruginosa* CFU per unit biovolume. Dispersing *P. aeruginosa* obtained from plating cells from the outflow of the microfluidic chamber normalized to biovolume of cells present in the microfluidic chamber ($P < 0.001$; $n = 6$). Reported pairwise comparisons are the result of Wilcoxon signed-rank test. All error bars indicated are standard errors.

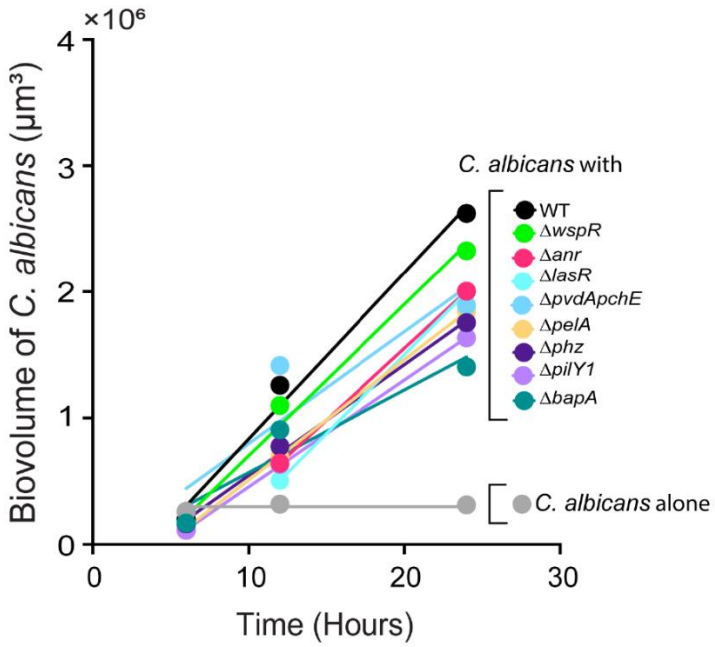

FIG. S5 Slopes of *C. albicans* growth yields. Best fit lines were generated by fitting kinetic biofilm biovolume data by least square regression. The slopes of the best fit lines for growth yields of *C. albicans* grown in the presence of the *P. aeruginosa* mutants were statistically different from the slope determined for *C. albicans* grown alone. ($P < 0.001$ for slope of *C. albicans* with *P. aeruginosa* mutants compared to slope of 0 for *C. albicans* alone as determined by extra sum-of-squares F test.)

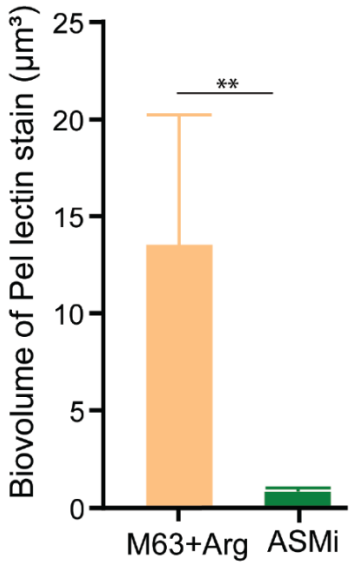

FIG. S6 The matrix polysaccharide Pel was stained and quantified in *P. aeruginosa* strain PA14 biofilms using a fluorescent dye bound to Pel-specific lectin in M63* medium plus arginine, a biofilm assay medium [99]), and ASMi medium ($P < 0.001$; $n = 6$). Reported pairwise comparisons determined by Wilcoxon signed-rank test. All error bars indicated are standard errors. *5X M63 is as follows: 17.5 g dibasic potassium phosphate, 7.5 g monobasic potassium phosphate, 5.0 g ammonium sulfate into sterile 500 ml H_2O. M63 is supplemented to obtain working concentrations of 0.4% l-arginine-monochloride and 1 mM $MgSO_4$.

4.7 Appendix 2

Effect of *P. aeruginosa* supernatant on *C. albicans* biofilms

We found that the addition of *P. aeruginosa* supernatant caused a dramatic decrease in *C. albicans* biofilm accumulation, most pronouncedly when *C. albicans* was inoculated in coculture with *P. aeruginosa* (Figure 1A A and B). Importantly, the PBS control treatment, in which *C. albicans* biomass was unaffected, demonstrates that addition of *P. aeruginosa* supernatants to the biofilm chamber influent does not reduce *C. albicans* accumulation due to a reduction of nutrient availability. Our first thought was that re-introduction of phenazines (46) or rhamnolipid surfactants (101) to the influent media might be primarily responsible for *C. albicans* biofilm biomass. However, supernatants from a *P. aeruginosa* Δ*phz* mutant, which produces no phenazines, resulted in the same outcome as introduction of WT supernatants. Supernatants from Δ*lasR* mutant cultures, which lacks many quorum sensing regulated secreted products including phenazines and rhamnolipids, were partially effective compared to the effects of WT supernatants, suggesting that the effects were likely multifactorial (Figure 2A). The observation that *P. aeruginosa* supernatant remained partially effective after protease treatment supports the model that multiple factors contributed to the effects on biovolume accumulation. Interestingly, it is worth noting that all supernatant activity was lost after boiling.

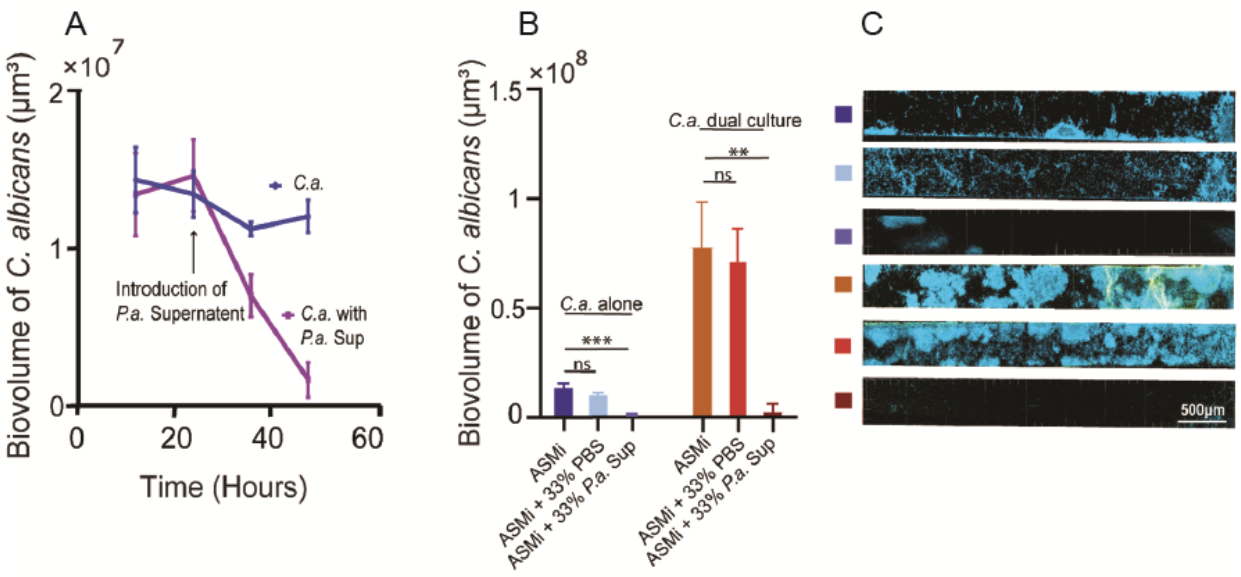

FIG. 1A Effect of *P. aeruginosa* supernatant on *C. albicans* biofilms (A) Biovolume of *C. albicans* biofilm initially grown in monoculture, followed by addition of *P. aeruginosa* supernatant at the time point marked by the arrow. (B) Biovolume of *C. albicans* mono species and dual species biofilms in the presence of different media influent. PBS is used as a control for addition of *P. aeruginosa* supernatants and media dilution. (n=6) (E) CLSM representative images of *C. albicans* and *C. albicans* + *P. aeruginosa* biofilms for conditions in C. For the control, sterile media was added in place of *P. aeruginosa* at the same time point (n=6). * denotes < 0.05. All error bars indicated are standard

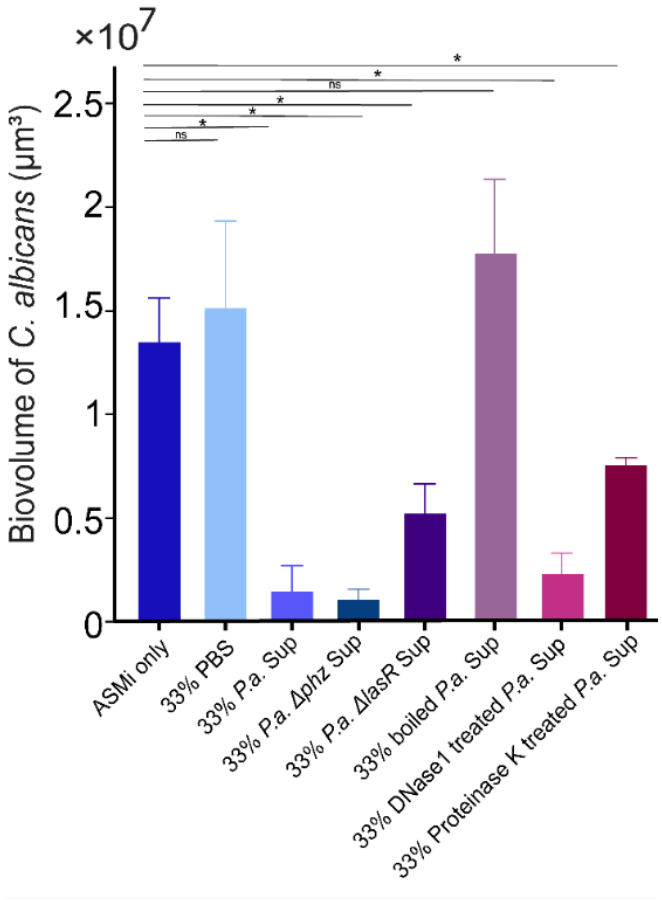

FIG. A2 Supernatants from *P. aeruginosa* mutants and enzyme treated supernatants. Supernatants either from *P. aeruginosa* mutants or supernatant from *P. aeruginosa* PA14 wildtype treated with *Proteinase K, Dnase1* or boiled and then used to grow *C. albicans* biofilms to identify the component in the supernatant responsible for decreased *C. albicans* growth yield (* denotes $p<0.05$; n=6). Reported pairwise comparisons are the result of Wilcoxon signed-rank test. All error bars indicated are standard error.

Previous studies have suggested that *P. aeruginosa* supernatants alone are not sufficient to inhibit *C. albicans* viability but did not specifically examine their effect on biomass retention to surfaces for biofilm production (19, 29). To explore this possibility, we grew biofilms of *C. albicans* in monoculture for 24 hs under regular ASMi flow, allowing them to reach their typical biomass steady state in biofilm chambers; after this 24 h period the medium influent was switched to a 2:1 mixture of ASMi and *P. aeruginosa* culture supernatant. After introduction of the supernatant, the *C. albicans* biofilms decreased linearly in total biomass nearly to zero in 24 h (Figure 1A). Altogether these results indicate

that the increased biomass accumulation of *C. albican* in the presence of *P. aeruginosa* is dependent on the mass transport of *P. aeruginosa* secreted products out of the system. When these supernatants are reintroduced, of *C. albicans* accumulation in the chambers ceased, and any pre-existing biomass was greatly reduced over time. This could be due to inhibited growth of *C. albicans*, inhibited attachment of *C. albicans* to substrata, induced dispersal, or a combination of these factors.

4.8 References

1. Nadell CD, Drescher K, Foster KR. 2016. Spatial structure, cooperation and competition in biofilms. Nat Rev Microbiol 14:589–600.https://doi.org/10.1038/nrmicro.2016.84.

2. Dufrêne YF, Persat A. 2020. Mechanomicrobiology: how bacteria sense and respond to forces. Nat Rev Microbiol 18:2272240.https://doi.org/10.1038/s41579-019-0314-2.

3. Flemming H-C, Wingender J, Szewzyk U, Steinberg P, Rice SA, KjellebergS. 2016. Biofilms: an emergent form of bacterial life. Nat Rev Microbiol14:563–575.https://doi.org/10.1038/nrmicro.2016.94.

4. Elias S, Banin E. 2012. Multi-species biofilms: living with friendly neighbors.FEMS Microbiol Rev 36:990–1004.https://doi.org/10.1111/j.1574-6976.2012.00325.x.

5. Bispo P, Haas W, Gilmore M. 2015. Biofilms in infections of the eye.Pathogens 4:111 136.https://doi.org/10.3390/pathogens4010111.

6. Bowen WH, Burne RA, Wu H, Koo H. 2018. Oral biofilms: pathogens, matrix, and polymicrobial interactions in microenvironments. Trends Micro-biol 26:229–242.https://doi.org/10.1016/j.tim.2017.09.008.

7. Silverstein A, Donatucci CF. 2003. Bacterial biofilms and implantable prosthetic devices. Int J Impot Res 15:S150–S154.https://doi.org/10.1038/sj.ijir.3901093.

8. Zhao G, Usui ML, Lippman SI, James GA, Stewart PS, Fleckman P, OlerudJE. 2013. Biofilms and inflammation in chronic wounds. Adv Wound Care2:389–399.https://doi.org/10.1089/wound.2012.0381.

9. Filkins LM, O'Toole GA. 2015. Cystic fibrosis lung infections: polymicrobial, complex, and hard to treat. PLoS Pathog 11:e1005258.https://doi.org/10.1371/journal.ppat.1005258.

10. Ciofu O, Tolker-Nielsen T, Jensen PØ, Wang H, Høiby N. 2015. Antimicrobial resistance, respiratory tract infections and role of biofilms in lung infections in cysti cfibrosis patients. Adv Drug Deliv Rev 85:7–23.https://doi.org/10.1016/j.addr.2014.11.017.

11. Stacy A, McNally L, Darch SE, Brown SP, Whiteley M. 2016. The biogeography of polymicrobial infection. Nat Rev Microbiol 14:93–105.https://doi.org/10.1038/nrmicro.2015.8.

12. Grahl N, Dolben EL, Filkins LM, Crocker AW, Willger SD, Morrison HG, Sogin ML,Ashare A, Gifford AH, Jacobs NJ, Schwartzman JD, Hogan DA. 2018. Profiling of bacterial and fungal microbial communities in cystic fibrosis sputum using RNA. mSphere 3:e00292-18.https://doi.org/10.1128/mSphere.00292-18.

13. Cutting GR. 2015. Cystic fibrosis genetics: from molecular understanding to clinical application. Nat Rev Genet 16:45–56.https://doi.org/10.1038/nrg3849.

14. Peters BM, Jabra-Rizk MA, O'May GA, Costerton JW, Shirtliff ME. 2012.Polymicrobial interactions: impact on pathogenesis and human disease. Clin Microbiol Rev 25:193–213.https://doi.org/10.1128/CMR.00013-11.

15. Fourie R, Pohl CH. 2019. Beyond antagonism: the interaction between Candida species and Pseudomonas aeruginosa. J Fungi 5:34.https://doi.org/10.3390/jof5020034.

16. Pierce GE. 2005. Pseudomonas aeruginosa, Candida albicans, and de-vice-related nosocomial infections: implications, trends, and potential approaches for control. J Ind Microbiol Biotechnol 32:309318.https://doi.org/10.1007/s10295-005-0225-2.

17. Nobile CJ, Johnson AD. 2015.Candida albicans biofilms and human disease.Annu Rev Microbiol 69:71–92.https://doi.org/10.1146/annurev-micro-091014-104330.18. Moradali

MF, Ghods S, Rehm BHA. 2017. Pseudomonas aeruginosa life-style: a paradigm for adaptation, survival, and persistence. Front CellInfect Microbiol 7:39.https://doi.org/10.3389/fcimb.2017.00039.

19. Hogan DA, Kolter R. 2002. Interactions: an ecological role for virulence factors. Science 296:222922232.https://doi.org/10.1126/science.1070784.

20. Christiaen SEA, Matthijs N, Zhang X-H, Nelis HJ, Bossier P, Coenye T.2014. Bacteria that inhibit quorum sensing decrease biofilm formation and virulence in Pseudomonas aeruginosaPAO1. Pathog Dis 70:271279.https://doi.org/10.1111/2049-632X.12124.

21. Chen AI, Dolben EF, Okegbe C, Harty CE, Golub Y, Thao S, Ha DG, WillgerSD, O'Toole GA, Harwood CS, Dietrich LE, Hogan DA. 2014. Candida albicans ethanol stimulates Pseudomonas aeruginosa WspR-controlled bio-film formation as part of a cyclic relationship involving phenazines. PLoSPathog 10:e1004480.https://doi.org/10.1371/journal.ppat.1004480.

22. Lewis KA, Baker AE, Chen AI, Harty CE, Kuchma SL, O'Toole GA, Hogan DA. 2019. Ethanol decreases Pseudomonas aeruginosa flagellar motility through the regulation of flagellar stators. J Bacteriol 201:e00285-19.https://doi.org/10.1128/JB.00285-19.

23. Grahl N, Demers EG, Lindsay AK, Harty CE, Willger SD, Piispanen AE,Hogan DA. 2015. Mitochondrial activity and Cyr1 are key regulators ofRas1 activation of *C. albicans* virulence pathways. PLoS Pathog 11:e1005133.https://doi.org/10.1371/journal.ppat.1005133.

24. Bergeron AC, Seman BG, Hammond JH, Archambault LS, Hogan DA,Wheeler RT. 2017. Candida albicans and Pseudomonas aeruginosa interact to enhance virulence of mucosal infection in transparent zebrafish. Infect Immun 85:e00475-17.https://doi.org/10.1128/IAI.00475-17.

25. Turner KH, Wessel AK, Palmer GC, Murray JL, Whiteley M. 2015. Essential genome of Pseudomonas aeruginosa in cystic fibrosis sputum. Proc Natl Acad Sci U S A 112:4114115.https://doi.org/10.1073/pnas.1419677112.

26. Darch SE, Simoska O, Fitzpatrick M, Barraza JP, Stevenson KJ, Bonnecaze RT, Shear JB, Whiteley M. 2018. Spatial determinants of quorum signalingin a Pseudomonas aeruginosa infection model. Proc Natl Acad Sci UA115:47794784.https://doi.org/10.1073/pnas.1719317115.

27. Flynn JM, Niccum D, Dunitz JM, Hunter RC. 2016. Evidence and role for bacterial mucin degradation in cystic fibrosis airway disease. PLoSPathog 12:e1005846.https://doi.org/10.1371/journal.ppat.1005846.

28. Hogan DA, Vik Å, Kolter R. 2004. A Pseudomonas aeruginosa quorum-sensing molecule influences Candida albicans morphology: Pseudomo-nas inhibition of *C. albicans* filamentation. Mol Microbiol 54:1212–1223.https://doi.org/10.1111/j.1365-2958.2004.04349.x

.29. Morales DK, Hogan DA. 2010. Candida albicans interactions with bacteria in the context of human health and disease. PLoS Pathog 6:e1000886.https://doi.org/10.1371/journal.ppat.1000886.

30. Friedman L, Kolter R. 2004. Genes involved in matrix formation in Pseudomonas aeruginosa PA14 biofilms. Mol Microbiol 51:675–690.https://doi.org/10.1046/j.1365-2958.2003.03877.x.

31. Jennings LK, Storek KM, Ledvina HE, Coulon C, Marmont LS, SadovskayaI, Secor PR, Tseng BS, Scian M, Filloux A, Wozniak DJ, Howell PL, Parsek MR. 2015. Pel is a cationic exopolysaccharide that cross-links extracellular DNA in the Pseudomonas aeruginosa biofilm matrix. Proc Natl AcadSci U S A 112:11353–11358.https://doi.org/10.1073/pnas.1503058112.

32. Hickman JW, Tifrea DF, Harwood CS. 2005. A chemosensory system that regulates biofilm formation through modulation of cyclic diguanylate levels. Proc Natl Acad Sci U S A 102:14422–14427.https://doi.org/10.1073/pnas.0507170102.

33. Jackson AA, Gross MJ, Daniels EF, Hampton TH, Hammond JH, ValletGely I, Dove SL, Stanton BA, Hogan DA. 2013. Anr and its activation byPlcH activity in Pseudomonas

aeruginosa host colonization and virulence. J Bacteriol 195:3093–3104.https://doi.org/10.1128/JB.02169-12

34. Dietrich LEP, Okegbe C, Price-Whelan A, Sakhtah H, Hunter RC, Newman DK. 2013. Bacterial community morphogenesis is intimately linked to the intracellular redox state. J Bacteriol 195:13711380.https://doi.org/10.1128/JB.02273-12.

35. de Bentzmann S, Giraud C, Bernard CS, Calderon V, Ewald F, Plésiat P,Nguyen C, Grunwald D, Attree I, Jeannot K, Fauvarque MO, Bordi C. 2012.Unique biofilm signature, drug susceptibility and decreased virulence inDrosophila through the Pseudomonas aeruginosa two-component sys-tem PprAB. PLoS Pathog 8:e1003052.https://doi.org/10.1371/journal.ppat.1003052.

36. Rodesney CA, Roman B, Dhamani N, Cooley BJ, Katira P, Touhami A,Gordon VD. 2017. Mechanosensing of shear by Pseudomonas aeruginosa leads to increased levels of the cyclic-di-GMP signal initiating biofilm de-velopment. Proc Natl Acad Sci U S A 114:5906–5911.https://doi.org/10.1073/pnas.1703255114.

37. O'Loughlin CT, Miller LC, Siryaporn A, Drescher K, Semmelhack MF, Bassler BL. 2013. A quorum-sensing inhibitor blocks Pseudomonas aeruginosa virulence and biofilm formation. Proc Natl Acad Sci U S A110:17981–17986.https://doi.org/10.1073/pnas.1316981110.

38. Harrison F, Buckling A. 2009. Siderophore production and biofilm formation as linked social traits. ISME J 3:632634.https://doi.org/10.1038/ismej.2009.9.

39. Hartmann R, Jeckel H, Jelli E, Singh PK, Vaidya S, Bayer M, Vidakovic L,Díaz-Pascual F, Fong JCN, DragošA, Besharova O, Nadell CD, Sourjik V,Kovács AT, Yildiz FH, Drescher K. 2019. BiofilmQ, a software tool forquantitative image analysis of microbial biofilm communities. https://doi.org/10.1101/735423.

40. Magdanova LA, Golyasnaya NV. 2013. Heterogeneity as an adaptive trait of microbial populations. Microbiology 82:1–10.https://doi.org/10.1134/S0026261713010074.

41. Grote J, Krysciak D, Streit WR. 2015. Phenotypic heterogeneity, a phenomenon that may explain why quorum sensing does not always result intruly homogenous cell behavior. Appl Environ Microbiol 81:5280–5289.https://doi.org/10.1128/AEM.00900-15.

42. Hogan DA, Gladfelter AS. 2015. Editorial overview: host-microbe interactions: fungi: heterogeneity in fungal cells, populations, and communities. Curr Opin Microbiol 26:vii–vix.https://doi.org/10.1016/j.mib.2015.07.003.

43.Yang L, Liu Y, Wu H, Hóiby N, Molin S, Song ZJ. 2011. Current under-standing of multi-species biofilms. Int J Oral Sci 3:74–81.https://doi.org/10.4248/IJOS11027.

44. Peleg AY, Hogan DA, Mylonakis E. 2010. Medically important bacterial–fun-gal interactions. Nat Rev Microbiol 8:340–349.https://doi.org/10.1038/nrmicro2313.

45. Trejo-Hernández A, Andrade-Domínguez A, Hernández M, Encarnación S.2014. Interspecies competition triggers virulence and mutability in Candida albicans–Pseudomonas aeruginosa mixed biofilms. ISME J 8:1974–1988.https://doi.org/10.1038/ismej.2014.53.

46. Morales DK, Grahl N, Okegbe C, Dietrich LE, Jacobs NJ, Hogan DA. 2013. Control of Candida albicans Metabolism and Biofilm and biofilm formation by Pseudomonas aeruginosa phenazines. mBio 4:e00526-12.https://doi.org/10.1128/mBio.00526-12.

47. Nadell CD, Xavier JB, Foster KR. 2009. The sociobiology of biofilms. FEMS Microbiol Rev 33:206–224.https://doi.org/10.1111/j.1574-6976.2008.00150.x.

48. Oliveira NM, Martinez-Garcia E, Xavier J, Durham WM, Kolter R, Kim W,Foster KR. 2015. Biofilm formation as a response to ecological competition. PLoS Biol13:e1002191.https://doi.org/10.1371/journal.pbio.1002191.

49. Schluter J, Nadell CD, Bassler BL, Foster KR. 2015. Adhesion as a weapon in microbial competition. ISME J 9:139–149.https://doi.org/10.1038/ismej.2014.174.

50. Al-Fattani MA. 2006. Biofilm matrix of Candida albicans and Candida tro picalis: chemical composition and role in drug resistance. J Med Micro-biol 55:999–1008.https://doi.org/10.1099/jmm.0.46569-0.

51. Zarnowski R, Sanchez H, Covelli AS, Dominguez E, Jaromin A, Bernhardt J,Mitchell KF, Heiss C, Azadi P, Mitchell A, Andes DR. 2018. Candida albicans biofilm induced vesicles confer drug resistance through matrix biogenesis. PLoS Biol 16:e2006872.https://doi.org/10.1371/journal.pbio.2006872.

52. Mitchell KF, Zarnowski R, Sanchez H, Edward JA, Reinicke EL, Nett JE,Mitchell AP, Andes DR. 2015. Community participation in biofilm matrix assembly and function. Proc Natl Acad Sci U S A 112:4092–4097.https://doi.org/10.1073/pnas.1421437112.

53.Rusconi R, Stocker R. 2015. Microbes in flow. Curr Opin Microbiol 25:.https://doi.org/10.1016/j.mib.2015.03.003

54. Wheeler JD, Secchi E, Rusconi R, Stocker R. 2019. Not just going with the flow: the effects of fluid flow on bacteria and plankton. Annu Rev CellDev Biol 35:213–237.https://doi.org/10.1146/annurev-cellbio-100818-125119.

55. Yawata Y, Nguyen J, Stocker R, Rusconi R. 2016. Microfluidic studies of biofilm formation in dynamic environments. J Bacteriol 198:2589–2595.https://doi.org/10.1128/JB.00118-16.

56. Rusconi R, Garren M, Stocker R. 2014. Microfluidics expanding the frontiers of microbial ecology. Annu Rev Biophys 43:65–91.https://doi.org/10.1146/annurev-biophys-051013-022916.

57. Persat A, Nadell CD, Kim MK, Ingremeau F, Siryaporn A, Drescher K,Wingreen NS, Bassler BL, Gitai Z, Stone HA. 2015. The mechanical world of bacteria. Cell 161:988–997.https://doi.org/10.1016/j.cell.2015.05.005.

58. Nadell CD, Bucci V, Drescher K, Levin SA, Bassler BL, Xavier JB. 2013. Cutting through the complexity of cell collectives. Proc R Soc B 280:20122770.https://doi.org/10.1098/rspb.2012.2770.

59. Hartmann R, Singh PK, Pearce P, Mok R, Song B, Díaz-Pascual F, Dunkel J,Drescher K. 2019. Emergence of three-dimensional order and structure in growing biofilms. Nat Phys 15:251–256.https://doi.org/10.1038/s41567-018-0356-9.

60. Liu Y, Tay J-H. 2002. The essential role of hydrodynamic shear force in the formation of biofilm and granular sludge. Water Res 36:1653–1665.https://doi.org/10.1016/S0043-1354(01)00379-7.

61. Stewart PS. 2014. Biophysics of biofilm infection. Pathog Dis 70:212–218.https://doi.org/10.1111/2049-632X.12118.

62. Ebrahimi A, Schwartzman J, Cordero OX. 2019. Cooperation and spatial self-organization determine rate and efficiency of particulate organic matter degradation in marine bacteria. Proc Natl Acad Sci U S A116:23309–23316.https://doi.org/10.1073/pnas.1908512116.

63. Kannan A, Yang Z, Kim MK, Stone HA, Siryaporn A. 2018. Dynamic switchingenables efficient bacterial colonization inflow. Proc Natl Acad Sci U S A115:5438–5443.https://doi.org/10.1073/pnas.1718813115.

64. Persat A, Stone HA, Gitai Z. 2014. The curved shape of Caulobacter crescentus enhances surface colonization inflow. Nat Commun 5:3824.https://doi.org/10.1038/ncomms4824.

65. Secchi E, Vitale A, Miño GL, Kantsler V, Eberl L, Rusconi R, Stocker R. 2020.The effect of flow on swimming bacteria controls the initial colonization of curved surfaces. Nat Commun 11:2851.https://doi.org/10.1038/s41467-020-16620-y.

66. Nadell CD, Ricaurte D, Yan J, Drescher K, Bassler BL. 2017. Flow environ-ment and matrix structure interact to determine spatial competition in Pseudomonas aeruginosa biofilms. Elife 6:e21855.https://doi.org/10.7554/eLife.21855.

67. Martínez-García R, Nadell CD, Hartmann R, Drescher K, Bonachela JA.2018. Cell adhesion and fluid flow jointly initiate genotype spatial distribution in biofilms. PLoS Comput Biol 14:e1006094.https://doi.org/10.1371/journal.pcbi.1006094.

68. Wucher BR, Bartlett TM, Hoyos M, Papenfort K, Persat A, Nadell CD. 2019.Vibrio cholerae filamentation promotes chitin surface attachment at the expense of competition in biofilms. Proc Natl Acad Sci U S A 116:14216–14221.https://doi.org/10.1073/pnas.1819016116.

69. Young KD. 2006. The selective value of bacterial shape. Microbiol MolBiol Rev 70:660–703.https://doi.org/10.1128/MMBR.00001-06.

70. Yang DC, Blair KM, Salama NR. 2016. Staying in shape: the impact of cell shape on bacterial survival in diverse environments. Microbiol Mol BiolRev 80:187–203.https://doi.org/10.1128/MMBR.00031-15.

71. Rusconi R, Guasto JS, Stocker R. 2014. Bacterial transport suppressed by fluid shear. Nature Phys 10:212–217.https://doi.org/10.1038/nphys2883.

72. Besemer K, Singer G, Hödl I, Battin TJ. 2009. Bacterial community composition of stream biofilms in spatially variable-flow environments. ApplEnviron Microbiol 75:7189–7195.https://doi.org/10.1128/AEM.01284-09

73. Besemer K, Singer G, Limberger R, Chlup AK, Hochedlinger G, Hödl I,Baranyi C, Battin TJ. 2007. Biophysical controls on community succession in stream biofilms. Appl Environ Microbiol 73:4966–4974.https://doi.org/10.1128/AEM.00588-07

74. Rossy T, Nadell CD, Persat A. 2019. Cellular advective-diffusion drives the emergence of bacterial surface colonization patterns and heterogeneity.Nat Commun 10:2471.https://doi.org/10.1038/s41467-019-10469-6.

75. Besemer K, Peter H, Logue JB, Langenheder S, Lindström ES, Tranvik LJ,Battin TJ. 2012. Unraveling assembly of stream biofilm communities. ISME J 6:1459–1468.https://doi.org/10.1038/ismej.2011.205.

76. Lecuyer S, Rusconi R, Shen Y, Forsyth A, Vlamakis H, Kolter R, Stone HA.2011. Shear stress increases the residence time of adhesion of Pseudomonas aeruginosa. Biophys J 100:3412350.https://doi.org/10.1016/j.bpj.2010.11.078.

77. Siryaporn A, Kim MK, Shen Y, Stone HA, Gitai Z. 2015. Colonization, competition, and dispersal of pathogens in fluid flow networks. Curr Biol25:1201–1207.https://doi.org/10.1016/j.cub.2015.02.074.

78. Dingemans J, Monsieurs P, Yu S-H, Crabbé A, Förstner KU, Malfroot A,Cornelis P, Van Houdt R. 2016. Effect of shear stress on Pseudomonas aeruginosa isolated from the cystic fibrosis lung. mBio 7:e00813-16.https://doi.org/10.1128/mBio.00813-16.

79. Mukherjee PK, Chand DV, Chandra J, Anderson JM, Ghannoum MA.2009. Shear stress modulates the thickness and architecture of Candida albicans biofilms in a phase-dependent manner. Mycoses 52:440–446.https://doi.org/10.1111/j.1439-0507.2008.01632.x.

80. Alves PM, Al-Badi E, Withycombe C, Jones PM, Purdy KJ, Maddocks SE.2018. Interaction between Staphylococcus aureus and Pseudomonas aeruginosa is beneficial for colonisation and pathogenicity in a mixed biofilm. Pathog Dishttps://doi.org/10.1093/femspd/fty003.

81. Carolus H, Van Dyck K, Van Dijck P. 2019. Candida albicans and Staphylococcus species: a threatening twosome. Front Microbiol 10:2162.https://doi.org/10.3389/fmicb.2019.02162.

82. Orazi G, Ruoff KL, O'Toole GA. 2019.Pseudomonas aeruginosa increases the sensitivity of biofilm-grown Staphylococcus aureus to membrane targeting antiseptics and antibiotics. mBio 10:e01501-19.https://doi.org/10.1128/mBio.01501-19.

83. Shing SR, Ramos AR, Patras KA, Riestra AM, McCabe S, Nizet V, Coady A.2020. The fungal pathogen Candida albicans promotes bladder coloniza tion of group B Streptococcus. Front Cell Infect Microbiol 9:437.https://doi.org/10.3389/fcimb.2019.00437.

84. Scoffield JA, Duan D, Zhu F, Wu H. 2017. A commensal streptococcus hijacks a Pseudomonas aeruginosa exopolysaccharide to promote bio-film formation. PLoS Pathog 13:e1006300.https://doi.org/10.1371/journal.ppat.1006300.

85. Gibson J, Sood A, Hogan DA. 2009. Pseudomonas aeruginosa-Candida albicans interactions: localization and fungal toxicity of a phenazine derivative. Appl Environ Microbiol 75:504–513.https://doi.org/10.1128/AEM.01037-08.

86. Azoulay E, Timsit JF, Tafflet M, de Lassence A, Darmon M, Zahar JR, AdrieC, Garrouste-Orgeas M, Cohen Y, Mourvillier B, Schlemmer B, OutcomereaStudy Group. 2006. Candida colonization of the respiratory tract and sub-sequent Pseudomonas

ventilator-associated pneumonia. Chest129:110–117.https://doi.org/10.1378/chest.129.1.110.

87. Earle KA, Billings G, Sigal M, Lichtman JS, Hansson GC, Elias JE, AmievaMR, Huang KC, Sonnenburg JL. 2015. Quantitative imaging of gut micro-biota spatial organization. Cell Host Microbe 18:478–488.https://doi.org/10.1016/j.chom.2015.09.002.

88. Welch JLM, Rossetti BJ, Rieken CW, Dewhirst FE, Borisy GG. 2016. Biogeography of a human oral microbiome at the micron scale. Proc Natl Acad SciU S A 113:E791–E800.https://doi.org/10.1073/pnas.1522149113.

89. Welch JLM, Hasegawa Y, McNulty NP, Gordon JI, Borisy GG. 2017. Spatialorganization of a model 15-member human gut microbiota established in gnotobiotic mice. Proc Natl Acad Sci U S A 114:E9105–E9114.https://doi.org/10.1073/pnas.1711596114.

90. Gallego-Hernandez AL, DePas WH, Park JH, Teschler JK, Hartmann R, JeckelH, Drescher K, Beyhan S, Newman DK, Yildiz FH. 2020. Upregulation of viru-lence genes promotes Vibrio cholerae biofilm hyper infectivity. Proc NatlAcad Sci U S A 117:11010–11017.https://doi.org/10.1073/pnas.1916571117.

91. Caldara M, Friedlander RS, Kavanaugh NL, Aizenberg J, Foster KR,Ribbeck K. 2012. Mucin biopolymers prevent bacterial aggregation by retaining cells in the free-swimming state. Curr Biol 22:2325–2330.https://doi.org/10.1016/j.cub.2012.10.028.

92. Wheeler KM, Cárcamo-Oyarce G, Turner BS, Dellos-Nolan S, Co JY,Lehoux S, Cummings RD, Wozniak DJ, Ribbeck K. 2019. Mucin glycansattenuate the virulence of Pseudomonas aeruginosa in infection. NatMicrobiol 4:2146–2154.https://doi.org/10.1038/s41564-019-0581-8.

93. Shanks RMQ, Caiazza NC, Hinsa SM, Toutain CM, O'Toole GA. 2006. Saccharomyces cerevisiae-based molecular tool kit for manipulation of genes from Gram-negative bacteria. Appl Environ Microbiol 72:5027–5036.https://doi.org/10.1128/AEM.00682-06.

94. Barelle CJ, Manson CL, MacCallum DM, Odds FC, Gow NA, Brown AJ.2004. GFP as a quantitative reporter of gene regulation in Candida albi-cans. Yeast 21:333–340.https://doi.org/10.1002/yea.1099.

95. Backer MDD, Maes D, Vandoninck S, Logghe M, Contreras R. 1999. Trans-formation of Candida albicans by electroporation. Yeast 15:160921618

96. Ng JMK, Gitlin I, Stroock AD, Whitesides GM. 2002. Components for integrated poly(dimethylsiloxane) microfluidic systems. Electrophoresis23:3461–3473.https://doi.org/10.1002/1522-2683(200210)23:20,3461::AID-ELPS3461.3.0.CO;2-8.

97. Holmén JM, Karlsson NG, Abdullah LH, Randell SH, Sheehan JK, HanssonGC, Davis CW. 2004. Mucins and their O-glycans from human bronchialepithelial cell cultures. Am J Physiol Lung Cell Mol Physiol 287:L824–L834.https://doi.org/10.1152/ajplung.00108.2004.

98. Sanders NN, Van Rompaey E, De Smedt SC, Demeester J. 2001.Structural alterations of gene complexes by cysticfibrosis sputum.Am J Respir Crit Care Med 164:486–493.https://doi.org/10.1164/ajrccm.164.3.2011041.

99.O'Toole GA. 2011. Microtiter dish biofilm formation assay. J Vis Exp2011:2437.https://doi.org/10.3791/2437.

100. de Lorenzo V, Timmis KN. 1994. Analysis and construction of stable phenotypes in gram-negative bacteria with Tn5- and Tn10-derivedminitransposons. Methods Enzymol 235:386–405.https://doi.org/10.1016/0076-6879(94)35157-0.

101. Jovanovic, M. *et al.* Rhamnolipid inspired lipopeptides effective in preventing adhesion and biofilm formation of Candida albicans. *Bioorganic Chem.* **87**, 209–217 (2019).

Conclusions

Microbes predominantly live in spatially structured communities called biofilms. These communities are very dynamic in nature and are shaped by interactions with their external environment and internally with other cells within the biofilm. These interactions lead to the emergence of properties and characteristics distinct to the biofilm community. Such biofilm-intrinsic characteristics impact the phenotypes of the cells within the biofilm; more importantly however they also impact the community composition and function. Studying community-intrinsic properties is, therefore, important for furthering our understanding of clinical, applied, and environmental microbiology.

The above studies exhibit scenarios where observed changes in phenotypes that occurred as a result of (i) microbial interactions that were not predictable from analyzing individual planktonic members and (ii) complex external environments; both in terms of mechanical forces like shear and nutrient media used. Therefore, biofilm properties are highly dependent on the system they occur in and as the realism of their natural niche increases, it enhances the probability of encountering and untangling biofilm-intrinsic properties in that environment. More of such studies of microbial interactions and ecology in complex environments that mirror natural environments are required, they will facilitate the discovery of biofilm properties and the factors that trigger them.

Once biofilm-specific properties are identified, the next goal would be to move towards a mechanistic understanding of the community-intrinsic properties. Molecular mechanisms involved community properties are still not well understood. Studies that use sequencing technologies combined with spatial and single cell analysis while maintaining an adequate level of biotic and abiotic complexity are very few and far apart. The transcriptional signatures across the biofilm could provide spatial information on metabolism and help with providing a holistic understanding of the biofilm system. Further, combining molecular biology techniques and high-resolution microscopy will we be able provide a fuller understanding of community-intrinsic properties.